AN ECG PRE-PROCESSING ALGORITHM FOR RELIABLE TRANSMISSION AND

RECOVERY OVER AN AWGN CHANNEL

by

Syed Muhammad Abdullah

APPROVED BY SUPERVISORY COMMITTEE:

_____

Dr. Lakshman S. Tamil, Chair

_____

Dr. Mehrdad Nourani

_____

Dr. John P. Fonseka

_____

Dr. Gopal Gupta

To family and friends

AN ECG PRE-PROCESSING ALGORITHM FOR RELIABLE TRANSMISSION AND

RECOVERY OVER AN AWGN CHANNEL

by

SYED MUHAMMAD ABDULLAH, BE, MSEE

DISSERTATION

Presented to the Faculty of

The University of Texas at Dallas

in Partial Fulfillment

of the Requirements

for the Degree of

DOCTOR OF PHILOSOPHY IN

ELECTRICAL ENGINEERING

THE UNIVERSITY OF TEXAS AT DALLAS

August 2017

ACKNOWLEDGEMENTS

AN ECG PRE-PROCESSING ALGORITHM FOR RELIABLE TRANSMISSION AND RECOVERY OVER AN AWGN CHANNEL

Syed Muhammad Abdullah, PhD
The University of Texas at Dallas, 2017

Supervising Professor: Dr. Lakshman S. Tamil

The history of telecardiology dates back to early 1960 when Electrocardiogram (ECG) was delivered via telecommunication transmission lines. Recent advances in wireless telecardiology have brought ease of access, efficiency, remote monitoring, improvement in patient's quality of life and significant reduction in health care costs. The transmission of ECG over wireless communication channel introduces several challenges compared to standard wireline monitoring of cardiovascular activity. In this work, a pre-processing algorithm is presented for reliable recovery of ECG signal corrupted by additive white Gaussian noise (AWGN) even at very low signal-to-noise ratio (SNR) conditions. At low SNR conditions, interference of noise corrupts the ECG signal to such an extent that the received ECG signals when compared to the original signals show unreliable results. The proposed method involves removal of redundancy in the original signal by a two-step approach: transform based compression using orthogonal wavelet basis function followed by entropy encoding. This is to increase the compression ratio but not at the expense of the quality of the reconstructed signal. This is important to preserve the content of clinical information. The aim of the proposed algorithm is to improve the fidelity of the received

ECG signal for accurate clinical interpretation. It is done by using data segmentation, data encoding, reassembly, features detection and signal reconstruction. These steps ensure that the diagnostically critical P-wave, QRS complex and T-wave are kept free of large reconstruction errors. The obtained results are evaluated in terms of compression ratio and PRMSD which are around 2.55:1 and 39.62% respectively at 3dB SNR. The visual perception of the reconstructed ECG signal also shows high quality signal recovery.

TABLE OF CONTENTS

LIST OF FIGURES

LIST OF TABLES

CHAPTER 1

INTRODUCTION

The reliable delivery of a patient's biomedical data such as ECG in real time is critical in emergency care. The architecture of health monitoring system to transmit ECG signal over noisy communication channel must ensure reliable transmission and recovery of signal that could withstand channel impairment such as noise that could significantly degrade the precision of ECG measurements. This chapter discuss research motivation, problem definition, implementation and contribution to the design of robust and error resilient ECG monitoring system.

1.1   Motivation and problem definition

According to Centers for Disease Control and Prevention (CDC), heart disease refers to several type of heart conditions such as Atrial Fibrillation, Aortic Aneurysm and Cardiomyopathy, etc. The coronary artery disease is most common type of heart disease. The narrowing of coronary arteries due to atherosclerosis restrict blood flow to the heart which can cause heart attack, killing over 370,000 people annually. More than 600,000 Americans die of heart disease each year [102] and it contribute to one in every four deaths in US. Every year 735,000 Americans have a heart attack, of these, 525,000 are first time attack and remaining 210,000 happen in people who had heart attack previously in their life [105]. In US, someone has a heart attack every 34 seconds and every 60 seconds someone dies from heart disease related event. These statistics show that cardiovascular diseases claim more lives than all forms of cancer combined.

There are several medical conditions and lifestyle choices that could put people at higher risk of heart disease, including:

- Diabetes

- Overweight and obesity

- High blood pressure and high cholesterol

- Physical inactivity

- Smoking and excessive alcohol use

- Hypertension

Early action is important in event of heart attack. Chest X-rays, coronary angiograms, electrocardiograms and stress tests are performed to determine the severity of heart disease. The chances of survival are greater when emergency treatment is administered immediately. In 2011, about 326,200 people experienced out-of-hospital cardiac arrests in US, out of which, 10.6% survived due to emergency medical services. The same year out of 19,300, 31.4% survived bystander-witnessed out-of-hospital cardiac arrest [102]. About 47% of deaths are attributed to cardiac disease occurring outside the hospital in people having heart disease; they either do not act or ignore early warning signs of heart attack. The economic impact of heart related disease on the US health care system continues to grow [104] with aging population. The direct and indirect cost of cardiovascular disease totals more than $320.1 billion per year including health care expenditures (e.g., hospitalization, rehabilitation services, physician visits, drugs, etc.) and loss of productivity from death and disability [102]. This economic impact could be reduced by intelligent, reliable and context aware health monitoring system which detect the disease in early stages and potentially save lives and cost associated with treatment of cardiovascular diseases.

The clinical significance of electrocardiogram (ECG or EKG) test is to examine the electrical conduction system of the heart over a period of time using electrodes on a patient's body. The electrical changes that arise from the heart muscle depolarization during each heart beat is detected by these electrodes and represents a *voltage* variation with *time*. The routine ECG screening procedure in patients without symptoms and those at low risk of coronary heart disease is not recommended as it may lead to misdiagnosis or false indication of existence of a problem [103]. Ambulatory ECG, Holter monitoring or continuous ECG monitoring is indispensable to monitor patients who show infrequently occurring of cardiac dysrhythmia which would unlikely be seen on a conventional short recording. This is also important in the event of heart attack when ECG done during a heart attack may look normal or unchanged from previous recording and need to be repeated over several hours and days to observe for changes.

Some key medical uses of ECG include:

1. Monitor the health of heart in patients with preexisting conditions such as high blood pressure, high cholesterol, smoking, diabetes and with family history of early heart disease.

2. Analyze the cause of symptoms of heart disease such as shortness of breath, palpitations, dizziness, seizures, chest pain, pericarditis and fainting.

3. Monitor the functionality of mechanical implant devices such as pacemakers.

4. Monitor any possible side effect of medication on heart activity.

5. Monitor the size and position of heart chambers

The research discussed here focused on the study of reliable recovery of ECG signal when it is corrupted by the additive white Gaussian noise (AWGN) under poor SNR

conditions using data buffering, lossless data compression, data denoising and ECG signal reconstruction.

The following section describes briefly the implementation of the proposed architecture and a detailed discussion is given in Chapter 4.

1.2   Problem Implementation

The proposed work addresses the challenges associated with the interference of ECG signal by white Gaussian noise over communication channel under low SNR conditions. The system architecture includes several modules each associated with a specific function.

Data analysis module performs raw compression on ECG signal using wavelet transform. This level 1 compression reduces the redundancy in the signal without compromising the vital information necessary for signal recovery and clinical analysis. The purpose of this step is to represent cardiac and non-cardiac cycle with minimum samples.

The minimum identified samples are further compressed at level 2 using Huffman coding. The encoded signal as shown in Chapter 4 represents original ECG signal with total length of code equals to 4.789 bits. During this process, no information is lost and encoded signal is transmitted as separate sign and data symbol stream.

AWGN model is used to study the superposition of white noise with ECG signal at varying low SNR. The proposed architecture simulates the scenario when bandpass signal power is overwhelmed by noise power at extremely low SNR. The recovery of original signal is accomplished using data recovery module.

Data recovery module detects key ECG signal features, reassemble, recover and reconstruct the received signal. The process of recovering the original signal starts with the

4

detection of P-wave, QRS complex and T-wave. These three repetitive electrical entities represent, atrial depolarization (P-wave), ventricular depolarization (QRS complex) and ventricular polarization (T-wave) of heart. The detection of P-wave, QRS complex and T-wave is based on variance and expected value of samples inside each corresponding window compared to a non-cardiac segment. Depending on the SNR of received signal, an adaptive threshold is used to determine whether the samples belong to key characteristic features of ECG signal or noise. The width of each window is then compared to the estimated duration of P-wave, QRS complex and T-wave of a normal ECG signal for the detection of these features. The window that may contains ST segment is first identified by doing the peak search and combining samples that result in less variation. The search for P-wave and QRS complex is then carried out on samples inside the adjacent left and right windows (reference to ST window) respectively. The detection of QRS complex and P-wave is based on doing the peak search and combining samples that yield maximum and least variation in search for QRS complex and P-wave.

The process of recovering QRS complex results in minimum amplitude distortion. The samples inside decoded *sign* symbol stream are scaled repeatedly and then *reassembled* with associated *data* samples to reconstructs QRS complex. *This is contrary to the procedure where signal is de-noised and then recovered which results in severe QRS complex distortion and impacts the quality of the recovered signal.*

The recovery of P and T-waves involve de-noising of ECG signal by discrete wavelet transform at level 4 using Daubechies-4 wavelet. The de-noising algorithm as explained in [5] is modified to recover P-wave and T-wave such that smoothing process does not significantly impact the quality of samples inside the observed P and ST segments. Using linear interpolation,

the denoised samples of P-wave and T-wave are then combined with the samples of recovered QRS complex.

1.3 Research Contribution

The real time transmission and recovery of ECG signal is a key deliverable of any health monitoring system that offers tele cardiology services related to cardiac diagnostics and monitoring for therapeutic purpose. The contribution of this work in the context of reliable ECG monitoring include:

(i) The presented work is an improvement in terms of accuracy over the existing solutions described in [5] and [101]. The proposed algorithm provides good performance even for very weak ECG signal that is corrupted by white Gaussian noise.

(ii) The design and implementation of m-ECG algorithm provides a framework for reliable recovery of ECG signal. It includes signal pre-processing, data segmentation, data encoding in data analysis module and data detection, reassembly and signal reconstruction in data recovery module.

(iii) The recovery of QRS complex with minimum distortion.

(iv) The compression of ECG signal and sampling of received signal is based on variance and expected value of sample amplitudes.

(v) A modified de-noising algorithm is proposed with adaptive threshold for the recovery of P-wave and T-wave in the presence of white Gaussian noise without compromising the morphology of the reconstructed ECG signal.

(vi) The mechanism to identify samples that may contain P-wave, QRS complex and T wave is based on threshold that uses signal-to-noise ratio and isolates cardiac samples from the noise.

1.4   Organization of the Dissertation

The recovery of ECG signal in different noisy environment aimed at improving signal-to-noise ratio is studied using various filter algorithms [5-12]. In this context, a novel ECG end-to-end system architecture using the proposed m-ECG algorithm is presented that demonstrates good performance in terms of signal detection, recovery and reconstruction. The proposed work is organized as follows.

Chapter 2 provides comprehensive background information on ECG signal processing techniques, signal denoising techniques and various signal coding schemes with associated challenges and metrics used to analyze the performance of compression algorithms. The use of time-frequency analysis of ECG signal yields simultaneous time-frequency localization of non-stationary signals. The fixed resolution of Short Time Fourier Transform (STFT) due to non-optimal window function provides uncertainty in knowing exact time-frequency information of the transformed signal. The use of Discrete Wavelet Transform (DWT) enables digital computation of ECG signal and provides time-scale representation using digital filter techniques where signal is analyzed at different resolution using filters with different cutoff frequencies. The dominant frequencies and non-significant frequencies in the original signal appear as high amplitude and low amplitude respectively in DWT transformed ECG signal where some level of compression is achieved by discarding low amplitude samples without any loss of information. The choice of ECG compression algorithm largely depends on sample rate, signal bandwidth,

noise level and average number of bits per compressed sample. The goal of data compression of biomedical signals, such as ECG involves representation of ECG signal using minimum number of bits without losing diagnostic information of original signal. Various types of ECG signal compression schemes are discussed along with relevant merits and challenges.

Detailed overview of referenced literature is presented in Chapter 3. Issues and challenges related to the transmission of ECG signal over communication channel such as QoS requirement, channel impairments, data loss and latency are discussed with reference to cellular network. The efficient use of available bandwidth of communication network involves *maximum data transfer with minimum redundancy*. ECG compression techniques include direct and transformation methods to achieve effective data compression with minimum reconstruction error. Detailed review of direct methods such as AZTEC, TP, CORTES and SAPA-2 are presented. Data compression algorithm using KLT, FFT, DCT and DWT are also presented. The reconstructed signal performance is generally measured using statistical measures such as compression ratio, mean square error and percent root mean square difference.

The architecture and implementation of proposed m-ECG algorithm is presented in Chapter 4. The recovery of ECG signal that is corrupted by additive white Gaussian noise channel (AWGN) is explained with detailed analysis of ECG feature detection, recovery, denoising and reconstruction. The design also includes the implementation of data analysis and data recovery modules to support reliable recovery of ECG signal when it is corrupted by white Gaussian noise under poor SNR.

Chapter 5 summarizes work and identifies future directions that are essential to design reliable pervasive health monitoring system that support wide range of biomedical signal

monitoring. The challenges associated with real time monitoring of ECG signal such as availability, accuracy and resilience to communication channel impairment are discussed.

1.5   Conclusion

The transmission of biomedical signal such as ECG over communication channel introduces several challenges compared to standard wireline monitoring of biomedical activities. The availability of high bandwidth, high data rate and low latency of next generation wireless communication network facilitates patient centric real time monitoring of biosignals. However, the design of such system gets complicated by frequent communication errors associated with noise. The use of error control mechanism for maintaining signal fidelity over communication channel is essential for acceptable signal recovery.

CHAPTER 2

BACKGROUND RESEARCH

The recent advancement in wireless networking technologies and mobile computing have made possible to deliver ubiquitous health care services and exchange of medical data anytime and anywhere. The availability of high transmission rates to provide connected health care depends on network performance such as bandwidth, latency, coverage and reliability at any given time. It is necessary to reduce the amount of data without loss of important bio-medical information while using lowest possible network resources.

This chapter presents brief background of commonly used techniques and methodology for (A) data conditioning and pre-processing (B) data de-noising and (C) data reconstruction. The details presented here are not intended to be comprehensive.

2.1   The Electrocardiogram (ECG) Signal

Electrocardiography displays the electrical activity of the heart captured over time by using external electrodes attached to the chest. The electrical changes on the chest that arise from heart muscle depolarization during heartbeat is detect by these electrodes. The location of the electrodes on the body influence different components of ECG signal including; amplitude, polarity and time duration of electrical waves characterized by peaks and valleys which in turn reflects the heart activity being normal or irregular or certain parts of heart are being stressed or enlarged. Besides measuring the rate and rhythm of heartbeat, it also provides evidence of blood flow to heart muscles.

The normal frequency range of ECG signal is 0.05Hz – 100Hz with 1mV – 10mV dynamic range [1]. The cardiac cycle is made up of multiple waves with signature pattern, duration and intensity; these waves are represented by letters P, Q, R, S, T and U. The performance of ECG monitoring system depends on the accuracy and reliable detection of QRS complex, P and T waves owing to the fact that they give information about the coordination between different events during a cardiac cycle [3]. The normal adult heart rate is 72 beats per minute and the duration from the beginning of a heartbeat to the beginning of the next heartbeat is about 0.83 sec [2] then by the definition of ECG signal the length of each cardiac event could be known [1].
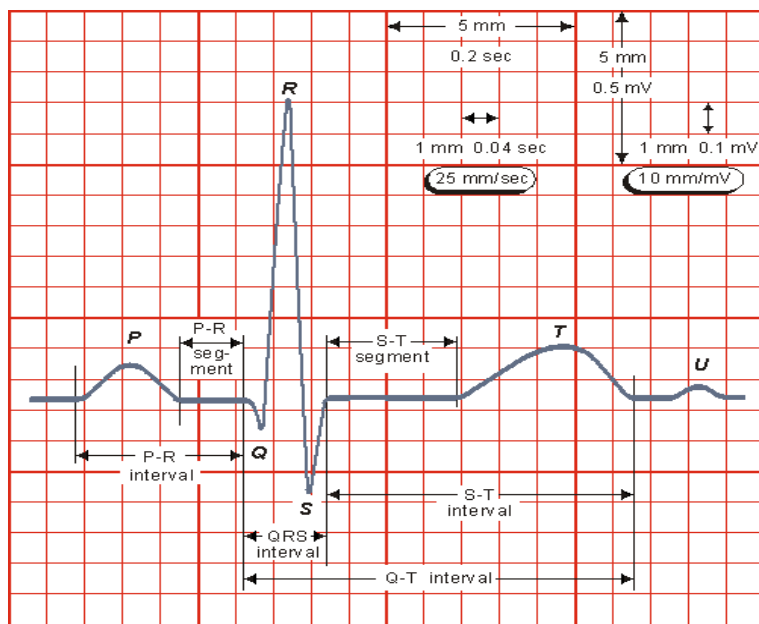
Figure 2.1. Normal Sinus Rhythm

The normal duration of key components of ECG waveform as shown in Fig. 2.1 are as follows:

- P-R segment: 0.12s – 0.2s

- Q-T segment: 0.35s – 0.44s

- S-T segment: 0.05s – 0.15s

- P-wave interval: 0.11s

- QRS complex: 0.08s – 0.12s

Moreover, the typical amplitude associated with the duration of characteristic wave is:

- P wave: 0.25mV

- R wave: 1.60mV

- Q wave: 25% of R wave

- T wave: 0.1mV – 0.5mV

2.2   ECG Signal Processing

The time domain methods employed earlier for ECG signal analysis often mask the information that could be readily seen in frequency domain or more accurately in time-frequency domain to study all features of ECG signal. In this section a detailed comparison between the time/frequency versus time-frequency analysis of ECG signal is presented.

2.2.1   Time/Frequency ECG signal analysis

A reversible transformation of signal from time to frequency and vice versa using Fourier Transform (FT) in most cases highlight information hidden in frequency domain of the signal which would otherwise not available in time domain. Let us take a closer look at how the transform works,

$$X(f) = \int_{-\infty}^{\infty} x(t) \cdot e^{-j\omega t} \, dt \qquad\qquad [2.1]$$

$$x(t) = \int_{-\infty}^{\infty} X(f) \cdot e^{j\omega t} \, df \qquad\qquad [2.2]$$

Equation (2.1) transform the time-domain signal *x(t)* by integrating it over all time, yielding the

spectral components that exists in the signal with no time resolution [4]. As the frequency

content of ECG varies in time, the need for an accurate description of ECG frequency contents

according to their location in time is essential [1]. Almost all biological signals including ECG

are non-stationary [4] which provides better insight of pathological conditions if represented by

time-frequency representation of heart's electrical activity.

2.2.2 Time-Frequency ECG signal analysis

Time-Frequency representation provides simultaneous time-frequency localization of time-

variant, non-stationary signals. The discussion in this section is limited to Short-time Fourier

Transform (STFT) followed by detailed application of wavelet transform applied to ECG signal.

Short Time Fourier Transform (STFT) transforms non-stationary signal into narrow time

intervals, narrow enough to be considered stationary followed by Fourier transform of each

segment thus providing spectral information of a separate time-slice of the signal with time and

frequency information. At any given time-frequency, the signal is analyzed by the following

relation:

$$STFT \, _x^f \, (t',f) = \int_t \big(x(t).W(t-t') \big) \cdot e^{-j2\pi ft} dt \qquad\qquad [2.3]$$

Where for every t' and f a new STFT coefficient is computed by the product of *x(t)* and its

complex conjugate window function *W(t)*. The window function influences the transformed

signal by its shape (Rectangular, Gaussian, Elliptic, Hann, etc.) and size. A wide window offers

poor time but good frequency resolution compared to a narrow window with better time at the

cost of poor frequency resolution. The choice of an appropriate support of window for signal

analysis is application dependent. If the frequency components of the signal are distinctly

defined, then sacrificing some spectral information will provide good time resolution in the transformed signal. It also shows that STFT gives a fixed resolution at all times due to non-optimal window support providing uncertainty in knowing the *exact* time-frequency information of transformed signal. It attempts to provide the information related to the *interval of frequencies* which are present in corresponding *time intervals.*

2.2.3   Wavelet Transform

Wavelet Transform (WT) provides simultaneous time-frequency information by overcoming problems related to resolution inherent to STFT. It offers variable resolution of the original signal where high frequencies are better resolved in time with less error compared to low frequencies that are resolved in frequency with less uncertainty. This Multiresolution Analysis (MRA) allows the signal with different frequencies to be analyzed with different resolution where each spectral component is not resolved equally as was the case with STFT [4].

ECG signal is characterized by high frequency component with distinct spectral contents for short duration and low frequency components for relatively longer duration. The use of WT provides good time resolution for high frequency and good frequency resolution for low frequency ECG spectral components.

The following section provides brief overview of theory of wavelet transform in terms of continuous and discrete signal transform with detailed account of application of discrete wavelet transform for the analysis of ECG signal including detection of cardiac events as discussed in section 2.1, signal de-noising and signal compression. The signal could be analyzed by choosing the most appropriate wavelet function which is a key advantage in contrast to single sinusoid feature of the Fourier analysis.

2.2.3.1 Continuous Wavelet Transform

The Continuous Wavelet Transform (CWT) is defined as follows:

$$CWT_x^{\psi}(\tau.s) = \Psi_x^{\psi}(\tau,s) = \frac{1}{\sqrt{|s|}} \int x(t) \cdot \psi^* \left(\frac{t-\tau}{s}\right) dt \qquad [2.4]$$

The transformed signal is convolution of the wavelet function $\psi^*(t)$ also known as the *mother wavelet* with signal *x(t)* and function of two variables; translation *(τ)* and scale parameter *(s)* respectively. The term mother wavelet represents a prototype for generating other window functions where the used windows are its dilated (s>1) or compressed (s<1) versions. A high scale provides bird's eye view and spans over the entire signal whereas low scale provides a detailed view of the signal that usually lasts for a short time.

The computation of CWT for a band limited signal involves limited interval of scales. The wavelet is placed at the beginning of the signal and set to (s=1), representing most compressed wavelet multiplied by the signal, integrated and subsequently normalized as shown in the equation (2.4). Once the wavelet function reaches the end of the signal, the scale is increased by a small value and the procedure is repeated for all *s* that culminates in the CWT of the given signal. According to equation (2.4), CWT is a representation of a square-integral function defined as:

$$< f(t), g(t) > = \int f(t) \cdot g^*(t) dt \qquad [2.5]$$

By comparing equation (2.4) and (2.5), CWT could be thought of as the inner product of test signal with the *basis function* $\psi_{\tau,s}^*(t)$:

$$CWT_x^{\psi}(\tau.s) = \Psi_x^{\psi}(\tau,s) = \int x(t) \cdot \psi_{\tau,s}^*(t) dt \qquad [2.6]$$

15

where,

$$\psi_{\tau,s}(t) = \frac{1}{\sqrt{s}} \psi\left(\frac{t-\tau}{s}\right) \qquad\qquad [2.7]$$

Thus CWT measures the similarity between the basis function and the signal's frequency

contents at a certain scale.

2.2.3.2 Discrete Wavelet Transform

The discretized continuous wavelet transform enables the digital computation of continuous

wavelet transform by sampling CWT. It provides highly redundant information as far as the

signal reconstruction is concerned. This redundancy in turn depends on the size of the signal and

resolution and involves significant computation time and resources. When the energy of the

signal is finite, the reconstruction of the original signal does not require all values of

decomposition provided using the wavelet that satisfies some admissibility conditions. In this

case, a continuous time signal is characterized by the knowledge of discrete waveform that

provides sufficient information for analysis and synthesis of the original signal with a significant

reduction in the computation time.

The Discrete Wavelet Transform (DWT) provides easier implementation when compared

to CWT. Like CWT, it provides time-scale representation of signal using digital filtering

techniques where filters of different cutoff frequencies are used to analyze the signal at different

resolution. Filtering a signal corresponds to the convolution of signal *x(n)* with the impulse

response *h(n)* of the low pass filter as follows:

$$x(n) * h(n) = \sum_{k=-\infty}^{\infty} x(k) \cdot h(n-k) \qquad\qquad [2.8]$$

The signal is also decomposed simultaneously using a high pass filter *g(n)*. The

decomposition obtained by successive high-pass and low-pass filtering of the time domain signal

yield detailed coefficients and coarse approximation coefficients respectively. When they are

applied to raw data vector it works as a smoothing filter to bring out data's detail information [5].

These two filters are related to each other and known as *quadrature mirror filter.* Low-pass filter

removes all the frequencies that are above half of the highest frequency in the signal thereby

changing the *resolution* to one half after filtering operation. After filtering, half of the samples

can be eliminated by *subsampling* by 2 without any loss of information according to the

Nyquist's rule as half the frequencies of the signal is removed by each of the corresponding

filters. The process of discarding every other sample and leaving the signal with half the number

of points which essentially doubles the *scale* constitutes level one decomposition and can be

mathematically expressed as follows:

$$y_{low}(k) = \sum_{n=-\infty}^{\infty} x(n) \cdot h(2k - n) \qquad [2.9]$$

$$y_{high}(k) = \sum_{n=-\infty}^{\infty} x(n) \cdot g(2k - n) \qquad [2.10]$$

where $y_{low}(k)$ and $y_{high}(k)$ are the outputs of the low-pass and high-pass filters respectively

following subsampling by 2. This hierarchical sub-band coding and multi-resolution analysis

which sometimes called *pyramidal* algorithm [5] can be repeated to further increase the

frequency resolution and the approximation coefficients decomposed with high and low pass

filters and then down-sampled. Fig. 2.2 illustrates this procedure, where *x(n)* is the original signal

to be decomposed using low-pass filter; *h(n)* and high-pass filter; *g(n)* respectively. The

frequency resolution (*f*) at each level is shown along with the corresponding approximation (A1, A2, etc.) and detailed (D1, D2, etc.) coefficients.
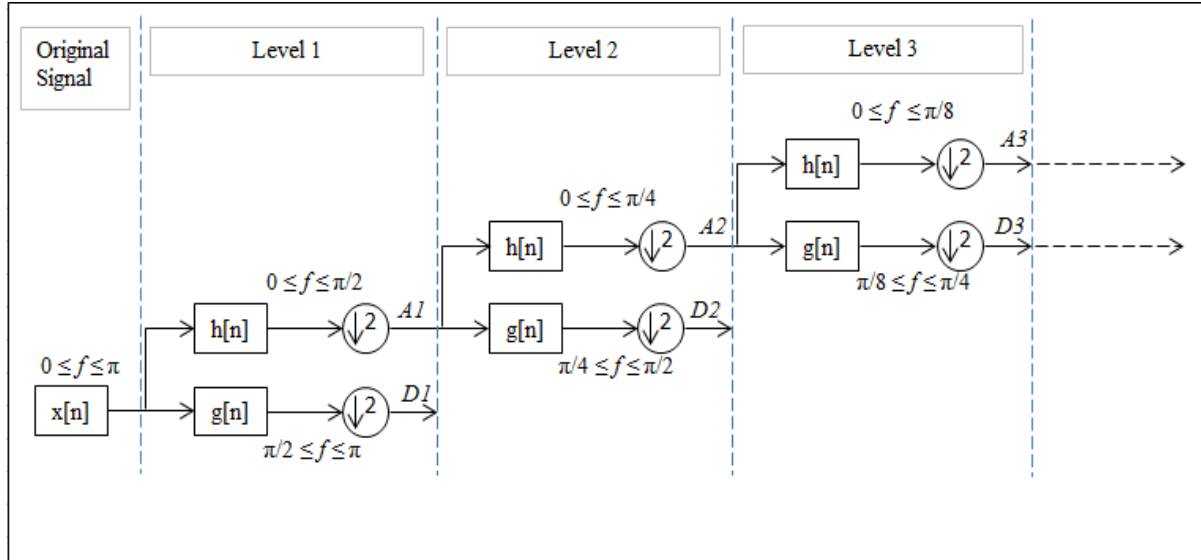
Figure 2.2. Multi-resolution wavelet analysis

The frequencies that are most prominent in the original signal will appear as high amplitudes in the region of the DWT signal that includes those frequencies. The frequency bands that are not very prominent in the original signal will have very low amplitudes and that part of the DWT signal can be discarded without any major loss of information – thus allowing data reduction [4].

The reconstruction procedure on other hand follows reverse order where signals at every level are *up-sampled* by 2, passed through the synthesis filters *g′(n)* and *h′(n)* and then added. The reconstruction at each level is achieved by the following relationship.

$$x(n) = \sum_{k=-\infty}^{\infty}((y_{low}(k) \cdot h(-n+2k)) + (y_{high}(k) \cdot g(-n+2k)))$$ [2.11]

The above relation shows analysis and synthesis filters being identical except for time reversal. Fig. 2.3 illustrates multi-resolution synthesis procedure where $h'(n)$ and $g'(n)$ are low-pass and high-pass reconstruction filters yielding approximation (A′3, A′2, etc.) and detail (D′3, D′2, etc.) coefficients at subsequent synthesis level.
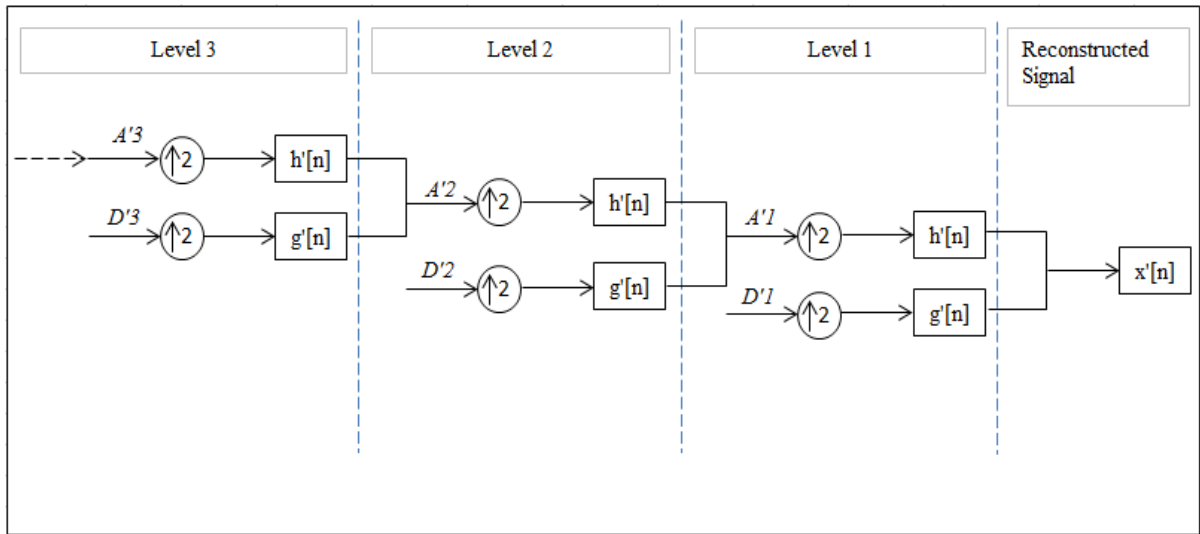
Figure 2.3. Multi-resolution wavelet synthesis

While wavelets are used in important applications such as computer vision, image compression and data analysis for characterizing behavior over a wide range of time scales, the wavelet techniques are equally useful in applications that involve signal de-noising.

2.3   Signal De-noising using Wavelet Transform

The process of noise removal or signal de-noising is the reconstruction of a signal from a noisy one. The two common approaches for signal de-noising include; de-noising in the original signal domain and de-noising in the processed domain. The wide range of applications in which de-noising is important for signal analysis include medical imaging and data analysis where the

removal of noise from biomedical signals requires specific care to avoid loss of useful information during the de-noising process. The scope of this dissertation is limited to the recovery of ECG signal that has been contaminated by additive white Gaussian noise. Different works have been done to design filtering algorithms aimed at improving the SNR and recovery of ECG signal from different noisy environment [5-9]. The use of Kernel/Spline estimators suppresses noise by broadening and erasing certain features but do not resolve local structures of the signal that is characterized by different scale and amplitudes. The Fourier transform based signal filtering cannot separate noise from signal where the noise and signal spectrum overlap.

For a broad class of signals that possess certain smoothness properties, wavelet based techniques are optimal or near optimal for signal recovery, the general wavelet-based method for de-noising involves:

- Decomposition: Applying wavelet transform to the noisy signal at level N

- Threshold detail coefficients: Appropriate threshold limit at each level to remove the noise

- Reconstruct: Compute inverse wavelet transform of the threshold detail and using original approximation coefficients to obtain a de-noised signal

The model of a noisy signal is the superposition of the signal *f(i)* and zero mean Gaussian white noise with variance of σ^2: $\eta(0, \sigma^2)$ [10]. The model is mathematically expressed using following equation:

$$s(i) = f(i) + e(i) \qquad\qquad [2.12]$$

where: *s(i)* – signal to be de-noised, *f(i)* – noise free signal, *e(i)* – noise.

2.3.1   Choice of wavelet and resolution levels

The selection of appropriate mother wavelet is important to better approximate and capture the

transient spikes of the original signal; it will not only determine how well the original signal is

estimated in terms of shape but will also influence the frequency spectrum of the de-noised

signal. The choice of mother wavelet could be based on visual inspection of signal of interest; it

could also be selected based on the correlation between the de-noised signal and signal of

interest as follows [12]:

$$\gamma = \frac{\sum (X-X')(Y-Y')}{\sqrt{\sum (X-X')^2 (Y-Y')^2}} \qquad\qquad [2.13]$$

The resulting transform is expected to be maximal when the input signal most resembles

the mother wavelet. The process of wavelet transformation involves signal decomposition at

different levels, the maximum level of wavelet transform applied to the signal depends on the

signal length and reduction of noise required thus improving the signal-to-noise (SNR) of the

original signal. Generally, when the signal has higher SNR with noticeable noise, the use of more

levels in order to extract the fine details of the signal is desirable compared to the signal with

poor SNR where the use of high levels say 8 or 10 of signal decomposition could remove much

of the desired information that could otherwise be captured using lower 4 or 5 decomposition

levels [12].

2.3.2   Wavelet Thresholding

Wavelet thresholding is a non-linear process to recover signal of interest corrupted by noise. The

threshold value is computed according to the model of the signal to be de-noised and the nature

of noise [11]. Using the model as described above in equation (2.12), each coefficient is

compared against a threshold in order to decide whether or not it qualifies as a desirable part of

original signal, this entails recovery of coefficients that are relatively stronger than the

background noise. Coefficients having small magnitude are considered as pure noise and are

subsequently set to zero. The process of wavelet thresholding is generally applied to the detail

coefficients such that the computed threshold does not lead to a large bias of the estimator nor it

increases the variance of the resulting threshold coefficients. The low frequency critical

components of the signal as represented by approximation coefficients are less impacted by the

noise and as such not subject to wavelet thersholding.

The threshold for wavelet coefficients using either *soft* or *hard* thresholding rule is

expressed as follows [11]:

$$T_{soft} = \begin{cases} x - Thr & x > Thr \\ 0 & |x| \leq Thr \\ x + Thr & x < -Thr \end{cases} \qquad [2.14]$$

$$T_{hard} = \begin{cases} x & |x| \geq Thr \\ 0 & |x| < Thr \end{cases} \qquad [2.15]$$

The simplest thresholding process or *hard* thresholding involve setting to zero the

elements whose absolute values are lower than the threshold *Thr*. The process of *soft*

thresholding is an extension of hard thresholding, first setting to zero the elements whose

absolute values are lower that the threshold and then shrinking the nonzero coefficients towards

0. The procedure to find the optimal value of threshold usually involve the estimation of noise

level; if signal under analysis is corrupted by white noise with variance σ^2, its standard deviation

can be estimated from the median of its detail coefficients:

$$\sigma = \ (|d(j,k)|) \ / \ 0.6745 \qquad\qquad [2.16]$$

Where |d(j,k)| is the median absolute deviation and the factor in the denominator, the *scale factor* depends on the distribution of *d(j,k)* and is equal to 0.6745 for a normally distributed data. Donoho and Johnstone [97] proposed a popular estimate of the noise level σ based on *Stein's unbiased risk estimate* (SURE) known as *VisuShrink* and is given as follows:

$$Thr = \ \sigma \sqrt{2.\log(N)} \qquad\qquad [2.17]$$

where *N* is the length of the ECG signal. The original ECG sequence could be reconstructed from the resulting threshold detail coefficients which yield denoised version of the original signal.

2.4   ECG Signal Compression

The monitoring of heart rate variability and diagnosis of cardiac abnormality involve ECG signal recording over long duration generating volume of data that lead to increasing demand on disk size to store information. In the particular case of data transmission across cellular networks and wireless communication systems it is very important to send maximum amount of data while using lowest possible network resources.

Any data compression of bio-medical signal including ECG must ensure the preservation of diagnostic information for correct medical diagnosis, increase the capacity of storage systems and reduce the transmission time between the patient and the health care provider. The goal is to represent ECG signal using fewest number of bits as accurately as possible by employing either *lossless* or *lossy* compression. In lossless compression, the signal is reconstructed as exact replica of the original signal and in lossy compression the reconstruction is done with certain amount of

distortion, small enough not to modify the diagnostic contents of the original signal. It may be necessary to perform noise filtering of the ECG signal prior to signal compression.

The factors that influence data compression largely depends on the sampling rate, signal bandwidth, noise level and the number of bits used to represent each sample of the original signal. A lossy compression method yield better compression performance at the cost of losing some clinical information whereas a lossless compression method offers moderate to high compression ratio without compromising the morphology of the original signal. The reliability requirement of signal transmission across wireless communication system makes lossless compression method for ECG compression an imperative choice for better medical diagnosis.

ECG signal compression techniques could also be classified into the following three major categories: (I) Direct data compression, (II) Transform based compression and (III) Parameter extraction. Direct and transform based data compression methods are reversible where the original signal could be recovered whereas the signal recovery is irreversible in parameter extraction technique of signal compression. Direct data compression techniques could be viewed as intelligent subsampling of original signal where the selection of successive significant samples is referenced to the properties of preceding samples so that the reconstruction error remains within certain tolerance. The performance of direct compression method is sensitive to the noise level in the ECG signal. AZTEC and SAPA are two well-known examples of direct method of data compression [13, 14]. Transformation based compression technique such as wavelet transform localizes the signal component in time-frequency space using time-frequency kernel and detects the redundancies utilizing energy distribution in the spectrum. It assumes that a compact signal representation exists in terms of the coefficients of a truncated orthonormal

expansion. Besides wavelet transform, orthogonal transform and Discrete Fourier Transform have also been used for ECG data compression.

The process of ECG data compression essentially involves two main steps: (I) reduction of redundancy in the original signal to produce a more compact signal (II) encoding the compact signal to produce an efficiently coded binary stream suitable for transmission or storage.

The scope of study in this dissertation is focused on employing lossless coding for ECG data compression. The intention through the proposed work is achieving maximum data reduction while preserving the morphology of ECG signal when transmitting across wireless communication network. The choice of using Huffman coding – a statistical compression algorithm for ECG data compression is mainly due to its best performance in real time data streaming over high speed wireless communication network and offer best efficiency in terms of compression ratio. The design of compression algorithm and structure of input data plays an important role in achieving high compression ratio and allow large amount of data transmission using lowest possible network resources. There are several measures such as compression ratio, PRMSD, RMS etc. which are used to evaluate the performance of compression algorithms.

(1) *Compression Ratio (CR)* expresses the effectiveness of data compression as a ratio between the number of bits required to represent the original signal to the number of bits required to represent the compressed signal.

$$CR = \frac{size\ of\ input\ data\ stream}{size\ of\ compressed\ output\ stream} \qquad [2.18]$$

(2) *Bit length* defines the average number of bits required to represent a sample of the ECG signal and is independent of sample rate and word length in contrast to compression ratio

(3) *Compression Percentage (CP)* expresses the compression rate as a percentage of the size of

the original data.

$$CP = \left(1 - {1}/{CR}\right) * 100 \ (\%) \tag{2.19}$$

The performance of lossy compression algorithm is characterized by measurement of

distortion in the reconstructed signal as excellent compression ratio and bit length could be

achieved at the expense of a severely distorted signal. The conditions such as sampling

frequency, bandwidth, precision and noise level use to record the original signal influence

compression ratio.

The following metrics define the complementary performance of compression algorithm

such as accuracy with which the diagnostic information in the original ECG signal is preserved.

For the original signal *x(n)* with *N* samples and the reconstructed signal *x̃(n)*, the following are

defined as:

(4) *Percent Root Mean Square Difference* calculates the deformation in the reconstructed signal

by point wise comparison with the original data.

$$PRMSD = \sqrt{\frac{\sum_{n=1}^{N}\left(x(n)-\tilde{x}(n)\right)^2}{\sum_{n=1}^{N}x^2(n)}} * 100 \ (\%) \tag{2.20}$$

Another definition of PRMSD called PRMSD1, is same as PRMSD but it subtracts the average

value of signal $\bar{x}$ from each original sample *x(n)* to eliminate the dc level.

$$PRMSD1 = \sqrt{\frac{\sum_{n=1}^{N}\left(x(n)-\tilde{x}(n)\right)^2}{\sum_{n=1}^{N}(x(n)-\bar{x}(n))^2}} * 100 \ (\%) \tag{2.21}$$

26

(5) *Root Mean Square Error* measures error between the original and the reconstructed signal as follows:

$$RMS = \sqrt{\frac{\sum_{n=1}^{N}(x(n)-\tilde{x}(n))^2}{N}}$$ [2.22]

(6) *Signal-to-Noise Ratio* measures the deformation as follows:

$$SNR = 10 \, log \, \frac{\sum_{n=1}^{N}(x(n)-\bar{x}(n))^2}{\sum_{n=1}^{N}(x(n)-\tilde{x}(n))^2} \, \text{(dB)}$$ [2.23]

where $\bar{x}$ is the average value of the original signal.

2.4.1 Huffman Coding

Huffman code is a particular type of *prefix code* that is commonly used for lossless data compression where no symbol is a prefix of another symbol. The output from the Huffman's algorithm can be viewed as a *variable-length code* where the length of the assigned code to each symbol depends on its probability of occurrence in the input data stream. Therefore, symbols that occur with highest frequency are generally represented using fewer bits than less common symbols which are assigned longer encoding bits. The process of coding is performed as follows and is shown in Fig. 2.4 for five symbols $\{a_1, a_2, a_3, a_4, a_5\}$ with associated probabilities P (a_1) = 0.4, P (a_2) = 0.25, P (a_3) = 0.25, P (a_4) = 0.05, and P (a_5) = 0.05.

1. The symbols are sorted and listed in order of descending probabilities.

2. The two symbols with the lowest probabilities are combined to create a new element with probability that is the sum of both symbols. A binary code [0 or 1] is assigned to each branch element.

27

3. Repeat steps 1 and 2 until a single *root* node is obtained.

4. The code for each symbol is obtained from the root of the tree to the corresponding symbol.

Symbol	Probability		Code
a_1	0.4	0	0
a_2	0.25	10	10
a_3	0.25	110	110
a_4	0.05	1110	1110
a_5	0.05	1111	1111
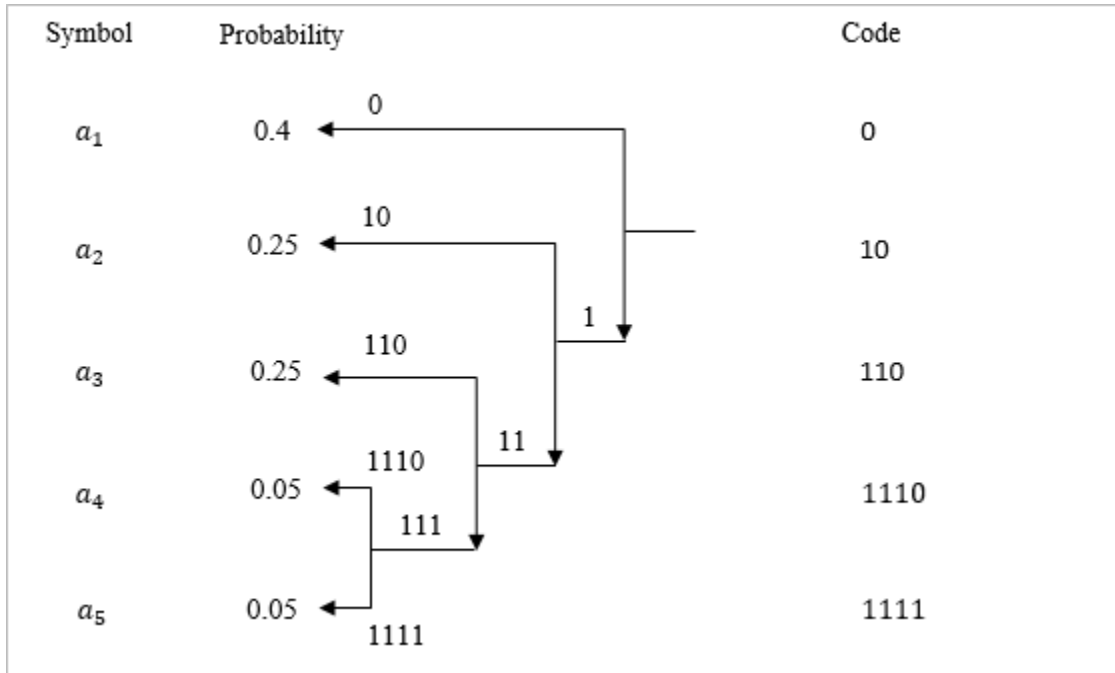
Figure 2.4. Huffman Coding Tree

The compression achieved by the Huffman code depends on the distribution of input symbols with average length that is close to the entropy of the source.

The average length of Huffman encoded signal can be calculated as:

$$Entropy = \sum_{j=0}^{n-1} P_j \, log_2 \frac{1}{P_j} \qquad [2.24]$$

Entropy is an important measure of data compression, it outlines the minimum number of bits required to encode the entire input signal with lossless compression and it could also be used to determine if data compression is worth attempting thereby evaluating the effectiveness of

28

compression. The number of bits in a compressed code when compared to the entropy of the signal reveal the optimal behavior of the compressed code.

2.5   Conclusion

In this chapter, various available signal processing techniques for ECG analysis in time, frequency and time-frequency domains were discussed. The use of time-frequency transform, such as wavelet transform greatly improves the clinical diagnosis and the correct interpretation of ECG signal.

The use of next generation wireless technologies in health care has led to an increase in pervasive monitoring of patients' vital signals. To make best use of bandwidth, speed and coverage of such infrastructure, data compression of original signal before transmitting it over the network is necessary. The choice of lossless data compression depends on system requirement and data structure to ensure reliable reconstruction of received signal.

CHAPTER 3

LITERATURE REVIEW

Patient monitoring plays a pivotal role in mobile health care system where reliability, efficiency and context awareness are the key attributes that influence the architecture of the system. The exploitation of wireless communication and multimedia technologies and their subsequent integration in the traditional health care system offers variety of medical services that are not possible with standard telephony communication alone [15].

This chapter presents a detailed overview of related works on pervasive patient monitoring of ECG signal using wireless infrastructure, signal processing techniques, effect of varying signal-to-noise ratio on the quality of the received signal and signal re-construction.

3.1   ECG Transmission over Communication Network

Mobile health system significantly impacts the delivery of healthcare services. The use of 2G and 2.5G networks to transmit 12-lead ECG to support transmission from ambulances and rural health emergency centers are shown in [16]. Istepanian *et al* demonstrate the transmission of ECG data and still images during emergency over GSM/GPRS network [17]. Wireless transmission of ECG and images from a rural health center and mobile ambulance using 2G/2.5G infrastructure was demonstrated by Kyriacou *et al.* in [18]. Clarke [19] proposed a reference architecture using General Packet Radio Service (GPRS) network to transmit ECG data from ambulances with wireless connectivity to sensors. The transmission of ECG and other parameters to support patients with chronic heart diseases using Global System for Mobile Communication (GSM) network and internet was studied by Salvador *et al.* [20]. The use of 2G

to transmit prehospital ECG to receiving stations in hospitals from symptom onset to reperfusion in time sensitive situations is shown by Clemmensen *et al.* [21]. Ambulatory emergency support through wireless transmission of ECG and images using 2G network was investigated by Kyriacou *et al.* [22]. Giovas *et al* [23] used GSM network to transmit 12-lead ECG data from a moving ambulance to a central hospital. A mobile emergency care system using German Telekom mobile data network to investigate the technical and conceptual suitability of such system where hospital was being informed more than 20 minutes in advance about the patient condition was undertaken [24]. In Uppsala, Sweden, Karlsten *et al.* [25] designed a 2G based time sensitive telemedicine and decision support system where ECG data was transferred from ambulance to the receiving medical facility over data network. Yan Xiao *et al.* [26] implemented a mobile based telemedicine system to transmit video and ECG signal from moving ambulance to desktop computer of the receiving physician. Pre hospital care involving transmission of ECG as a pilot project in Singapore between three emergency ambulances and emergency department was studied by Anantharaman *et al.* [27]. Rodriguez *et al.* [28] designed a mobile ECG transmission system to transmit single-lead ECG data via GSM mobile telephony. AMBULANCE [29] was developed as a portable medical device that allowed telediagnosis and transmission of ECG and still images of patient from an emergency site to a physician using GSM network. The Poket Doktor [30] by Hall *et al* designed to provide a flexible, scalable method of storing and communicating critical electronic medical record information using personal handheld electronic devices. Reponen *et al.* [31] proposed a personal digital assistant (PDA) based on GSM digital cellular phone to transmit computerized tomography. Anliker *et al* [37] implemented an advanced care and alert portable telemedical monitor (AMON) for acute

cardiac and respiratory patients. The wearable medical monitor collects and evaluates multiple vital signs and transmit data to a medical center over GSM link. Arjun *et al.* [40] proposed a distributed secure system where biomedical data being collected by wearable sensors is transmitted to the health monitoring center over GSM network. Alahmadi *et al.* [39] proposed an approach based on smart mobile e-health monitoring system that uses multi-level intelligent framework to share and analyze patient's data over GSM network. Prentza *et al.* [44] discuss e-Vital and CHS projects that make use of a 2G network to bring improvement to emergency treatments, routine check-ups and medical consultations.

The use of 3G mobile network to transmit bio-signals and images of the patient have been demonstrated by many applications. A cost-effective portable teletrauma sysem that simultaneously transmit patient's video, medical images and ECG signal over a commercially available 3G wireless data service was demonstrated by Yuechun *et al.* [32]. OTELO [33], an end-to-end mobile tele-echography system used an ultra-light robot to evaluate quality of service issues defined in terms of throughput, packet-delay and jitter over a 3G connectivity link. Richard *et al.* [34] proposed a methodology for measurement-based performance assessment of 3G network to support m-health services. An integrated 3G based ubiquitous health care monitoring system with ECG diagnosis algorithm on a cell phone is discussed in [35] where the physiological signs of a patient from a wireless sensor is transmitted directly to a PDA using 3G wireless network. MobiHealth [36] project was developed using UMTS network for continuous monitoring and transmission of vital signals to the hospital. Viruete *et al* [38] analyzed and measured a multi-collaborative wireless telemedicine system over a 3G mobile network. The system was designed to communicate from an ambulance with medical specialists in a remote

hospital through UMTS network. The performance analysis of joint transmission of voice, real-time video, ECG, heart sound and file transfer for both uplink and downlink over High Speed Packet Access (HSPA) was presented by D. Vouyioukas *et al.* [41]. The quality of service (QoS) was examined by prioritization of m-health services and it suggested improvements to HSPA system parameters. The use of context information in mobile health service platform using 3G wireless communication network to support m-health service delivery was investigated by K. Wac *et al.* [42]. The proposed model made use of context information in a QoS aware m-health service platform in defining end-user QoS and impact of communication network infrastructure on the delivered QoS.

R. Istepanian *et al.* [45] addresses some of the scenarios and characteristics of next generation mobile telemedicine systems that offer high communication speed, high capacity, low per-bit transmission cost and IP-based technology to deliver effective medical care and provide choices to both patients and care-givers that fit their lifestyle while maintaining access to critical medical information. In [43], Pravin *et al* highlight main problems associated with mobile patient monitoring system as follows:

(a) Lack of sufficient bandwidth for transmitting bio-signals due to wireless network coverage or congestion resulting in high latency.

(b) QoS requirements to transmit bio-signal also need to take into consideration issues such as network delay and jitter.

(c) The loss of data during transmission over the network need to be minimized so that the health care professionals have access to high quality bio-signals.

3.2   ECG Compression Techniques

The ECG signal represent various features of heart's electrical activity and is characterized by P, Q, R, S and T wave respectively [46], where:

(A): P wave marks the depolarization of atria. When the heart chambers receive the blood from the body, the left atrium is depolarized which collects the oxygen rich blood from the lungs and the right atrium collects oxygen deficient blood from the body.

(B): QRS complex represents the depolarization of left ventricle which sends oxygen rich blood to the body and the right ventricle sends the oxygen deficient blood to the lung. Due to the larger muscle mass of ventricles the amplitude of QRS complex is significantly large compared to P-wave.

(C): T wave represents the ventricles repolarization or relaxed state before the atria prepares for the next beat.

The real time ECG signal transmission over communication network for both monitoring and diagnostic purposes involve massive volume of digital data that makes ECG data compression an important area of research in biomedical signal processing. The preservation of main characteristic features of ECG signal during compression as defined above in (A-C) are important as it is used by cardiologists to analyze heart activity and note any disorder. The effectiveness of ECG compression technique is often described in terms of achieving a good compression ratio while preserving relevant signal information, execution time and measure of error loss as percent-mean-square difference [47]. Existing data compression techniques for ECG signals are broadly categorized as direct data and transformation methods. They are discussed below:

3.2.1 Direct Method for ECG Data Compression

The direct method of ECG data compression involves detection and elimination of redundancies and yield minimum distortion. Dedicated techniques such as Amplitude Zone Time Epoch Coding (AZTEC) by Cox *et al.* [48] for preprocessing of real-time ECG signal were developed for rhythm analysis. The algorithm converts raw ECG data into horizontal lines (plateaus) and slopes. The amplitude of the line and its length are stored as value for each plateau and the value of slope is saved whenever a plateau of three samples or more can be formed. The reconstruction of the signal is achieved by expanding plateaus and slopes into discrete sequence of data points. Compression ratio of 5:1 for ECG signal sampled at 200Hz with 12bit resolution is achieved per ref. [50].

The Turning Point (TP) data reduction algorithm by Mueller [49] processes three data points at a time and eliminate one point from every pair of points in the ECG trace. This depends on which point preserves the slope of the original three points. The turning point method yield a compression factor of 50% whereby the reconstructed signal resembles the original signal with some distortion [50].

The coordinate reduction time encoding system (CORTES) algorithm by Abenstein and Tompkins [51] combines the best features of TP and AZTEC to reduce data without losing the clinical information content. CORTES applies TP algorithm to the high frequency regions and AZTEC algorithm to the isoelectric regions of the ECG signal. The signal reconstruction is achieved by expanding the plateaus into the discrete data points and interpolating between TP data points. As per [50], CORTES algorithm reports a compression ratio of 4.8:1.

Gardenhire [52] reported ECG compression method – Fan, by replacing the original signal with straight line segments such that none of the points lies farther from line segment than predetermined threshold. A related technique that also approximates ECG waveform with straight line segments known as Scan-Along Polygon Approximation (SAPA) was presented by Ishijima *et al*. [53] as set of three algorithms. The SAPA-2; one of the three SAPA algorithms showed best result by comparing the deviation between the approximated line and the original signal against a predetermined error tolerance.

Stewart *et al.* [54] described delta coding with threshold for compression of three lead ECG signal by eliminating data according to a preset error threshold. The data is considered redundant for elimination when absolute value of the difference between adjacent samples in any of the three ECG lead signal is less than the threshold, otherwise it is retained. Ruttimann *et al*. [55] studied the performance of Differential Pulse Code Modulation (DPCM) system with linear prediction as a function of the order of the predictor. They concluded that linear predictor of order higher than two does not result in increased data compression. The performance comparison of DPCM using a second order linear predictor versus a second order interpolator was demonstrated [56] with results showing superior performance with the latter.

J. R. Cox *et al.* [57] proposed Huffman coding technique by employing second order predictor system for ECG data compression. The code words of resulting second difference ECG data was partitioned into two sets: frequent data set and an infrequent data set. Huffman coding was applied to the frequent code words set while fixed word length coding was applied to the infrequent set. ECG data compression using Huffman coding is also implemented in [58] and [59].

The implementation of two asynchronous data compression techniques is described based on picking out the peaks of the ECG signal in one case and adaptive peaking in the second case as per ref. [60]. The basic operation of such techniques involve extraction of parameters such as amplitude, slope changes and points of maxima and minima. Signal reconstruction is accomplished by joining these points by polynomial fitting techniques such as straight lines. T. S. Ibiyemi [61] proposed a data compression technique on similar principle by clipping the signal and using zero-crossing intervals as features. The system was validated by experiments using ECG of rat's heart. Imai *et al*. [62] proposed efficient encoding method for ECG using spline functions. The method consists of two steps; extraction algorithm that extracts ECG features from A/D converter and restoration algorithm that restores the original ECG signal from the extracted samples using spline functions. The spline function performs a smoothing operation and thereby achieves root mean square error that is half the AZTEC method for given compression ratio.

Jalaleddine *et al*. [63] proposed data compression method for ECG by substituting a periodic signal by one cycle period and a count of the total number of cycles that occur, in the signal. The underlining assumption treats ECG as quasi-periodic signal that does not change significantly as a result of change in the heart function. The proposed scheme involves detection of QRS complex as a repetitive wave in the ECG signal. The difference between generated QRS template and actual QRS complex result in a low amplitude and slow varying difference signal that when compressed using Fan compression algorithm results in better performance in terms of higher compression ratio. In another study, preliminary evaluation of this scheme yielded no significant improvement over Fan compression algorithm [50].

3.2.2   Transform Method for ECG Data Compression

The use of transformation data compression techniques for ECG compression involve input signal preprocessing by orthogonal transforms such as Karhunen-Loeve Transform (KLT), Fast Fourier Transform (FFT), Discrete Cosine Transform (DCT) and Discrete Wavelet Transform (DWT). The compression is achieved based on energy distribution of the signal, properly encoding the transformed output and reducing the data required to adequately represent the original signal. The signal reconstruction involves inverse transformation to recover the original signal without losing relevant clinical information for accurate detection and classification. Al-Nashash [64] modeled ECG as quasi-periodic signal and proposed a data compression technique using Fourier series by estimating Fourier coefficients using FFT algorithm or adaptive least mean square (LMS) algorithm. Saberkari *et al*. [65] investigated a different frequency domain transform for ECG signal compression. They used compression ratio (CR) and percent root mean square difference (PRD) as figure of merit and showed that Discrete Sine Transform (DST) has the least compression ratio whereas Discrete Cosine Transform (DCT-II) offered most percent root mean square difference. The DCT is widely used for data compression such as image, speech and ECG as it yields nearly optimal performance in the signals that exhibit high correlation in adjacent samples. Batista *et al*. [66] proposed ECG compression method based on optimized quantization of DCT coefficients that was previously used for image compression. The proposed method achieved CR of 9.3:1 for PRD equal to 2.5%. Allen *et al*. [67] studied the tradeoffs between accuracy, speed and compression ratio using DCT for ECG data compression. The goal of the study was to select a small subset of transform coefficients that contain most information about the signal without introducing noticeable error during reconstruction. The use

of DCT and Laplacian Pyramid (LP) based compression method for ECG signal was proposed by Aggarwal et al. [68]. The proposed method involves transformed coefficients being threshold using user defined PRD. The lookup table then stores the map for zero and non-zero coefficients, the non-zero coefficients are quantized by Max-Lloyd quantizer followed by arithmetic coding. Huffman coding was used to encode the lookup table. Ahmed et al. [70] studied the ECG data compression using Haar transform, DCT and KLT for a single lead canine ECG to achieve CR of 3:1. Reddy *et al*. [75] used Fourier descriptors for ECG data compression. The two-lead ECG data segmented into QRS complex and S-Q interval are Fourier transformed with an overall compression ratio of 7. Lee *et al*. [76] described a real time ECG compression algorithm for a digital holter system that achieved a CR of 8.82:1 and PRD of 1.82. The algorithm involved applying DCT on a processed ECG data which is encoded using Huffman coding compression to achieve high level of compression.

The use of Walsh transform to implement a real-time ECG data compression system was investigated [77] using mean squared error (MSE) and linear filtering techniques. Frangakis *et al*. [78] also proposed a fast Walsh transform based ECG data compression algorithm for multi-microprocessor based system. De Perez *et al*. [79] presented ECG data compression technique based on exponential quantization of ECG Walsh spectrum. The proposed method yields CR of 8:1.5 with additional reduction of high frequency recording noise besides simplicity and speed. Shridhar *et al*. [80] compared the performance of three data reduction techniques for ECG data compression: linear prediction using DPCM, FT and slope change detection. Their analysis revealed that slope change detection when applied to pre-filtered data showed a MSE below 1% compared to FT for a single lead ECG compression.

KLT transform also known as Principal Component transform represents the input signal

with least number of orthonormal functions for a given RMS error [50]. Olmos et al. [69]

analyzed Karhunen-Loeve transform (KLT) technique for ECG data compression. The

application of KLT to entire beat and to independent windows yielded CR of 12.1 with a mean

MSE of 0.3% and CR of 17.21 with a mean MSE of 0.44% respectively. Womble *et al*. [71],

[73]- [74] used data compression technique using Karhunen-Loeve series for ECG data to

achieve CR of 12:1. Young et al. [72] analyzed the application of principal component theory or

KLT to study ECG classification.

The use of Discrete Wavelet Transform (DWT) makes it suitable to analyze and extract

information from non-stationary signals such as ECG. The time-frequency resolution properties

along with localization feature of wavelet makes it a robust tool to study the behavior of non-

stationary signals that are characterized by drifts and abrupt changes. Rajoub [81] used DWT to

pre-processed ECG signal and achieved a compression ratio of 24:1 with PRD as low as 1.08%

by using run length encoding (RLE) on resulting wavelet decomposition coefficients and binary

representation for significant coefficients. Yan *et al*. [82] proposed ECG data compression

method based on integer to integer wavelet transform for a Holter system. The delay

performance of ECG compression algorithm for time-critical data transmission over CDMA

network, based simulation model with mobile channel noise was studied by Kim *et al*. [83]. They

proposed a wavelet-based ECG compression algorithm with a low delay property for

instantaneous and continuous ECG transmission over wireless network by waveform

partitioning, adaptive frame sizing and wavelet compression to attain low delay and high signal

fidelity. Istepanian *et al*. [17] evaluated ECG compression performance using optimal zonal

wavelet coding (OZWC) and wavelet transform of higher order statistics based coding (WHOSC) for real time low bandwidth telemedicine application. The proposed method enhances medical data compression with high compression ratio (CR) and low normalized rms error (NRMSE). Ramakrishnan *et al*. [84] showed that ECG coding scheme involving linear prediction of significant wavelet coefficients increased the compression ratio while the error remained uniform throughout the ECG cycle and QRS complex remained free of maximum reconstruction error. MULTIWAVE – a multiresolution wavelet based algorithm for ECG data compression by Thakor *et al*. [85] achieved variable data compression rates of 2:1, 4:1, 8:1 and so on at each successive scale better than TURNING POINT algorithm. The algorithm decomposed the signal into coarse and fine samples and analyzed the signal at successive scales by convolution with an orthonormal set of filters, followed by decimation. The 1D case of set partitioning in hierarchical trees compression algorithm (SPIHT) used by Lu *et al*. [86] to compress wavelet ECG data codec was more efficient in terms of computation as well as compression when compared to other ECG compression schemes.

Hilton [87] proposed wavelets and wavelet packet based compression algorithm to compress Holter ECG data by 8:1 compression. A similar approach using wavelet packet based algorithm for the compression of a single lead ECG signal was investigated by Brian [89] using KL transform.

Al-Busaidi et al. [88] used ECG compression technique involving discrete wavelet transform (DWT), bit-field preserving (BFP) and run length encoding (RLE) method to achieve desired data compression. The compressed packets are decomposed into blocks and compressed again to fit inside the available payload before transmission. Crowe *et al*. [90] investigated the

application of wavelet transform to the study of ECG and heart rate variability data for data compression using efficient pyramidal algorithm. Ahmeda *et al.* [91] described a hybrid technique based on combination of wavelet transform and linear prediction to achieve effective data compression of 20:1 with PRD less than 4%. A novel algorithm for wavelet based ECG signal coding was proposed by Kumari *et al.* [92] by using both horizontal and vertical bit scanning – a concept similar to Huang's Partition Parity Coding (PPC) and intra band coding to achieve high compression ratio. The subsequent application of adaptive entropy coding provided high quality signal reconstruction.

Chen *et al.* [94] proposed wavelet based method for the compression of ECG data. It involved the application of DWT to the ECG signal where the resulting DWT coefficients are quantized with uniform scalar dead-zone equalizer and subsequently decomposed into four symbol streams. An adaptive arithmetic coder was then used for entropy coding of the symbol stream resulting in a CR of 14:1. Blanco *et al.* [94] studied the impact of increasing compression ratio on the quality of reconstructed signal using wavelet transform. The quality of the reconstructed signal should be analyzed together with different parameters, such as a joint use of CR and PRD otherwise considering only the PRD and the CR parameters independently could hide the real performance of the compressor.

Manikandan et al. [95] proposed a wavelet threshold based ECG signal compression technique using uniform scalar zero zone quantizer (USZZQ) and Huffman coding on differencing significance map (DSM). The significant wavelet coefficients selected based on energy efficiency at each sub-band are quantized with uniform scalar zero zone quantizer. The indices of wavelet coefficients are stored in significance map which is encoded using Huffman

coding. The proposed technique achieved a CR of 18.7:1 with lower PRD on record 117 from MIT-BIH arrhythmia data base compared to other threshold based methods.

Brechet *et al.* [96] discussed ECG and EMG data compression based on discrete wavelet packet transform decomposition. The mother wavelet was selected based on minimal distortion of the decoded signal for fixed compression ratio. The basis of wavelet packets was selected for given mother wavelet. The proposed method yields a CR in the range of 50%-90%.

3.3   Conclusion

In this chapter various techniques discussed in the published literature on ECG data compression are presented. The context was achieving high data compression and high quality reconstruction of ECG signal. The techniques are divided into two main groups based on direct and transform based signal compression methods. The criteria to choose one over the other depends on preserving minimum essential information required to ensure reliable clinical diagnosis of ECG signal.

CHAPTER 4

M-ECG ALGORITHM

This chapter presents a simple and reliable algorithm for recovery of ECG signal that is corrupted by additive white Gaussian noise (AWGN) at moderate to low SNR conditions with relevant assumptions. When the signal is transmitted over wireless network, it picks up several sources of noise that prevents accurate extraction of useful information making it irrelevant for clinical analysis. Different studies have proposed design of algorithms to improve signal-to-noise (SNR) and ECG recovery under different noise conditions [6], [8], [98]. In this context, m-ECG algorithm is developed that provides adequate and near accurate recovery of ECG signal that is corrupted by WGN.

4.1   Problem Framework

The m-ECG algorithm is based on wavelet transform applied to ECG signal followed by data pre-processing and signal encoding. This technique provides high compression with less reconstruction error when the signal is subjected to extreme low SNR conditions.

The signal reconstruction involves data decoding, data reassembly, features detection and recovery and signal denoising to recover the original signal. The proposed algorithm is novel and efficient to reduce the data size while maintaining the reconstructed signal quality.

The ECG signal processing model in the context of the stated problem framework is depicted in Fig. 4.1.
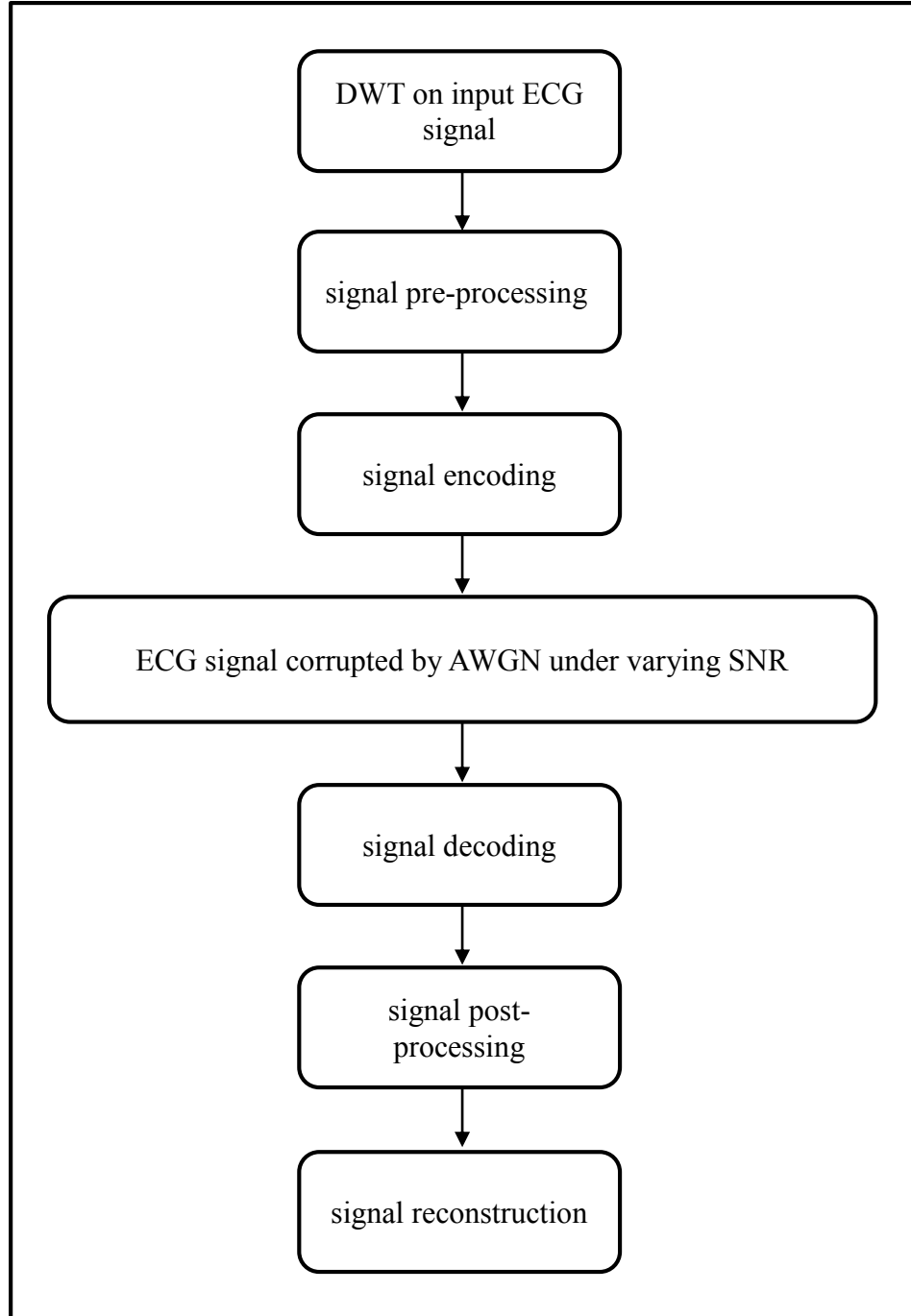
Figure 4.1. ECG signal processing model

The input ECG signal for testing and evaluation is sourced from MIT-BIH Arrhythmia Database [99]. The performance of m-ECG algorithm is measured in terms of compression ratio (CR) and distortion of the reconstructed ECG signal. A more detailed description of ECG processing model using m-ECG algorithm is shown in Fig. 4.2.
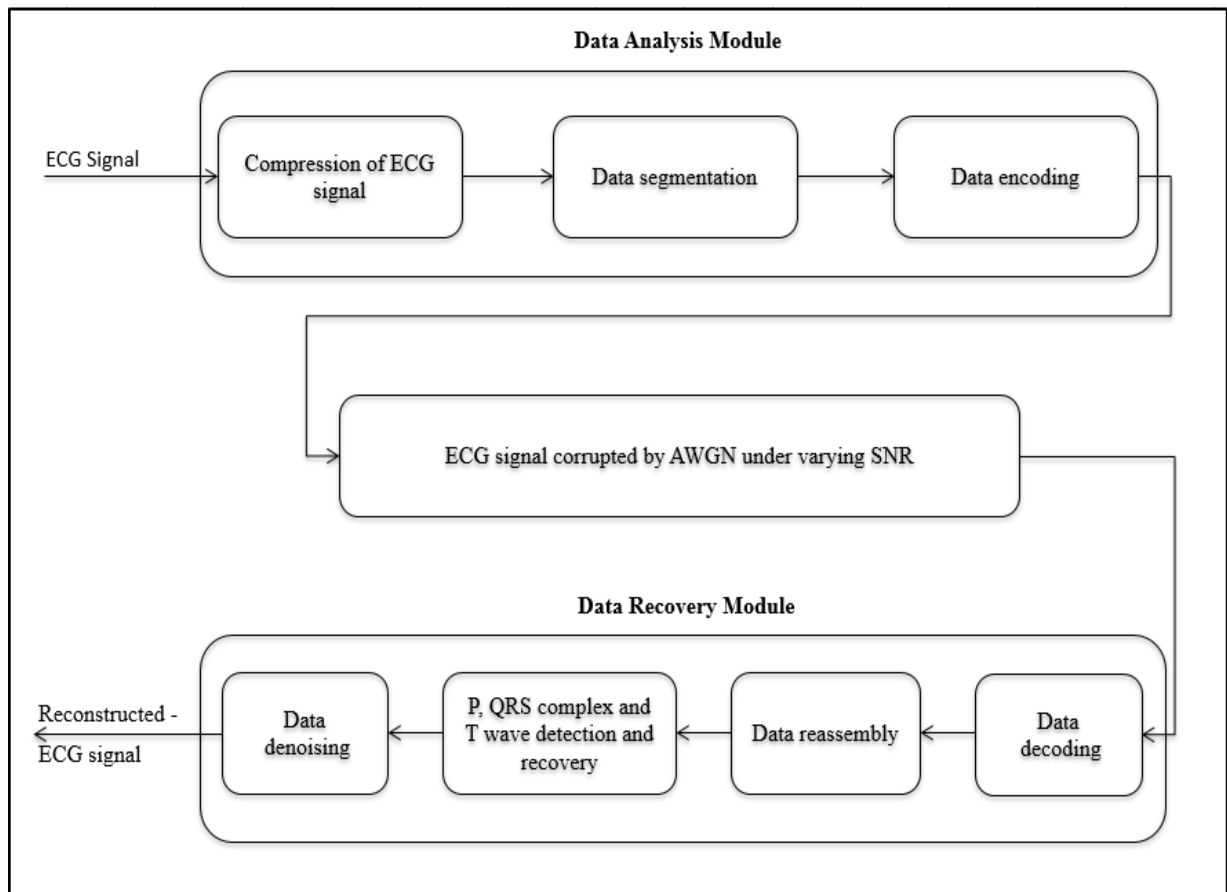
Figure 4.2. ECG signal processing using m-ECG algorithm

The design and implementation of m-ECG algorithm in context of data analysis module and data recovery module along with associated components are discussed in the following sections.

4.2   Data Analysis Module

The data analysis module performs signal pre-processing on input ECG signal using discrete

wavelet transform, data segmentation and data encoding. The ECG signal [99] is used as input

and all components of data analysis module are implemented in MATLAB [100]. The key

characteristic features of input ECG signal are as follows:

1. Length of signal: 1024 samples (*simulation results are shown using 300 samples*)

2. Frequency range: 0.01Hz – 300Hz

3. Amplitude range: 0.05mV – 4.0mV

The detail of each block is discuss in the following sections.

4.2.1   Compression of ECG signal

The time localized feature extraction of non-stationary ECG signal is accomplished using

wavelet function, Daubechies at level 4 – db4. The choice of wavelet at this decomposition level

not only reduces the amount of data required to adequately represent the original signal but also

provides better approximation by capturing the transients of the original signal. The multilevel

wavelet decomposition of input signal yields approximate coefficient cA4 and detailed cD1-cD4

coefficients.

The selection of significant DWT coefficients involves the application of *soft* fixed-form

threshold that realizes minimum of the maximum mean square error performance multiplied by a

small factor proportional to logarithmic length of input signal.

$$Thr = \sqrt{2.\log(\text{length of signal})} \qquad\qquad [4.1]$$

47

The resulting *level 1 compressed* signal as shown in Fig. 4.3 contains fewer detailed coefficients that accurately approximate the original signal. This compressed signal retains 80% - 85% energy of the original ECG signal by preserving key characteristic features and removing redundant samples.
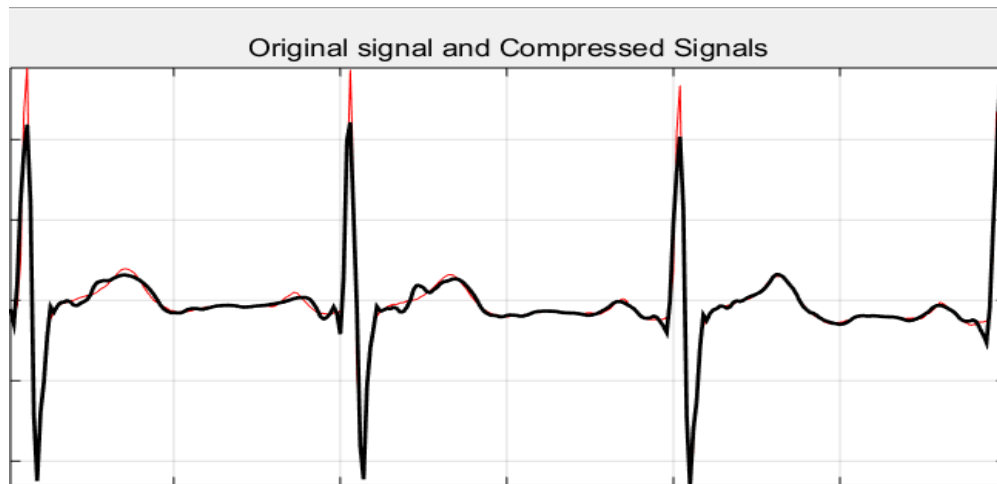
Figure 4.3. Level 1 compression using DWT – Original (RED), Compressed (BLACK)

4.2.2   Data Segmentation

The compressed ECG samples are represented using *n-uint16* where each sample is stored as *uint8* sign and *uint8* data. If the data is accurately stored using uint8 then its associated uint8 sign contains all zeros otherwise it holds sign or overflow bits.

The data segmentation process structures the compressed data in separate sign and data bits in order to achieve higher compression by using Huffman encoding where sign symbols stream and data symbols stream are encoded separately.

The data segmentation process is shown in Fig. 4.4 where each sample of compressed ECG signal is represented using sign and data bits.
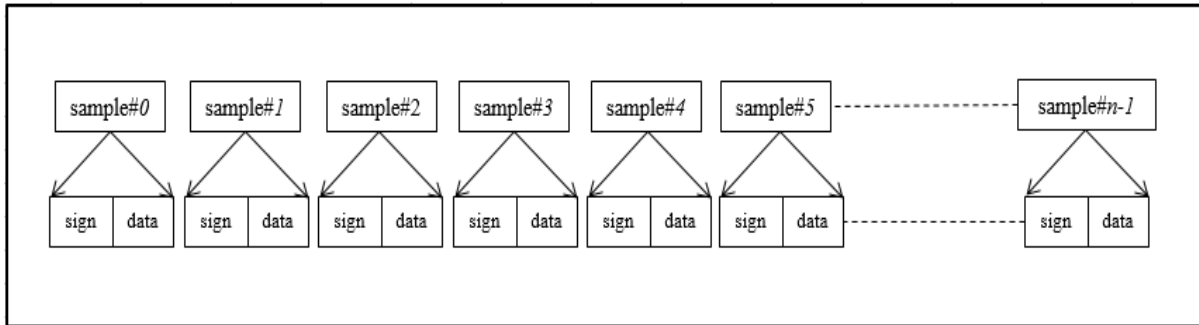
Figure 4.4. Data segmentation of compressed ECG signal

4.2.3   Data Encoding

The lossless compression at *level 2* involve Huffman coding of the previously compressed ECG signal. The compressed ECG signal with data and sign symbols are encoded separately to achieve maximum data reduction while preserving key characteristic features.

The length of code depends upon the statistical frequency of each symbol in the ECG signal. The sign (*ss#*) and data symbols (*ds#*) are grouped separately as shown in Fig. 4.5. The associated probabilities of sign and data symbols are used to create Huffman code dictionary (Table 4.1) that contains information of distinct signal values with associated code-words. The average length among all code-words in the dictionary is weighted according to the symbol probability and number of bits in the code vector. The effectiveness of compression is then measured in terms of compression ratio:

$$CR = \frac{size\ of\ input\ data\ stream}{size\ of\ compressed\ output\ stream} \qquad [4.2]$$
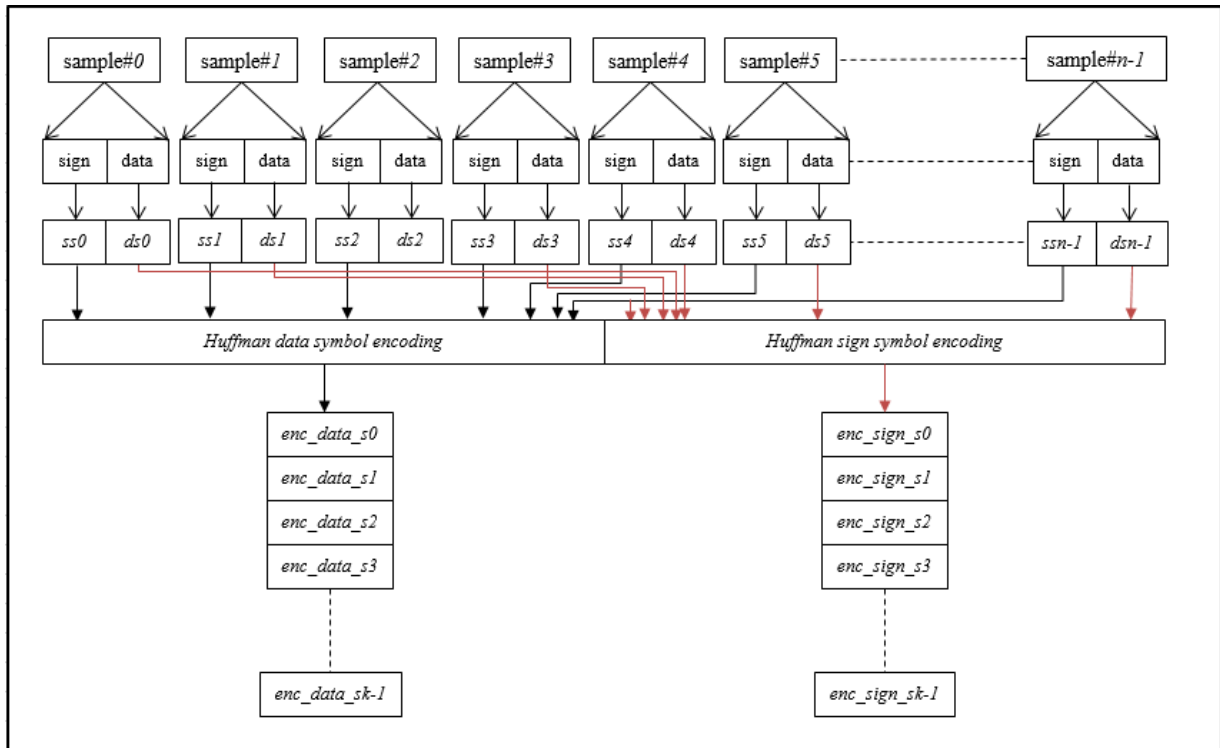
Figure 4.5. Sign and data symbols encoding

The application of Huffman coding to ECG signal results in compressed signal with total length of code equals to 4.789 bits compared to 4.735 bits which is the entropy of the signal obtained using equation (2.23). The structure of the input data, the design of the compression scheme and its implementation are the key factors in determining the compression ratio and deciding whether the data compression is beneficial (reducing the amount of data to be sent over the network) or deteriorates the performance of the communication network by increased delay associated with data compression and decompression.

This completes the pre-processing of the ECG signal by using data analysis module. The impact of AWGN on encoded sign and data symbol stream will be discussed in the next section.

Table 4.1. Encoded ECG signal using Huffman coding

Symbols	Probability	Code Vector	Length of each code
0	0.133	[0,1,1]	0.399
1	0.013	[1,0,0,1,1,1]	0.078
2	0.008	[0,1,0,1,0,0,0]	0.056
3	0.003	[1,1,0,0,0,0,0,1]	0.024
4	0.005	[0,1,0,0,1,0,0,0]	0.04
7	0.002	[0,1,0,0,1,0,0,1,1]	0.018
8	0.002	[0,1,0,0,1,0,0,1,0]	0.018
9	0.007	[1,0,0,0,1,1,1]	0.049
10	0.002	[0,1,0,0,1,1,1,0,1]	0.018
12	0.005	[1,1,1,0,1,1,1]	0.035
13	0.005	[1,1,1,0,1,1,0]	0.035
16	0.003	[1,1,0,0,0,0,0,0]	0.024
18	0.003	[1,1,0,0,0,0,1,1]	0.024
20	0.003	[1,1,0,0,0,0,1,0]	0.024
21	0.002	[0,1,0,0,1,1,1,0,0]	0.018
22	0.002	[0,1,0,0,1,1,1,1,1]	0.018
24	0.003	[1,1,0,0,1,1,0,1]	0.024
26	0.003	[1,1,0,0,1,1,0,0]	0.024
27	0.002	[0,1,0,0,1,1,1,1,0]	0.018
28	0.003	[1,1,0,0,1,1,1,1]	0.024
30	0.002	[0,1,0,0,1,1,0,0,1]	0.018
32	0.003	[1,1,0,0,1,1,1,0]	0.024
33	0.002	[0,1,0,0,1,1,0,0,0]	0.018
36	0.002	[0,1,0,0,1,1,0,1,1]	0.018
37	0.002	[0,1,0,0,1,1,0,1,0]	0.018
38	0.002	[1,0,0,0,0,0,1,0,1]	0.018
40	0.002	[1,0,0,0,0,0,1,0,0]	0.018
41	0.003	[1,1,0,0,1,0,0,1]	0.024
42	0.002	[1,0,0,0,0,0,1,1,1]	0.018
47	0.003	[1,1,0,0,1,0,0,0]	0.024
48	0.002	[1,0,0,0,0,0,1,1,0]	0.018
49	0.002	[1,0,0,0,0,0,0,0,1]	0.018
51	0.002	[1,0,0,0,0,0,0,0,0]	0.018
52	0.002	[1,0,0,0,0,0,0,1,1]	0.018

Symbols	Probability	Code Vector	Length of each code
56	0.008	[0,1,0,1,0,1,1]	0.056
59	0.005	[1,1,1,0,0,0,1]	0.035
61	0.002	[1,0,0,0,0,0,1,0]	0.018
62	0.003	[1,1,0,0,1,0,1,1]	0.024
64	0.002	[1,0,0,0,0,1,1,0,1]	0.018
66	0.005	[1,1,1,0,0,0,0]	0.035
68	0.002	[1,0,0,0,0,1,1,0,0]	0.018
69	0.002	[1,0,0,0,0,1,1,1,1]	0.018
72	0.002	[1,0,0,0,0,1,1,1,0]	0.018
74	0.003	[1,1,0,0,1,0,1,0]	0.024
78	0.003	[1,0,1,1,0,1,0,1]	0.024
80	0.002	[1,0,0,0,0,1,0,0,1]	0.018
92	0.002	[1,0,0,0,0,1,0,0,0]	0.018
97	0.003	[1,0,1,1,0,1,0,0]	0.024
125	0.002	[1,0,0,0,0,1,0,1,1]	0.018
128	0.002	[1,0,0,0,0,1,0,1,0]	0.018
130	0.002	[0,1,0,1,1,0,1,0,1]	0.018
144	0.002	[0,1,0,1,1,0,1,0,0]	0.018
146	0.002	[0,1,0,1,1,0,1,1,1]	0.018
155	0.002	[0,1,0,1,1,0,1,1,0]	0.018
160	0.003	[1,0,1,1,0,1,1,1]	0.024
169	0.002	[0,1,0,1,1,0,0,0,1]	0.018
175	0.002	[0,1,0,1,1,0,0,0,0]	0.018
188	0.002	[0,1,0,1,1,0,0,1,1]	0.018
190	0.003	[1,0,1,1,0,1,1,0]	0.024
194	0.002	[0,1,0,1,1,0,0,1,0]	0.018
195	0.002	[0,1,0,1,1,1,1,0,1]	0.018
197	0.003	[1,0,1,1,0,0,0,1]	0.024
199	0.002	[0,1,0,1,1,1,1,0,0]	0.018
200	0.005	[1,1,1,0,0,1,1]	0.035
201	0.002	[0,1,0,1,1,1,1,1,1]	0.018
202	0.007	[1,0,0,0,1,1,0]	0.049
203	0.002	[0,1,0,1,1,1,1,1,0]	0.018
204	0.002	[0,1,0,1,1,1,0,0,1]	0.018
206	0.002	[0,1,0,1,1,1,0,0,0]	0.018
207	0.002	[0,1,0,1,1,1,0,1,1]	0.018

Symbols	Probability	Code Vector	Length of each code
208	0.012	[1,1,0,1,0,1]	0.072
209	0.002	[0,1,0,1,1,1,0,1,0]	0.018
210	0.01	[1,1,1,0,1,0]	0.06
211	0.005	[1,1,1,0,0,1,0]	0.035
212	0.006	[1,1,0,0,0,1,1]	0.042
213	0.006	[1,1,0,0,0,1,0]	0.042
214	0.008	[0,1,0,1,0,1,0]	0.056
215	0.003	[1,0,1,1,0,0,0,0]	0.024
216	0.013	[1,0,0,1,1,0]	0.078
217	0.007	[1,0,0,1,0,0,1]	0.049
218	0.005	[1,1,1,1,1,0,1]	0.035
219	0.003	[1,0,1,1,0,0,1,1]	0.024
220	0.002	[0,1,0,1,0,0,1,0,1]	0.018
221	0.006	[1,0,1,0,1,0,1]	0.042
222	0.013	[1,0,0,1,0,1]	0.078
223	0.002	[0,1,0,1,0,0,1,0,0]	0.018
224	0.018	[0,1,0,0,0,1]	0.108
225	0.007	[1,0,0,1,0,0,0]	0.049
226	0.012	[1,1,0,1,0,0]	0.072
227	0.008	[1,0,0,0,1,0,1]	0.056
228	0.006	[1,0,1,0,1,0,0]	0.042
229	0.01	[0,1,0,0,0,0,1]	0.07
230	0.01	[0,1,0,0,0,0,0]	0.07
232	0.006	[1,0,1,0,1,1,1]	0.042
233	0.003	[1,0,1,1,0,0,1,0]	0.024
234	0.008	[1,0,0,0,1,0,0]	0.056
235	0.003	[1,0,1,1,1,1,0,1]	0.024
236	0.003	[1,0,1,1,1,1,0,0]	0.024
237	0.002	[0,1,0,1,0,0,1,1,1]	0.018
238	0.003	[1,0,1,1,1,1,1,1]	0.024
239	0.003	[1,0,1,1,1,1,1,0]	0.024
240	0.025	[1,0,1,0,0]	0.125
241	0.005	[1,1,1,1,1,0,0]	0.035
242	0.02	[1,1,1,1,0]	0.1
243	0.003	[1,0,1,1,1,0,0,1]	0.024
244	0.005	[1,1,1,1,1,1,1]	0.035

.

Symbols	Probability	Code Vector	Length of each code
245	0.003	[1,0,1,1,1,0,0,0]	0.024
246	0.006	[1,0,1,0,1,1,0]	0.042
248	0.003	[1,0,1,1,1,0,1,1]	0.024
249	0.003	[1,0,1,1,1,0,1,0]	0.024
250	0.008	[0,1,0,0,1,0,1]	0.056
251	0.005	[1,1,1,1,1,1,0]	0.035
253	0.002	[0,1,0,1,0,0,1,1,0]	0.018
254	0.023	[1,1,0,1,1]	0.115
255	0.345	[0,0]	0.69

4.3   Analyzing ECG signal impairment due to AWGN

The studied model of noisy ECG signal as discussed in section 2.3 is the superposition of the signal *f(i)* and a zero mean Gaussian white noise with variance of σ^2: $\eta\ (0, \sigma^2)$:

$$s(i) = f(i) + e(i) \qquad\qquad [4.3]$$

where *s(i)* is the signal to be de-noised, *f(i)* is the noise free signal and *e(i)* is the noise. The noise *e(i)* is additive, statistically independent and impacts every single frequency component over the whole length of received ECG signal.

The problem implementation uses additive white Gaussian noise (AWGN) with varying signal-to-noise ratio and measures the distortion of reconstructed ECG signal. The AWGN does not account for fading, interference, dispersion or frequency selectivity. It is a simple model that is useful in understanding system behavior and channel background noise before other impairments are considered.

The study of radio propagation model to predict path loss or effective coverage area of the transmitter is beyond the scope of research.

The received ECG signal that is corrupted by AWGN at SNR of 20dB, 15dB, 10dB and 3dB is shown in Fig. 4.6 – Fig. 4.9 respectively. The interference with noise results in severe distortion and attenuation of P-wave, QRS-complex and T-wave which are the characteristic features of ECG signal. As the noise level continues to increase, the detection and recovery of these features under poor SNR becomes extremely challenging.

The m-ECG algorithm addresses the problem related to reliable and clinically acceptable ECG signal recovery even under poor SNR conditions. The recovered ECG signal in general and the reconstructed QRS complex in particular shows high fidelity and exceptional reproducibility when compared to the studies undertaken by Chourakri *et al*. [5] and Rabiul *et al*. [101].

The decoding of received signal, reassembly, detection and recovery of key characteristic features using m-ECG algorithm is discussed under data recovery module.
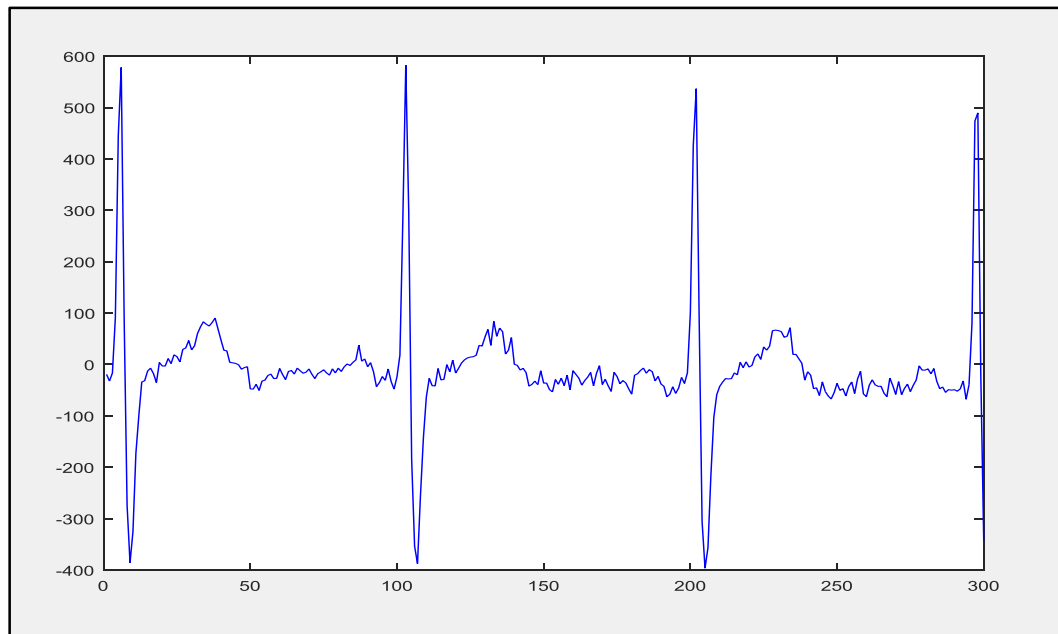
Figure 4.6. ECG signal corrupted by AWGN at 20dB SNR
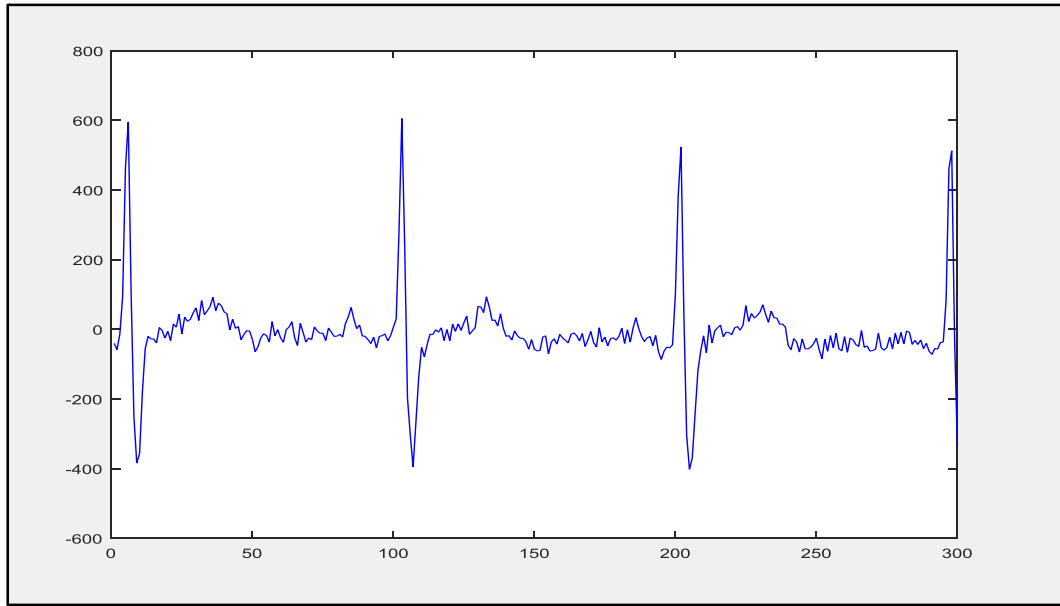
Figure 4.7. ECG signal corrupted by AWGN at 15dB SNR
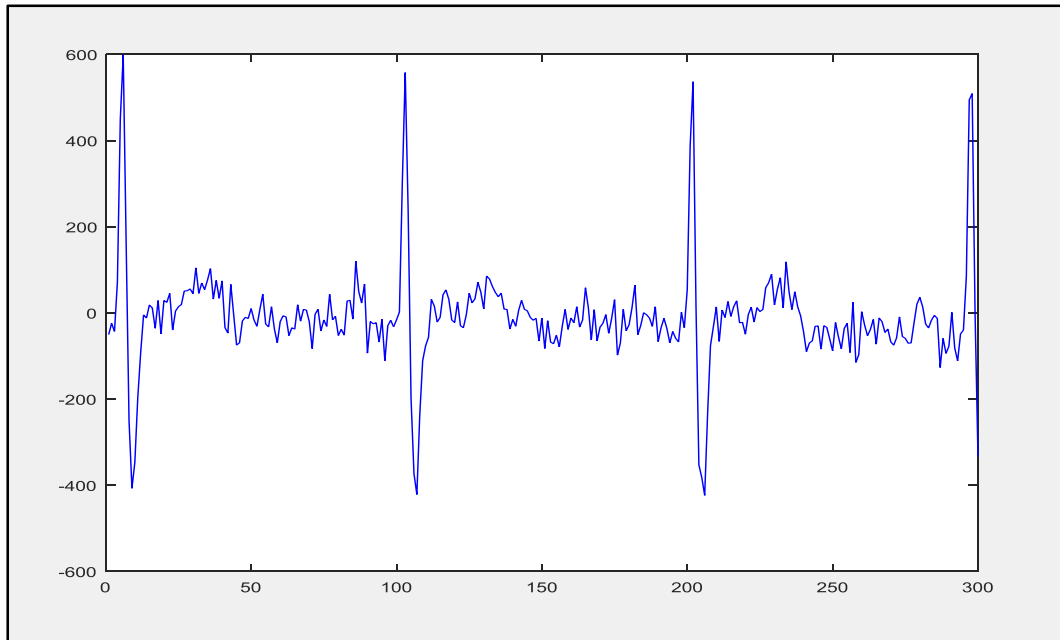
Figure 4.8. ECG signal corrupted by AWGN at 10dB SNR
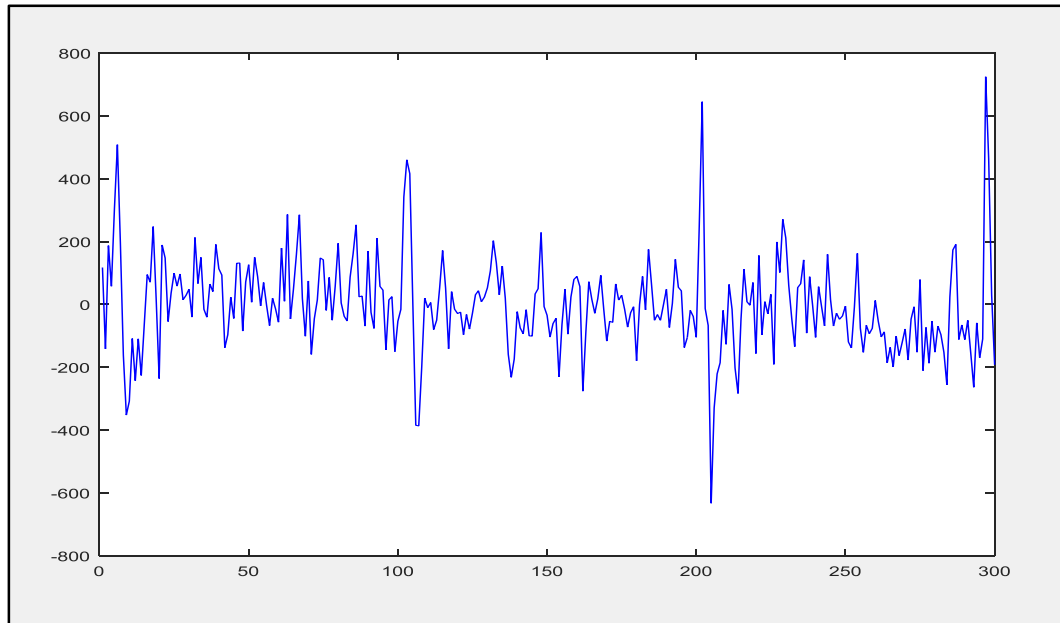
Figure 4.9. ECG signal corrupted by AWGN at 3dB SNR

4.4   Data Recovery Module

The decoding, recovery and reconstruction of received ECG signal that is corrupted by WGN is the key deliverable of data recovery module. The recovery of ECG signal involves the decoding of received symbols. The resulting sign and data symbols are then combined to create reassembled ECG signal which is then used for the detection of P wave, QRS complex and T wave. The detection process also uses empirical threshold to isolate noise samples. The recovered QRS complex is then combined with the denoised samples of P-wave and T-wave using linear interpolation and yield reconstructed ECG signal.

The distortion of recovered ECG signal using m-ECG algorithm is measured in terms of percent root mean square difference (PRMSD), compression ratio (CR) and signal-to-noise ratio (SNR) as shown in Table 4.4.

57

4.4.1 Data Decoding

The received sign (*rec_enc_sign_s#*) and data (*rec_enc_data_s#*) symbols are decoded using Huffman decoding. The decoder use symbol probabilities to decompress the data as sign (*ss#*) and data (*ds#*) as shown in Fig. 4.10. These sign and data symbols are then reassembled during data reassembly process.
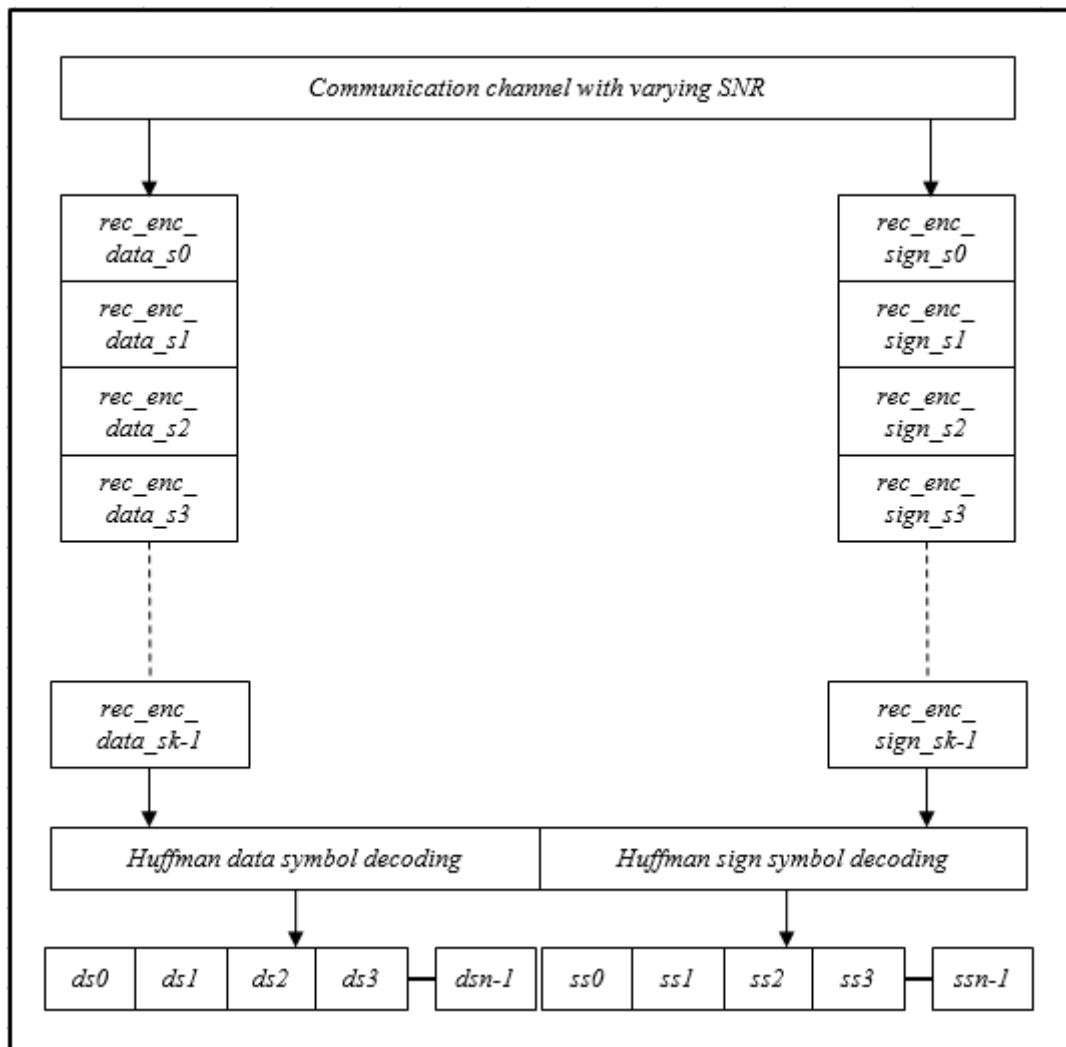
Figure 4.10. Sign and data symbols decoding

4.4.2 Data Reassembly

The data reassembly process combines decoded sign (*ss#*) symbol with its associated data symbol (*ds#*) and yield an ECG sample as shown in Fig. 4.11. This process is repeated for all decoded sign and data symbols and the resulting ECG samples are sequentially combine to create reassembled ECG signal as shown in Fig. 4.12. This reassembled ECG signal is used for the detection and recovery of P wave, QRS complex and T wave.
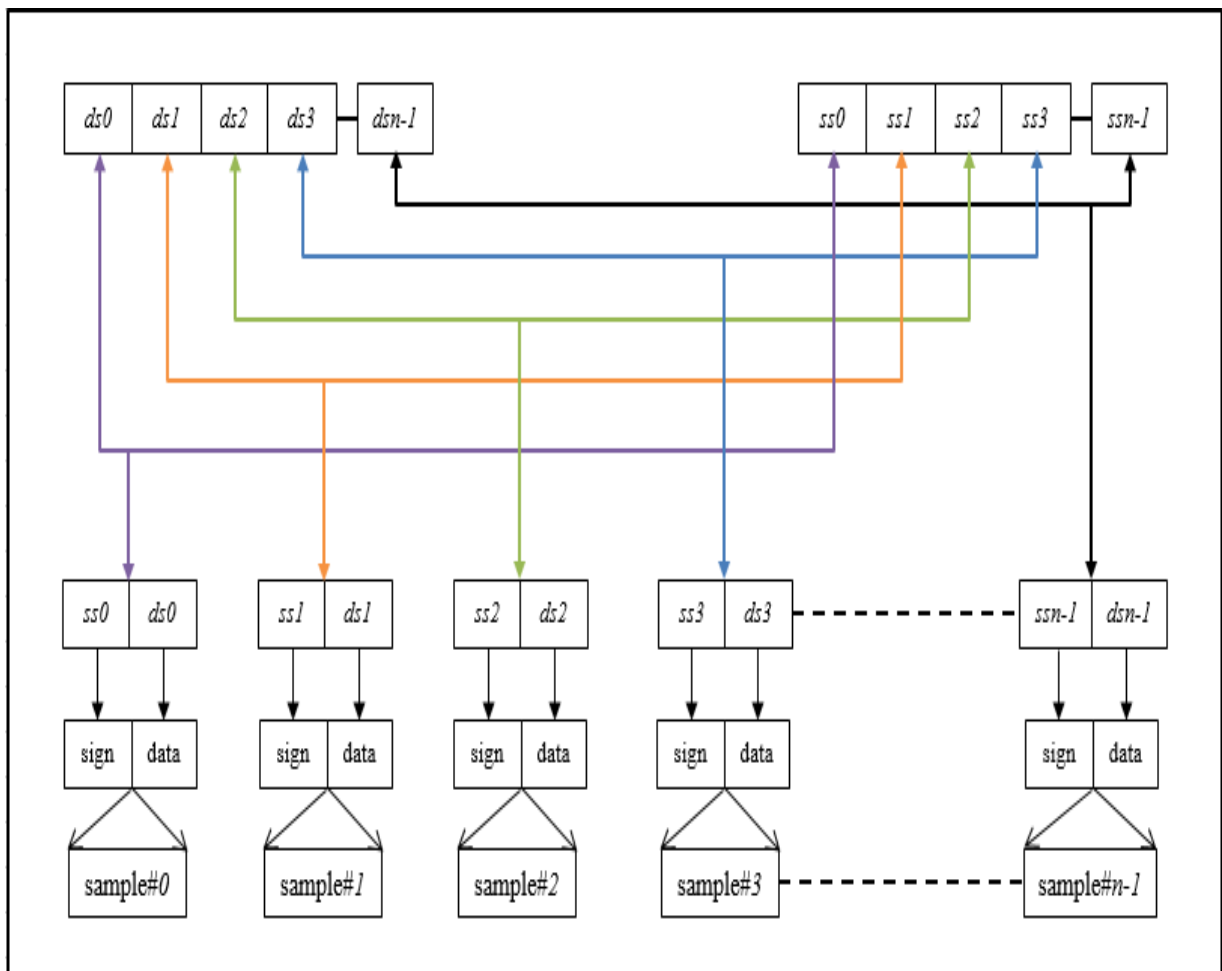
Figure 4.11. Data reassembly process
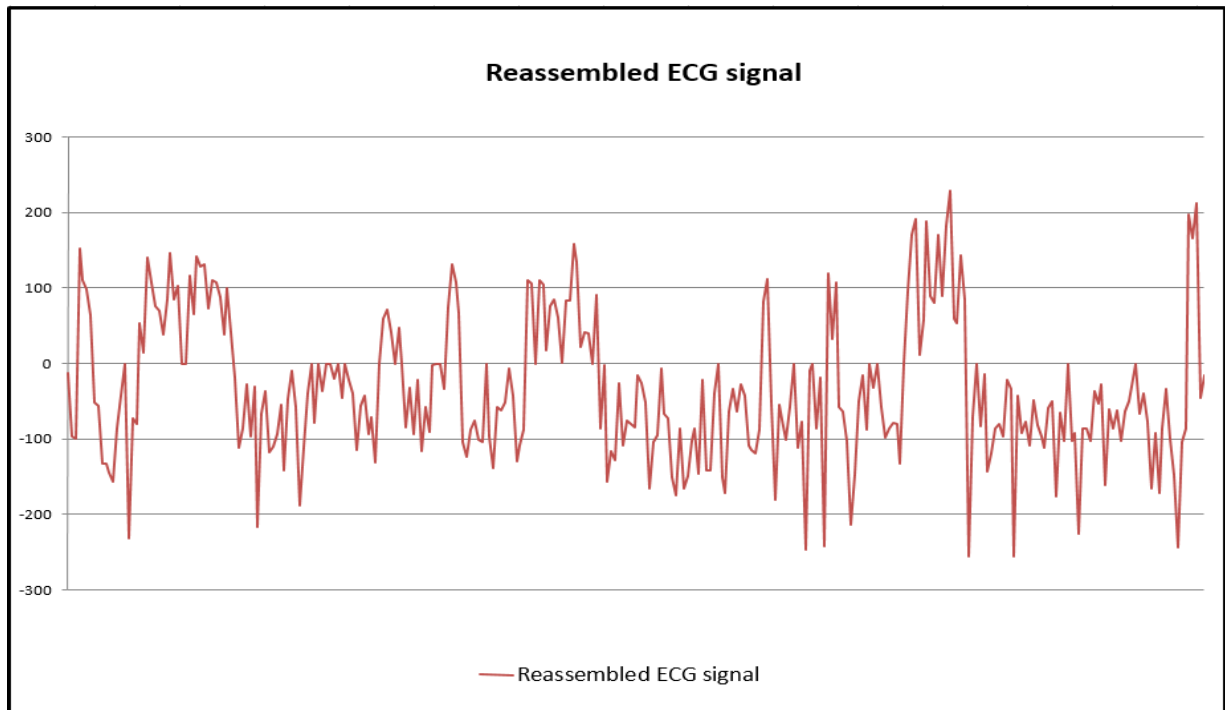
Figure 4.12. Reassembled ECG signal at 3dB SNR

Table 4.2 shows first 300 sign and data symbols that were used to create the reassembled ECG signal at SNR of 3dB.

Table 4.2. Reassembled sign and data symbols

Symbol #	Sign symbols: ss#	Data symbol: ds#
0	255	243
1	255	159
2	255	157
3	0	152
4	0	110
5	0	98
6	0	64
7	255	205
8	255	200
9	255	124
10	255	123

Symbol #	Sign symbols: ss#	Data symbol: ds#
11	255	111
12	255	100
13	255	170
14	255	213
15	255	255
16	255	24
17	255	183
18	255	176
19	0	53
20	0	14
21	0	141
22	0	108
23	0	76
24	0	70
25	0	38
26	0	85
27	0	146
28	0	85
29	0	103
30	0	0
31	0	0
32	0	116
33	0	65
34	0	142
35	0	128
36	0	131
37	0	73
38	0	110
39	0	107
40	0	88
41	0	39
42	0	100
43	0	41
44	255	238
45	255	144
46	255	170
47	255	229
48	255	159

Symbol #	Sign symbols: ss#	Data symbol: ds#
49	255	226
50	255	40
51	255	189
52	255	219
53	255	138
54	255	146
55	255	162
56	255	201
57	255	114
58	255	209
59	255	247
60	255	199
61	255	68
62	255	145
63	255	216
64	255	255
65	255	177
66	255	255
67	255	219
68	255	255
69	255	255
70	255	236
71	255	255
72	255	211
73	255	255
74	255	234
75	255	216
76	255	141
77	255	200
78	255	214
79	255	162
80	255	185
81	255	125
82	0	0
83	0	59
84	0	72
85	0	41
86	0	0

Symbol #	Sign symbols: ss#	Data symbol: ds#
87	0	47
88	0	0
89	255	172
90	255	224
91	255	163
92	255	235
93	255	140
94	255	199
95	255	165
96	255	254
97	255	255
98	255	255
99	255	223
100	0	74
101	0	131
102	0	107
103	0	67
104	255	152
105	255	133
106	255	169
107	255	180
108	255	155
109	255	152
110	255	255
111	255	160
112	255	117
113	255	198
114	255	194
115	255	204
116	255	250
117	255	213
118	255	127
119	255	147
120	255	169
121	0	111
122	0	106
123	0	0
124	0	111

Symbol #	Sign symbols: ss#	Data symbols: ds#
125	0	105
126	0	17
127	0	76
128	0	85
129	0	61
130	0	1
131	0	83
132	0	83
133	0	158
134	0	134
135	0	22
136	0	42
137	0	40
138	0	0
139	0	91
140	255	170
141	255	254
142	255	99
143	255	140
144	255	128
145	255	230
146	255	147
147	255	181
148	255	176
149	255	171
150	255	240
151	255	230
152	255	204
153	255	91
154	255	152
155	255	161
156	255	249
157	255	189
158	255	183
159	255	106
160	255	81
161	255	170
162	255	91

Symbol #	Sign symbols: ss#	Data symbols: ds#
163	255	107
164	255	154
165	255	170
166	255	110
167	255	234
168	255	114
169	255	114
170	255	217
171	255	255
172	255	106
173	255	85
174	255	193
175	255	223
176	255	192
177	255	229
178	255	213
179	255	147
180	255	142
181	255	137
182	255	169
183	0	82
184	0	112
185	255	205
186	255	75
187	255	201
188	255	182
189	255	155
190	255	198
191	255	255
192	255	145
193	255	179
194	255	9
195	255	247
196	255	255
197	255	170
198	255	238
199	255	14
200	0	119

Symbol #	Sign symbols: ss#	Data symbols: ds#
201	0	33
202	0	107
203	255	198
204	255	192
205	255	154
206	255	43
207	255	109
208	255	206
209	255	240
210	255	169
211	255	255
212	255	224
213	255	255
214	255	198
215	255	158
216	255	170
217	255	178
218	255	176
219	255	124
220	255	255
221	0	96
222	0	170
223	0	191
224	0	11
225	0	58
226	0	188
227	0	90
228	0	81
229	0	170
230	0	89
231	0	182
232	0	229
233	0	59
234	0	54
235	0	144
236	0	85
237	255	0
238	255	185

Symbol #	Sign symbols: ss#	Data symbols: ds#
239	255	255
240	255	173
241	255	242
242	255	113
243	255	137
244	255	170
245	255	176
246	255	159
247	255	234
248	255	222
249	255	0
250	255	214
251	255	164
252	255	179
253	255	147
254	255	207
255	255	175
256	255	160
257	255	145
258	255	197
259	255	206
260	255	80
261	255	191
262	255	153
263	255	255
264	255	153
265	255	164
266	255	31
267	255	170
268	255	170
269	255	154
270	255	220
271	255	203
272	255	229
273	255	95
274	255	195
275	255	170
276	255	194

Symbol #	Sign symbols: ss#	Data symbols: ds#
277	255	153
278	255	192
279	255	206
280	255	225
281	255	255
282	255	190
283	255	217
284	255	179
285	255	90
286	255	164
287	255	85
288	255	170
289	255	222
290	255	156
291	255	109
292	255	13
293	255	152
294	255	170
295	0	198
296	0	166
297	0	213
298	255	211
299	255	240

4.4.3   Detection of P-wave, QRS complex and T-wave

The process of ECG signal recovery starts with the detection of P-wave, QRS complex and T-wave. This section describes the procedure undertaken by m-ECG algorithm to detect key features of ECG waveform that is corrupted by WGN when SNR is < 5dB. The detection of these features under poor SNR conditions were found to be extremely challenging but were readily identified by the proposed detection scheme. The steps involved in the detection process are described as follows:

Step 1: The noise samples are isolated by doing *peak* search for max *x(n)* samples along the complete length of reassembled ECG signal. The collocated peak samples with minimum variance are grouped together inside a *window*. The width of each window depends on the number of its peak and adjacent samples. The length of each window is then compared to the duration of normal PR interval (*from the onset of P-wave to the beginning of QRS complex*), QRS complex and ST interval (*from the onset of ST segment till the end of T-wave*) as described in section 2.1. This step is shown in Fig. 4.13.
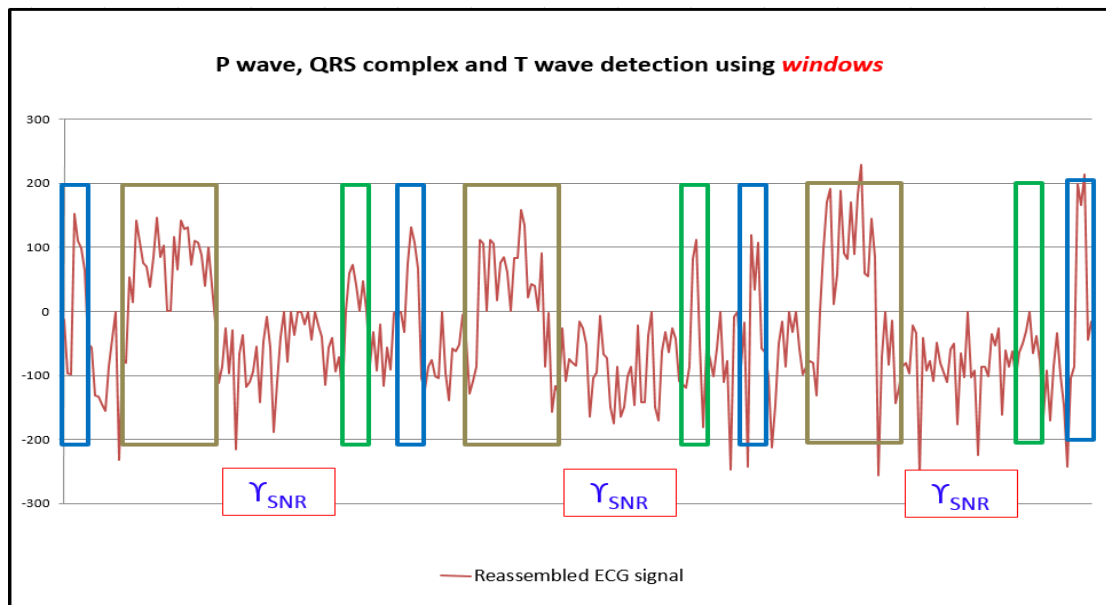
Figure 4.13. ECG features detection using windows

Step 2: Select the window(s) with maximum width and calculate the variance and expected value of its samples using equation (4.4) and (4.5) respectively. If the expected value of samples inside the window is higher than the expected value of noise samples (Υ_{SNR}), then the selected window may contain T-wave inside the ST interval.

$$E(X) = \frac{1}{N}\sum_{i=1}^{N} x_i \tag{4.4}$$

$$VAR(X) = \frac{1}{N}\sum_{i=1}^{N}(x_i - E(X))^2 \tag{4.5}$$

Fig. 4.14 shows window '1' with possible T wave.
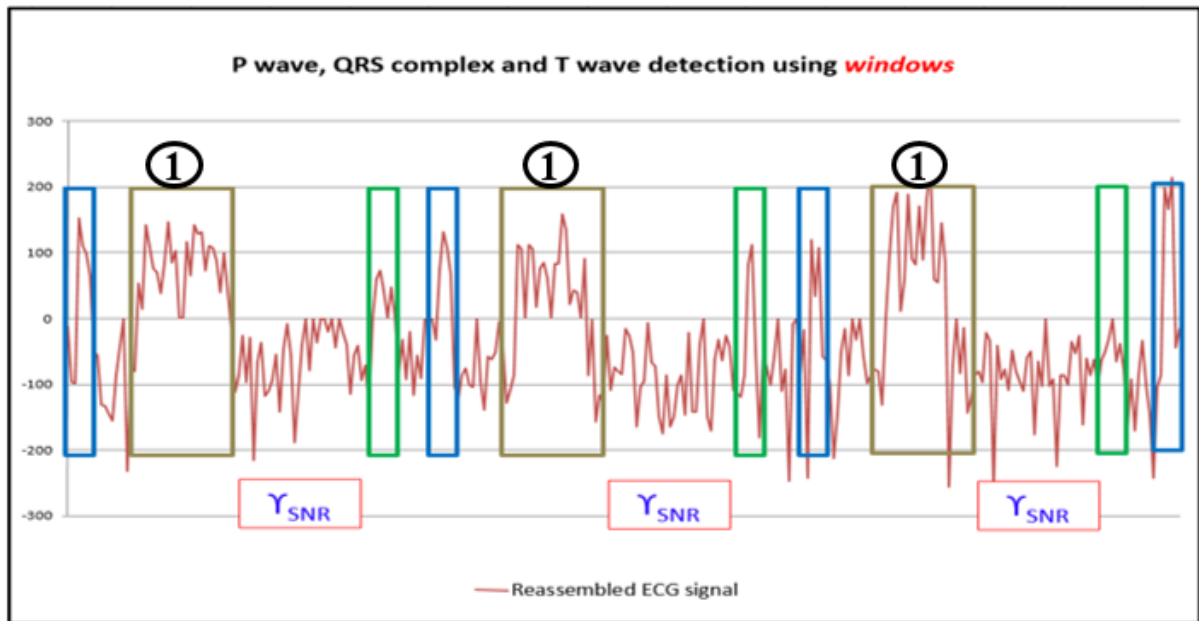
Figure 4.14. Window '1' with possible T-wave

Step 3: The search for P-wave and QRS complex is done on samples inside the adjacent window on both sides of window '1'. The variance and expected value of samples are then calculated. If the expected value of samples inside the window is higher than the expected value of noise samples (Υ_{SNR}), then window '3' and window '2' may contains P-wave and QRS complex respectively. Fig. 4.15 shows window '3' and window '2' with possible P-wave and QRS complex.
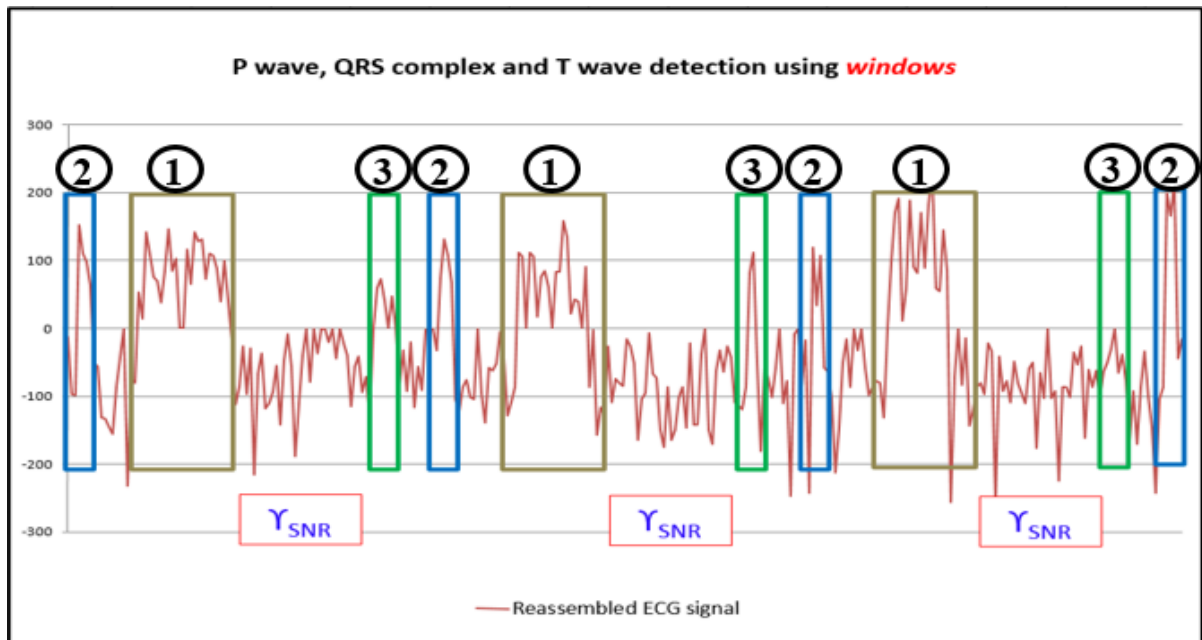
Figure 4.15. Window '2' and window '3' with possible P-wave and QRS complex

Step 4: If the initial search failed to recover P-wave, QRS complex and T-wave during the data recovery process then the length of each window is either increased or decreased until all key characteristic features of ECG signal are recovered. Fig. 4.16 summarizes these steps in a flow chart.

Υ_{SNR} represents expected value of noise samples between P and T wave that do not contain important clinical information. The average value of these samples change with the SNR of received signal which is used as threshold to discard very low amplitude samples inside the window without any major loss of information for the recovery of P-wave, QRS complex and T-wave. The value of Υ_{SNR} is selected from a lookup table, a higher threshold drops more samples from the window which will impact the recovery of characteristic features. Selecting a lower threshold add insignificant samples to the window which in turn add more noise.

This completes ECG feature detection. The recovery of P-wave, QRS complex and T-wave will be discussed in next sections.
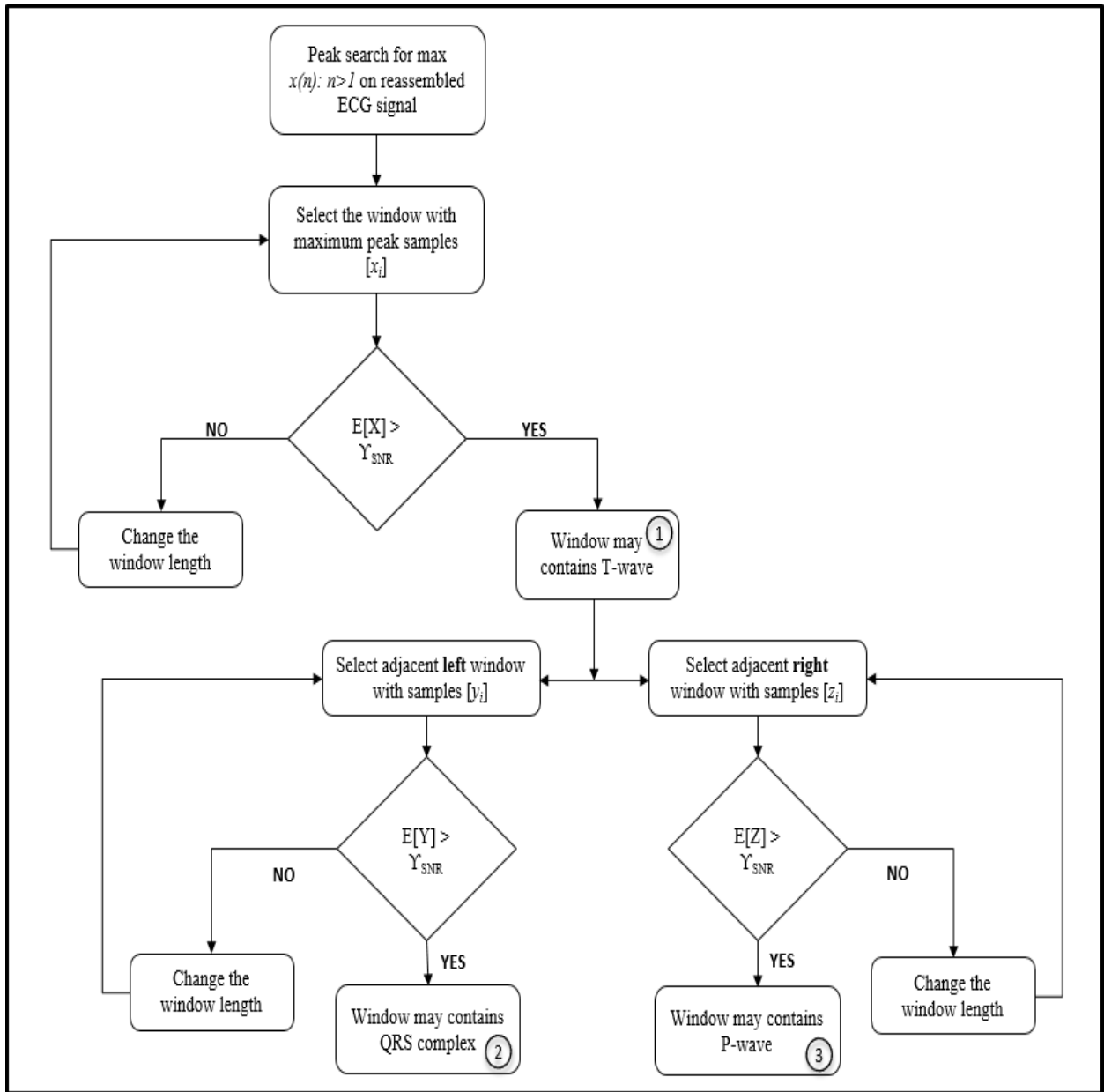
Figure 4.16. Flow chart: ECG feature detection process

4.4.4   Recovery of QRS complex

The sign symbols inside window '2'are used to recover and reconstruct the QRS complex with minimum distortion. As shown in Table 4.2, reassembled sign symbols represent sign and overflow bits of each data sample. If data symbol is accurately represented using *uint8*, it has null (*zeros*) in the corresponding sign symbol, otherwise it holds the overflow data bits or the sign extension (*255*) of corresponding data symbol.

When the ECG signal is corrupted by WGN at low SNR (<3dB being worst case analysis), simulation result shows that contents of received sign symbol stream recovers with less uncertainty compared to data using parametric estimation where each sign symbol is rounded to either *zero* or *255*.

When SNR is high, the data recovery module combines the data symbol to its corresponding sign symbol and constructs the reassembled ECG signal. If the reassembled signal is of good quality to detect P-wave, QRS complex and T-wave then reconstructed ECG signal shows very low distortion.

When SNR is extremely low (<3dB) it may result in erroneous detection of P-wave, QRS complex and T-wave in the reassembled signal. Under this condition, redundant sign symbols are used to recover sign or overflow bits of associated data symbol using parametric estimation.

Once the window with possible QRS complex is detected, it is recovered by using sign symbols. Fig. 4.17 shows QRS complex recovery algorithm where A_R and A_S represents the amplitude of R wave and S wave of recovered QRS complex. A_{Rnom} and A_{Snom} represents amplitude of R wave and S wave of normal QRS complex. The QRS complex is recovered here with less noise and signal distortion compared to Chourakri *et al*. [5] and Rabiul *et al*. [101].
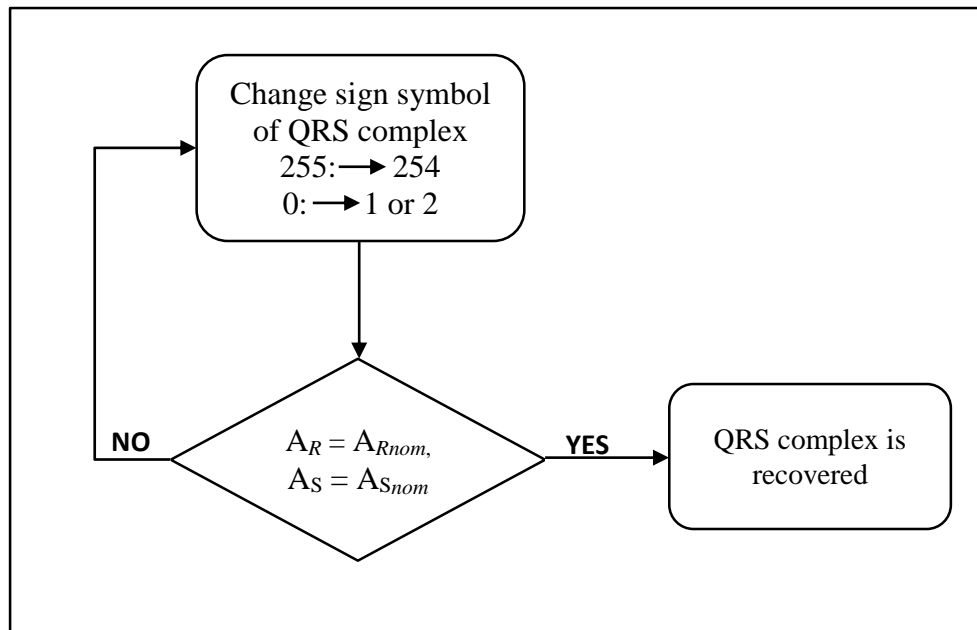
Figure 4.17. Recovery of QRS complex using sign vector

The steps involve in the QRS complex recovery process are described as follows:

Step 1: The sign symbols are scaled high or low to recover the QRS complex. The positive cycle, R wave of QRS complex is increased from 0 to either 1 or 2. The negative cycle, S wave of QRS complex is decreased from 255 to 254.

Step 2: Compare amplitude, $\mathbf{A_R}$ and $\mathbf{A_S}$ to the amplitude of R and S wave of normal QRS complex. The new sign symbol that yield amplitude closer to the amplitude of R and S wave of normal QRS complex is selected and then combined with associated data symbol.

Step 3: Repeat above steps until QRS complex is recovered.

Table 4.3 shows first 300 samples of reassembled ECG signal (see section 4.4.2) with modified sign symbols (*in red*) for the recovery of QRS complex. This reassembled ECG signal was corrupted by WGN at SNR of 3dB.

74

Table 4.3. QRS complex recovery using sign symbols

Symbol #	Original Sign symbols: ss#	Scaled Sign symbols: ss#	Data symbols: ds#
0	255	255	243
1	255	255	159
2	255	255	157
3	0	0	152
4	0	1	110
5	0	2	98
6	0	0	64
7	255	254	205
8	255	254	200
9	255	254	124
10	255	255	123
11	255	255	111
12	255	255	100
13	255	255	170
14	255	255	213
15	255	255	255
16	255	255	24
17	255	255	183
18	255	255	176
19	0	0	53
20	0	0	14
21	0	0	141
22	0	0	108
23	0	0	76
24	0	0	70
25	0	0	38
26	0	0	85
27	0	0	146
28	0	0	85
29	0	0	103
30	0	0	0
31	0	0	0
32	0	0	116
33	0	0	65
34	0	0	142
35	0	0	128

Symbol #	Original Sign symbols: ss#	Scaled Sign symbols: ss#	Data symbols: ds#
36	0	0	131
37	0	0	73
38	0	0	110
39	0	0	107
40	0	0	88
41	0	0	39
42	0	0	100
43	0	0	41
44	255	255	238
45	255	255	144
46	255	255	170
47	255	255	229
48	255	255	159
49	255	255	226
50	255	255	40
51	255	255	189
52	255	255	219
53	255	255	138
54	255	255	146
55	255	255	162
56	255	255	201
57	255	255	114
58	255	255	209
59	255	255	247
60	255	255	199
61	255	255	68
62	255	255	145
63	255	255	216
64	255	255	255
65	255	255	177
66	255	255	255
67	255	255	219
68	255	255	255
69	255	255	255
70	255	255	236
71	255	255	255
72	255	255	211
73	255	255	255

Symbol #	Original Sign symbols: ss#	Scaled Sign symbols: ss#	Data symbols: ds#
74	255	255	234
75	255	255	216
76	255	255	141
77	255	255	200
78	255	255	214
79	255	255	162
80	255	255	185
81	255	255	125
82	0	0	0
83	0	0	59
84	0	0	72
85	0	0	41
86	0	0	0
87	0	0	47
88	0	0	0
89	255	255	172
90	255	255	224
91	255	255	163
92	255	255	235
93	255	255	140
94	255	255	199
95	255	255	165
96	255	255	254
97	255	255	255
98	255	255	255
99	255	255	223
100	0	0	74
101	0	1	131
102	0	2	107
103	0	0	67
104	255	255	152
105	255	254	133
106	255	254	169
107	255	254	180
108	255	255	155
109	255	255	152
110	255	255	255
111	255	255	160

Symbol #	Original Sign symbols: ss#	Scaled Sign symbols: ss#	Data symbols: ds#
112	255	255	117
113	255	255	198
114	255	255	194
115	255	255	204
116	255	255	250
117	255	255	213
118	255	255	127
119	255	255	147
120	255	255	169
121	0	0	111
122	0	0	106
123	0	0	0
124	0	0	111
125	0	0	105
126	0	0	17
127	0	0	76
128	0	0	85
129	0	0	61
130	0	0	1
131	0	0	83
132	0	0	83
133	0	0	158
134	0	0	134
135	0	0	22
136	0	0	42
137	0	0	40
138	0	0	0
139	0	0	91
140	255	255	170
141	255	255	254
142	255	255	99
143	255	255	140
144	255	255	128
145	255	255	230
146	255	255	147
147	255	255	181
148	255	255	176
149	255	255	171

Symbol #	Original Sign symbols: ss#	Scaled Sign symbols: ss#	Data symbols: ds#
150	255	255	240
151	255	255	230
152	255	255	204
153	255	255	91
154	255	255	152
155	255	255	161
156	255	255	249
157	255	255	189
158	255	255	183
159	255	255	106
160	255	255	81
161	255	255	170
162	255	255	91
163	255	255	107
164	255	255	154
165	255	255	170
166	255	255	110
167	255	255	234
168	255	255	114
169	255	255	114
170	255	255	217
171	255	255	255
172	255	255	106
173	255	255	85
174	255	255	193
175	255	255	223
176	255	255	192
177	255	255	229
178	255	255	213
179	255	255	147
180	255	255	142
181	255	255	137
182	255	255	169
183	0	0	82
184	0	0	112
185	255	255	205
186	255	255	75
187	255	255	201

Symbol #	Original Sign symbols: ss#	Scaled Sign symbols: ss#	Data symbols: ds#
188	255	255	182
189	255	255	155
190	255	255	198
191	255	255	255
192	255	255	145
193	255	255	179
194	255	255	9
195	255	255	247
196	255	255	255
197	255	255	170
198	255	255	238
199	255	255	14
200	0	1	119
201	0	2	33
202	0	0	107
203	255	254	198
204	255	254	192
205	255	254	154
206	255	255	43
207	255	255	109
208	255	255	206
209	255	255	240
210	255	255	169
211	255	255	255
212	255	255	224
213	255	255	255
214	255	255	198
215	255	255	158
216	255	255	170
217	255	255	178
218	255	255	176
219	255	255	124
220	255	255	255
221	0	0	96
222	0	0	170
223	0	0	191
224	0	0	11
225	0	0	58

Symbol #	Original Sign symbols: ss#	Scaled Sign symbols: ss#	Data symbols: ds#
226	0	0	188
227	0	0	90
228	0	0	81
229	0	0	170
230	0	0	89
231	0	0	182
232	0	0	229
233	0	0	59
234	0	0	54
235	0	0	144
236	0	0	85
237	255	255	0
238	255	255	185
239	255	255	255
240	255	255	173
241	255	255	242
242	255	255	113
243	255	255	137
244	255	255	170
245	255	255	176
246	255	255	159
247	255	255	234
248	255	255	222
249	255	255	0
250	255	255	214
251	255	255	164
252	255	255	179
253	255	255	147
254	255	255	207
255	255	255	175
256	255	255	160
257	255	255	145
258	255	255	197
259	255	255	206
260	255	255	80
261	255	255	191
262	255	255	153
263	255	255	255

Symbol #	Original Sign symbols: ss#	Scaled Sign symbols: ss#	Data symbols: ds#
264	255	255	153
265	255	255	164
266	255	255	31
267	255	255	170
268	255	255	170
269	255	255	154
270	255	255	220
271	255	255	203
272	255	255	229
273	255	255	95
274	255	255	195
275	255	255	170
276	255	255	194
277	255	255	153
278	255	255	192
279	255	255	206
280	255	255	225
281	255	255	255
282	255	255	190
283	255	255	217
284	255	255	179
285	255	255	90
286	255	255	164
287	255	255	85
288	255	255	170
289	255	255	222
290	255	255	156
291	255	255	109
292	255	255	13
293	255	255	152
294	255	255	170
295	0	0	198
296	0	1	166
297	0	1	213
298	255	255	211
299	255	254	240

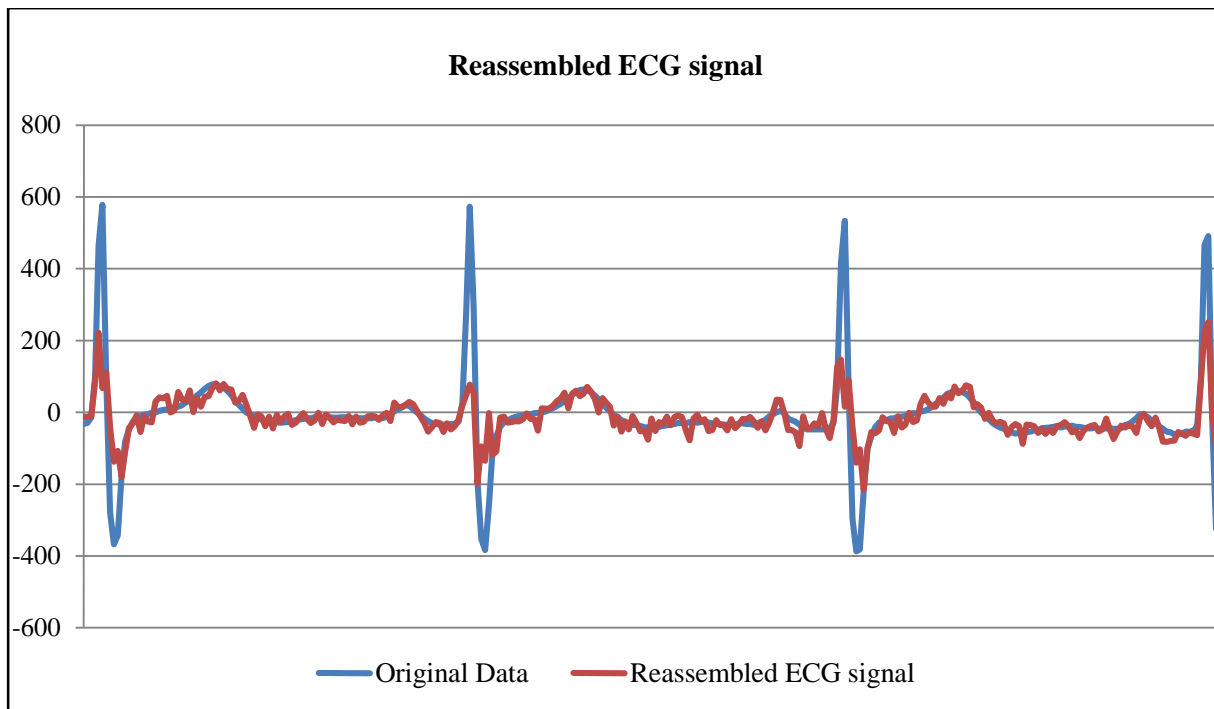Fig. 4.18 shows QRS complex that is corrupted by WGN at SNR of 15dB.

Figure 4.18. QRS complex distortion by WGN at 15dB SNR

The QRS complex in Fig. 4.18 could be easily detected in the reassembled ECG signal. The recovery of QRS complex with minimum distortion is shown in Fig. 4.19 and Fig. 4.20 The sign symbols are scaled high or low and then compared to the amplitude of R wave and S wave of normal QRS complex. Fig. 4.19 depicts an overshoot in R wave when the original sign symbol '0' is increased to '2'. This error is corrected in Fig. 4.20 when new sign symbol '1'yield the amplitude of R wave that is comparable to the R wave of normal QRS complex.

During the QRS complex recovery process, some level of distortion was observed at QR and RS transition. This distortion was due to the samples with erroneous sign symbols that were estimated incorrectly during data reassembly process.
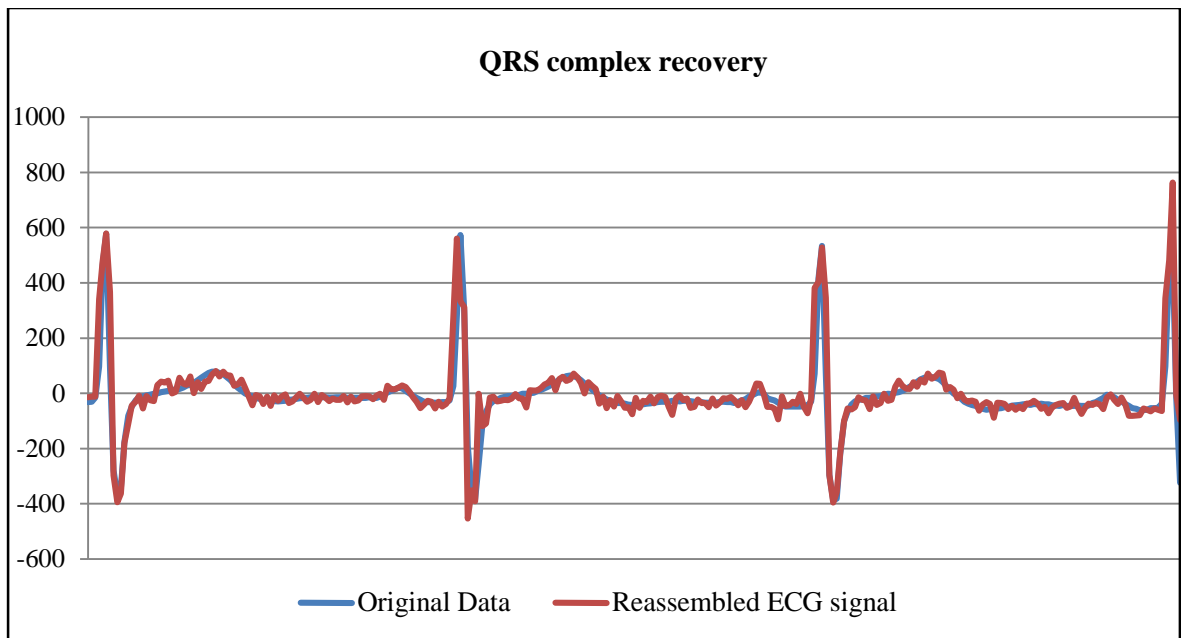
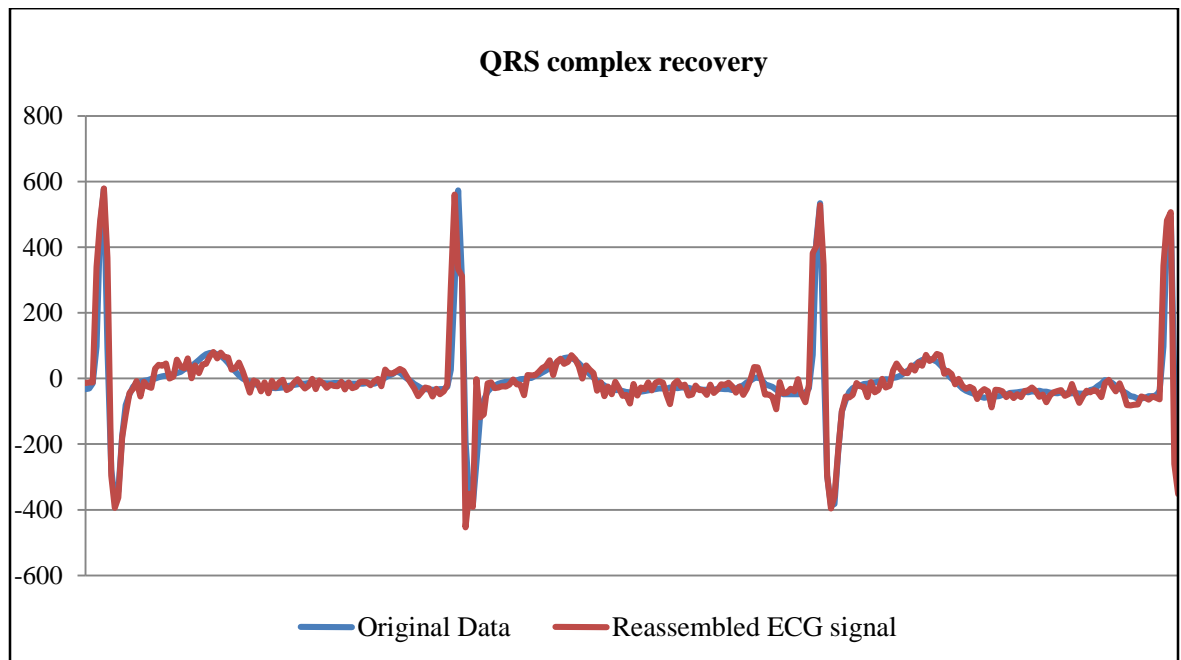Figure 4.19. R wave overshoot due to sign symbol scaling error

Figure 4.20. QRS complex recovery

4.4.5   Signal denoising for the recovery of P-wave and T-wave

The objective of signal denoising is to estimate the reassembled ECG signal by employing noise reduction techniques *without* compromising important clinical information. The recovery of P and T-wave involves denoising of reassembled ECG signal in transform domain using discrete wavelet transform because of its good localization properties in time and frequency. The denoising process decomposes signal using digital filters and yield approximate and detail coefficient using wavelet shrinkage and thresholding method. The threshold discards the insignificant detail coefficients without substantially affecting the signal fidelity and the resulting noise free P and T wave are recovered without smoothing out the wave structure.

The denoising algorithm proposed by Chourakri *et al*. [5] was modified for the recovery of P wave and T wave and is based on classical wavelet denoising scheme as proposed by Donoho [97]. The obtained noise free P and T-waves were constructed in time domain using modified coefficients and linear signal interpolation. The recovery process is explained as follows:

Step 1: Apply DWT at level 1 on reassembled ECG signal using Daubechies wavelet function 'db4' to estimate WGN and identify detail coefficient sequence (cD1) and approximation coefficient sequence (cA1) respectively. The detail coefficients are subjected to threshold using the equation (2.16) and (2.17).

Step 2: Apply DWT at level 4 on reassembled ECG signal using wavelet function 'db4' and identify 4 detail sequence (cnD4, cnD3, cnD2 and cnD1) and approximation sequence (cnA4). The detail coefficients are subjected to threshold using the equation (2.16) and (2.17) that result in the detail coefficient sequence (cnDT4, cnDT3, cnDT2 and cnDT1).

Step 3: Apply DWT at level 4 on the *residual* signal obtained from step 1 using wavelet function 'db4' and identify 4 detail sequence (crD4, crD3, crD2 and crD1) and approximation sequence (crA4).

Step 4: Generate noise free detail coefficient as follows:

$$cnfD1 = cnDT1 - crD1$$

$$cnfD2 = cnDT2 - crD2$$

$$cnfD3 = cnDT3 - crD3$$

$$cnfD4 = cnDT4 - crD4$$

Step 5: Reconstruct the denoised ECG signal using inverse discrete wavelet transform (IDWT) with detail sequence (cnfD4, cnfD3, cnfD2 and cnfD1) and approximation sequence (cnA4).

These denoised samples are then combined with recovered QRS complex using linear interpolation. This modified denoising algorithm not only suppresses the noise but also preserve the shape of P-wave and T-wave in the denoised signal. The analysis of different DWT levels shows that level 1 approximation sequence is dominated by WGN and set of peaks that are related to R wave whereas level 1 detail sequence is submerged in WGN.

This completes the recovery of P-wave and T-wave. Fig. 4.21 summarizes these steps in a flow chart.

Reassembled ECG signal

DWT at level 1 using db4:
- Detail coefficient: cD1
- Approximation coefficient: cA1

DWT at level 4 using db4:
- Detail coefficient: [cnD4, cnD3, cnD2, cnD1]
- Approximation coefficient: [cnA4]

Threshold detail coefficient:

$$Thr = \sigma \sqrt{2.\log(N)}$$

$$\sigma = (|d(j,k)|) / 0.6745$$

Threshold detail coefficient:

$$Thr = \sigma \sqrt{2.\log(N)}$$

$$\sigma = (|d(j,k)|) / 0.6745$$

Residual signal =
[received signal - denoised signal]

Detail coefficient: [cnDT4, cnDT3, cnDT2, cnDT1]

DWT at level 4 using db4:
- Detail coefficient: [crD4, crD3, crD2, crD1]
- Approximation coefficient: [crA4]

$cnfD1 = cnDT1 - crD1$
$cnfD2 = cnDT2 - crD2$
$cnfD3 = cnDT3 - crD3$
$cnfD4 = cnDT4 - crD4$

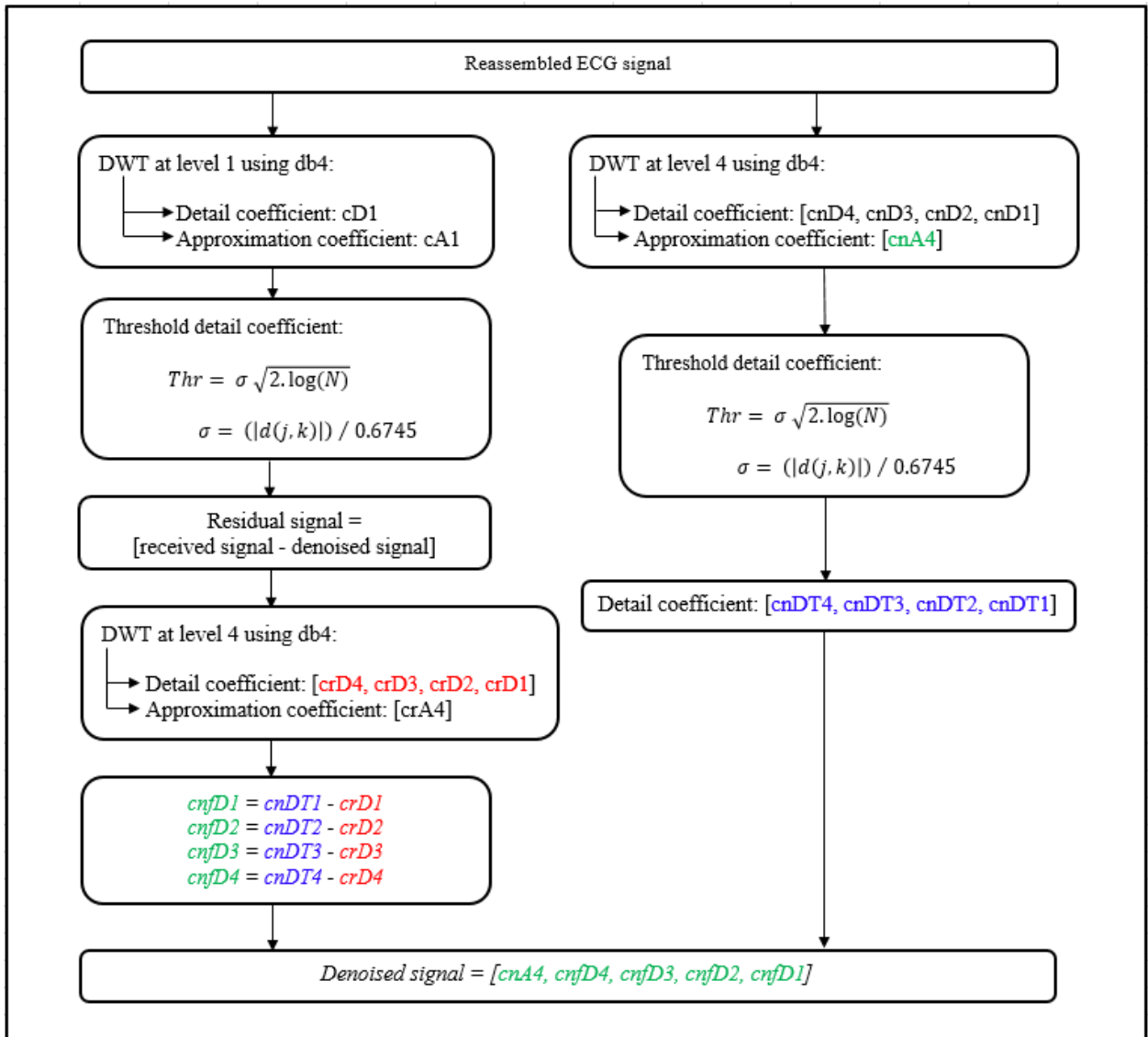Denoised signal = [cnA4, cnfD4, cnfD3, cnfD2, cnfD1]

Figure 4.21. Recovery of P-wave and T-wave

The recovery and reconstruction of ECG signal that is corrupted by WGN at 3dB SNR is summarized as follows. *The resolution of reconstructed ECG signal (100.dat) is limited to first 300 samples for qualitative analysis.*

The reassembled ECG signal with significantly distorted QRS complex and corrupted P-wave and T-wave are shown in Fig. 4.22.
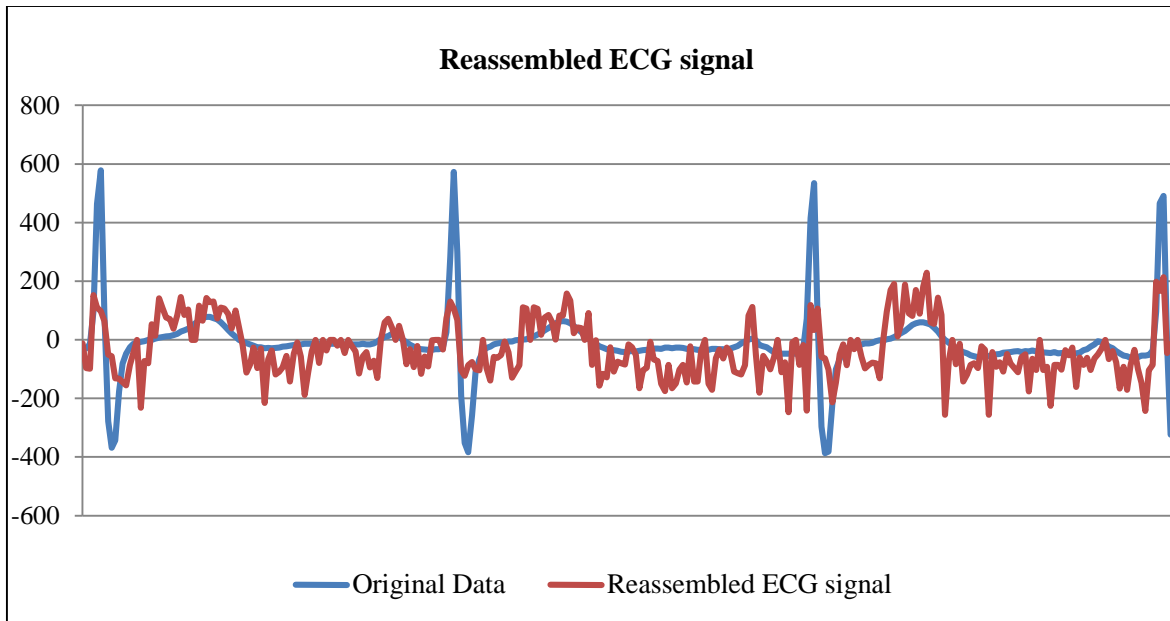
Figure 4.22. Recovery of ECG signal at 3dB SNR

The recovery of QRS complex by changing the sign symbol stream is shown in Fig. 4.23 and Fig. 4.24.
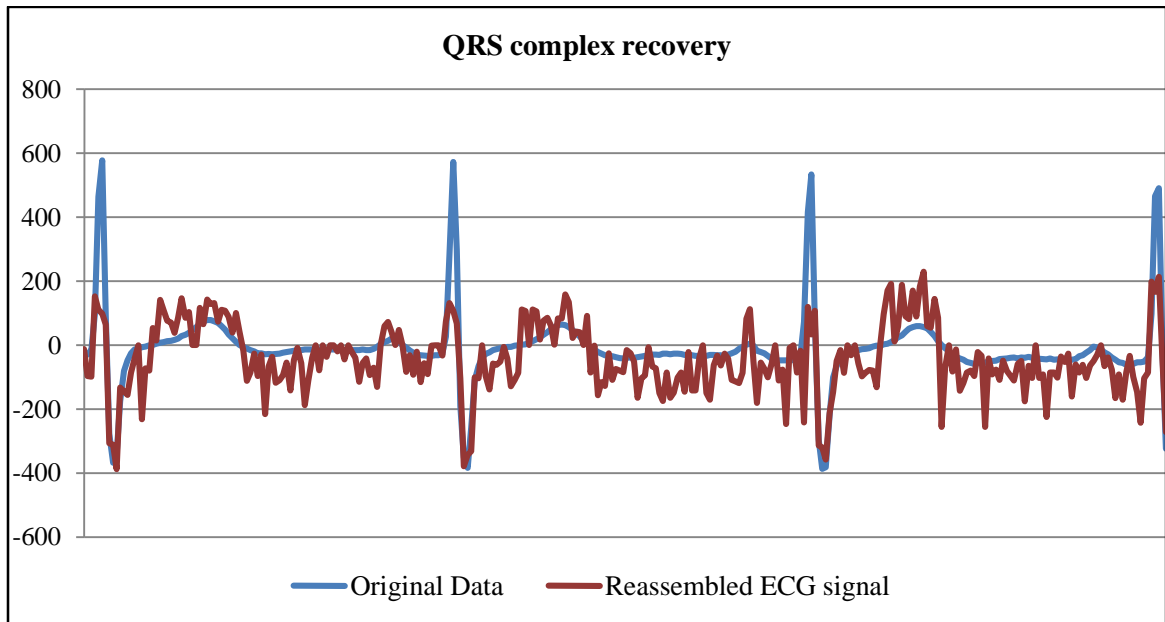

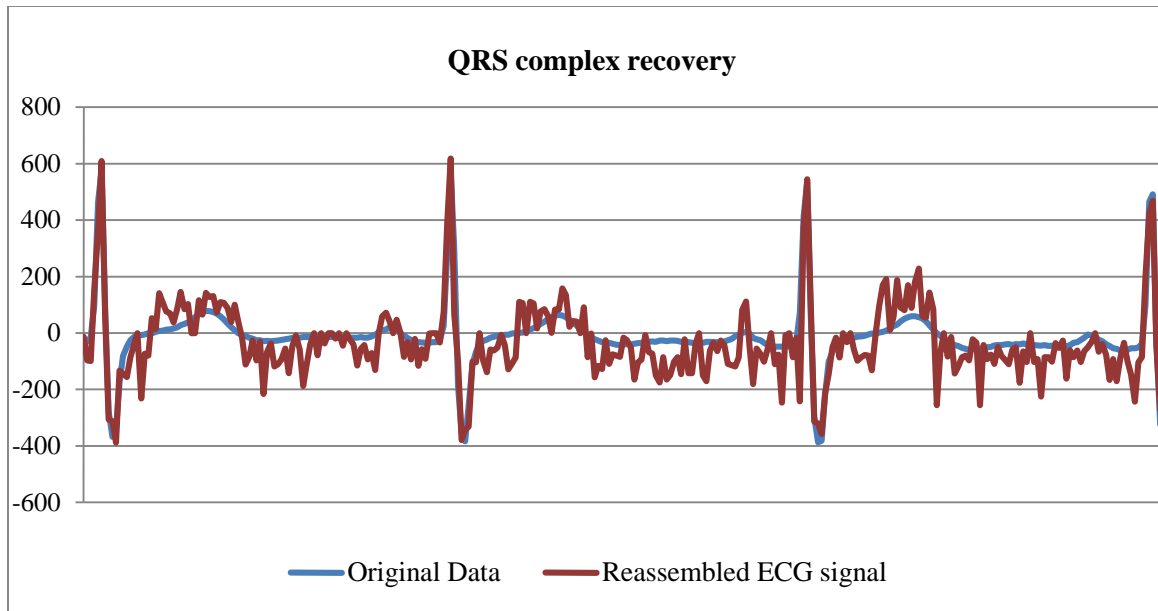Figure 4.23. Recovery of QRS complex by scaling sign symbols

Figure 4.24. Recovery of QRS complex with modified sign symbol

The reconstructed ECG signal is shown in Fig. 4.25 with recovered QRS complex and denoised P-wave and T-wave.
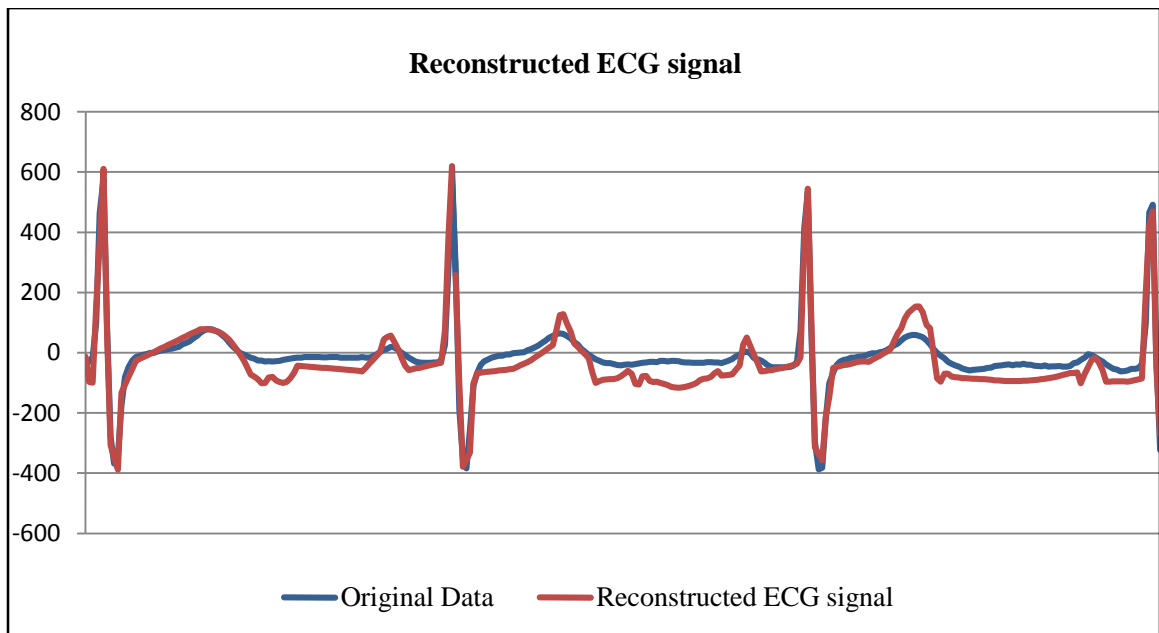

Figure 4.25. Reconstructed ECG signal at 3dB SNR

The comparative result is shown in Fig. 4.26 where QRS complex is recovered with significant

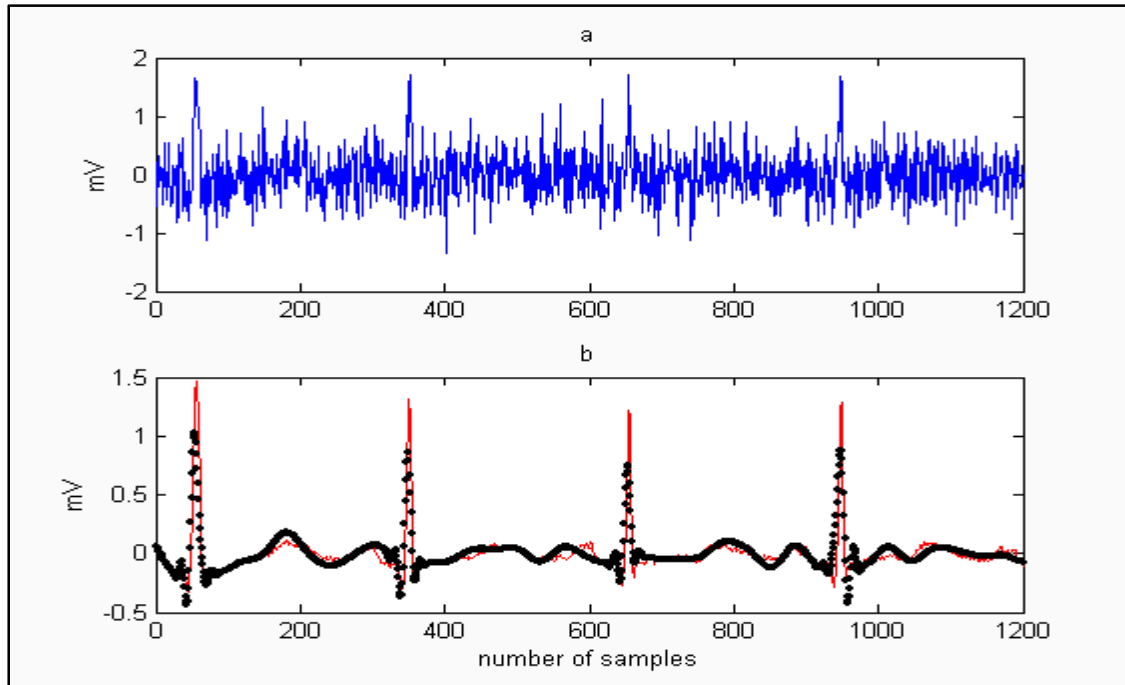distortion when ECG signal is corrupted by AWGN.

Figure 4.26. Correlation of the original ECG (RED) and denoised signal (BLACK) - [5]

Table 4.4 shows the distortion measured in reconstructed ECG signal over 300 samples, where

the received ECG signal was corrupted by AWGN at 3dB.

Table 4.4. Distortion measured in reconstructed ECG signal

Record	PRMSD (%)	PRMSD1 (%)	Compression Ratio	SNR (dB)
100	39.62	41.62	2.55:1	7.61
116	42.13	44.71	2.71:1	6.31
117	43.31	45.12	2.63:1	6.72

4.5   Conclusion

This chapter discussed the architecture and implementation of m-ECG algorithm that can help in

reliable and clinically acceptable ECG signal recovery when corrupted by WGN under poor SNR

conditions. **The novel approach improves signal fidelity through pre-processing, data**

buffering, data encoding, data segmentation, ECG feature detection and denoising. The

comparative result with [5] demonstrate performance improvement using m-ECG algorithm with

minimum QRS complex distortion and high resolution P-wave and T-wave recovery.

CHAPTER 5

CONCLUSION AND FUTURE WORK

This chapter summarizes the research carried out for this dissertation and the future direction that can advance research to achieve a reliable, stable, scalable and ubiquitous health monitoring system that supports wide range of medical monitoring of bio-signals. The performance of such a system is a tradeoff between transmission efficiency and reliable ECG signal recovery.

5.1   Conclusion

The m-ECG algorithm developed here provides a framework for reliable ECG recovery when the signal is corrupted by AWGN even at very low signal-to-noise ratio by employing pre-processing, data segmentation, data encoding, data reassembly, detection, and denoising. The design and implementation of m-ECG algorithm offer good performance against white Gaussian noise even when the signal-to-noise ratio drops to near 0dB. The performance of the m-ECG algorithm is evaluated using ECG data record downloaded from MIT-BIH arrhythmia database. The white Gaussian noise signal with varying SNR was simulated for the purpose of testing.

The use of transform based compression followed by lossless encoding significantly reduced the size of ECG signal. The aim in ECG compression is to increase the compression ratio but not at the expense of quality of the reconstructed signal.

The use of wavelet transform for signal denoising significantly distorts the amplitude of QRS complex. The proposed methodology attempts to recover the signal with negligible distortion by repeated scaling of the sign symbols. This technique keeps the diagnostically critical QRS region free from large reconstruction errors. The obtained results for P-wave and T-

wave similarly showed high efficiency in suppressing the corrupted noise and recovering critical ECG signal components without compromising relevant clinical information. The signal reconstruction is achieved by linear interpolation of QRS complex with denoised P and T waves.

The signal detection process is another important aspect of the work presented here, where the reassembled signal is segmented based on variance and expected value of peak and adjacent samples. The empirical threshold that is based on the signal-to-noise ratio isolates peak samples from non-cardiac samples. This adaptive threshold forces the samples that are not the part of cardiac event as noise and changes its value when SNR changes. This improves signal detection and reconstruction with minimal error.

5.2   Future Research

There are many areas in the work presented here that require further analysis and improvement that could be extended to include interesting ideas and research directions in mobile health care monitoring.

ECG feature detection when information about *noise* distribution is not known could be based on non-parametric approach such as the kth-nearest neighbor, however detection of cardiac events using Bayesian estimation yields minimum variance when prior information about the noise distribution is known. The m-ECG algorithm assumes *normal* noise distribution and use of parametric estimation process to detect QRS complex, PR interval and ST segment respectively. Non-parametric approaches should be explored for ECG feature detection as in most of the cases the channel noise is not known apriori.

93

The proposed scheme of data segmentation where it segregates data and sign symbols for reliable recovery of ECG signal when it is corrupted by AWGN could be extended to other bio-medical signals such EEG and EMG.

The data latency associated with signal compression and decompression can be exacerbated by network congestion, packet loss and delay variations. The use of fast dictionary-based compression algorithm such as LZW and others that we have discussed in chapter 3 could be investigated for high bandwidth communication networks that provide the best compression and decompression using the efficient signal coder and decoder.

The AWGN channel model is commonly used to simulate background channel noise under study; further research to analyze the behavior of more complex frequency selective nonlinear multi-terminal channels with application to cellular system is required in the context of pervasive monitoring of vital biomedical signals.

The real time monitoring of ECG signal should be context aware, where the system intelligently uses the m-ECG algorithm to detect and reconstructs the ECG signal and subsequently raise alarm in event of emergency.

REFERENCES

[1] C. Saritha, V. Sukanya, Y. Narasimha Murthy. "ECG Signal Analysis Using Wavelet Transforms", *in Bulgarian Journal of Physics, vol. 35, no. 1, pp. 68-77*, Feb 2008.

[2] C. Hsiao-Chiu. "Power-Saving Encoding Schemes for Wireless ECG Signal Transmissions", *in IEEE 7th International Conference on Complex, Intelligent and Software Intensive Systems (CISIS), pp. 559-564,* July 2013.

[3] U. Varshney. "Enhancing Wireless Patient Monitoring by Integrating Stored and Live Patient Information", *in IEEE 19th International Symposium on Computer-Based Medical Systems, pp. 501-506,* Jan 2006.

[4] http://web.iitd.ac.in/~sumeet/WaveletTutorial.pdf

[5] S. A. Chouakri, F. Bereksi-Reguig, S. Ahmaidi, O. Fokapu. "Wavelet denoising of the electrocardiogram signal based on the corrupted noise estimation", *in IEEE Conference on Computers in Cardiology, pp. 1021-1024*, September 2005.

[6] M. Unser, A. Aldroubi. "A review of wavelets in biomedical applications", *in Proceedings of the IEEE, vol. 84, no. 4, pp. 626-638*, April 1996.

[7] J. E. A. Sheild, D. L. Kirk. "The use of digital filters in enhancing the fetal electrocardiogram", *in Journal of Biomedical Engineering, vol. 3, no. 1, pp. 44-48,* January 1981.

[8] J. Pan, W. J. Tompkins, "A Real-Time QRS Detection Algorithm", *in IEEE Transactions on Biomedical Engineering, vol. BME-32, no. 3, pp. 230-236*, March 1985.

[9] V. De, Y. Olivier. "R-Wave Detection in the Presence of Muscle Artifacts", *in IEEE Transactions on Biomedical Engineering, vol. BME-31, no. 11, pp. 715-717*, November 1984.

[10] M. Alfaouri, K. Daqrouq. "ECG Signal Denoising by Wavelet Transform Thresholding", *in American Journal of Applied Sciences, vol. 5, no. 3, pp. 276-281*, March 2008.

[11] S. A. Chouakri, O. Djaafri. A. Taleb-Ahmed. "Wavelet transform and Huffman coding based electrocardiogram compression algorithm: Application to telecardiology", *in Journal of Physics, vol. 454, no.1, doi:10.1088/1742-6596/454/1/012086*, August 2013.

[12] C. Rami. "Signal Denoising using Wavelets", *in project report. Department of Electrical Engineering Technion, Israel Institute of Technology,* February 2012.

[13] J. R. Cox, F. M. Nolle, H. A. Fozzard, G. C. Oliver. "AZTEC, a preprocessing program for real time ECG rhythm analysis", *in IEEE Transactions on Biomedical Engineering, vol. BME-15, no. 2, pp. 128-129,* April 1968.

[14] M. Ishijima, S-B. Shin, G. H. Hostetter, J. Sklansky. "Scan-Along Polygonal Approximation for Data Compression of Electrocardiograms", *in IEEE Transactions on Biomedical Engineering, vol. BME-30, no. 11, pp. 723-72*9, November 1983.

[15] B. Woodward, R. S. H. Istepanian, C. I. Richards. "Design of a telemedicine system using a mobile telephone", *in IEEE Transactions on Information Technology in Biomedicine, vol. 5, no. 1, pp. 13-15*, March 2001.

[16] F. Chiarugi, D. Trypakis, V, Kontogiannis, P. J. Lees, C. E. Chronaki, M. Zeaki, N. Giannakoudakis, D. Vourvahakis, M. Tsiknakis, S. C. Orphanoudakis. "Continuous ECG monitoring in the management of pre-hospital health emergencies*", in IEEE Conference on Computers in Cardiology, pp. 205-208,* September 2003.

[17] R. S. H. Istepanian, L. J. Hadjileontiadis, S. M. Panas. "ECG data compression using wavelets and higher order statistics methods", *in IEEE Transaction on Information Technology in Biomedicine*, *vol. 5, no. 2, pp. 108-115*, June 2001.

[18] E. Kyriacou, S. Pavlopoulos, A. Berler, M. Neophytou, A. Bourka, A. Georgoulas, A. Anagnostaki, D. Karayiannis, C. Schizas, C. Pattichis, A. Andreou, D. Koutsouris. "Multi-purpose health care telemedicine system with mobile communication link support", *in Biomedical Engineering online, 2:7,* March 2003.

[19] M. Clarke. "A reference architecture for telemonitoring", *in Studies in Health Technology and Informatics, vol. 103, pp. 381-384*, 2004.

[20] C. H. Salvador, M. P. Carrasco, M. A. G. de Mingo, A. M. Carrero, J. M. Montes, L. S. Martin, M. A. Cavero, I. F. Lozano, J. L. Monteagudo. "Airmed-cardio: a GSM and Internet services-based system for out-of-hospital follow-up of cardiac patients", *in IEEE Transactions on Information Technology in Biomedicine, vol. 9, no. 1, pp. 73-85*, March 2005.

[21] P. Clemmensen, M. Sejersten, M. Sillesen, D. Hampton, G. S. Wagner, S. Loumann-Nielsen. "Diversion of ST-elevation myocardial infarction patients for primary angioplasty based on wireless prehospital 12-lead electrocardiographic transmission directly to the cardiologist's handheld computer: a progress report", *in Journal of Electrocardiology, vol. 38, no. 4, pp. 194-198*, October 2005.

[22] E. Kyriacou, S. Pavlopoulos, D. Koutsouris. "An emergency telemedicine system based on wireless communication technology", *in M-Health: Emerging Mobile Health Systems, R. H. Istepanian, S. Laxminarayan, C. S. Pattichis (eds.), New York, Springer, pp. 401-416,* 2006.

[23] P. Giovas, D. Thomakos, O. Papazachou, D. Papadoyannis. "Medical aspects of prehospital cardiac telecare", *in M-Health: Emerging Mobile Health Systems, R. H. Istepanian, S. Laxminarayan, C. S. Pattichis (eds.), New York, Springer, pp. 389-400,* 2006.

[24] U. Schachinger, R. Kretschmer, C. Neumann, M. Nerlich. "NOAH. A mobile emergency care system. Notfall-Organizations –und Arbeitshilfe", *in Studies in Health Technology and Informatics, vol. 64, pp. 85-92.* 1999.

[25] R. Karlsten, B. A. Sjogvist. "Telemedicine and decision support in emergency ambulances in Uppsala", *in Journal of Telemedicine and Telecare, 6, pp. 1-7,* 2000.

[26] X. Yan, D. Gagliano, M. LaMonte, P. Hu, W. Gaasch, R. Gunawadane. "Design and evaluation of a real time mobile telemedicine system for ambulance transport", *in Journal of High Speed Networks, 9, pp. 47-56,* January 2000.

[27] V. Anantharaman, L. Swee Han. "Hospital and emergency ambulance link: using IT to enhance emergency pre-hospital care", *in International Journal of Medical Informatics*, *vol. 61, no. 2-3, pp. 147-161*, May 2001.

[28] A. Rodriguez, J. L. Villalar, M. T. Arredondo, M. F. Cabrera, F. Del Pozo. "Transmission trials with a support system for the treatment of cardiac arrest outside hospital", *in Journal of Telemedicine and Telecare*, *7, suppl. 1, 6*0-2, February 2001.

[29] S. Pavlopoulos, E. Kyriacou, A. Berler, S. Dembeyiotis, D. Koutsouris. "A novel emergency telemedicine system based on wireless communication technology – AMBULANCE", *in IEEE Transactions on Information Technology in Biomedicine, vol. 2, no. 4, pp. 261-267*, December 1998.

[30] E. S. Hall, D. K. Vawdrey, C. D. Knutson, J. K. Archibald. "Enabling remote access to personal electronic medical records", *in IEEE Engineering in Medicine and Biology Magazine, vol. 22, no. 3, pp. 133-139*, June 2003.

[31] J. Reponen, E. Ilkko, L. Jyrkinen, O. Tervonen, J. Niinimaki, V. Karhula, A. Koivula. "Initial experience with a wireless personal digital assistant as a teleradiology terminal for reporting emergency computerized tomography scans", *in Journal of Telemedicine and Telecare*, *6(1), 45*-9, February 2002.

[32] C. Yuechun, A. Ganz. "A mobile teletrauma system using 3G networks", *in IEEE Transactions on Information Technology in Biomedicine, vol. 8, no. 4, pp. 456-462*, December 2004.

[33] S. Garawi, R. S. H. Istepanian, M. A. Abu-Rgheff. "3G wireless communications for mobile robotic tele-ultrasonography systems", *in IEEE Communications Magazine, vol. 44, no. 4, pp. 91-96*, April 2006.

[34] B. Richard, W. Katarzyna, H. A. Van, N. Victor, K. Dimitri. "Goodput Analysis of 3G wireless networks supporting m-health services", *in 8th International Conference on Telecommunications, ConTEL, pp. 99-106,* June 2005.

[35] C. Wan-Young, Y. Chiew-Lian, S. Kwang-Sig, R. Myllyla. "A cell phone based health monitoring system with self-analysis processor using wireless sensor network technology", *in 29th Annual International Conference of IEEE Engineering in Medicine and Biology, EMBS200, pp. 3705-3708,* August 2007.

[36] W. Katarzyna, B. Richard, K. Dimitri, H. A. Van, J. Val, W. Ing, H. Rainer. "Mobile health care over 3G networks: The MobiHealth pilot system and service", *in the proceedings of Global Mobile Congress, pp. 71-76,* October 2004.

[37] U. Anliker, J. A. Ward, P. Lukowicz, G. Troster, F. Dolveck, M. Baer, F. Keita, E. B. Schenker, F. Catarsi, L. Coluccini, A. Belardinelli, D. Shklarski, M. Alon, E. Hirt, R. Schmid, M. Vuskovic. "AMON: a wearable multiparameter medical monitoring and alert system", *in IEEE Transactions on Information Technology in Biomedicine, vol. 8, no. 4, pp. 415-427*, December 2004.

[38] E. A. V. Navarro, J. R. Mas, J. F. Navajas. "Analysis and measurement of a wireless telemedicine system", *in IEEE Pervasive Health Conference and Workshop, pp. 1-6*, December 2006.

[39] A. Alahmadi, B. Soh. "A smart approach towards a mobile e-health monitoring system architecture", *in IEEE International Conference on Research and Innovation in Information Systems (ICRIIS), pp. 1-5*, November 2011.

[40] A. Durresi, M. Durresi, L. Barolli. "Secure Ubiquitous Health Monitoring System", *in Network-Based Information Systems – 2nd International Conference, NBiS 2008, Turin, Italy, September 1-5, 2008. Proceedings, New York, Springer, pp. 273-282.* 2008.

[41] D. Vouyioukas, I. Maglogiannis, D. Komnakos. "Emergency m-health services through high speed 3G systems: simulation and performance", *in Transactions of the Society for Modeling and Simulation International, vol. 83, no. 4, pp. 329-345*, April 2007.

[42] K. Wac, H. A. Van, B. Richard, T. Broens. "Context-aware QoS provisioning in an m-health service platform", *in International Journal of Internet Protocol Technology, vol. 2, no. 2, pp. 102-108*, 2007.

[43] P. Pravin, J. Val, B. F. Bert-Jan, H. Hermie. "A framework for the comparison of mobile patient monitoring systems", *in Journal of Biomedical Informatics*, *vol. 45, no. 3, pp. 544-556*, June 2012.

[44] A. Prentza, S. Maglavera, L. Leondaridis. "Delivery of healthcare services over mobile phones: e-vital and CHS paradigms", *in 28th Annual International Conference of IEEE Engineering in Medicine and Biology Society, EMBS'06, pp. 3250-3253,* August 2006.

[45] R. Istepanian, N. Philip, X. H. Wang, S. Laxminarayan. "Non-Telephone Healthcare: The role of 4G and emerging mobile systems for future health systems", *in Studies in Health Technology and Informatics, vol. 103, pp. 465-470*, 2004.

[46] www.hcs.harvard.edu/~weber/HomePage/Papers/ECGCompression/

[47] L. Sörnmo, P. Laguna. "Electrocardiogram (ECG) Signal Processing", *in Wiley Encyclopedia of Biomedical Engineering,* April 14 2006.

[48] J. R. Cox, F. M. Nolle, H. A. Fozzard, G. C. Oliver. "AZTEC, a Preprocessing Program for Real-Time ECG Rhythm Analysis", *in IEEE Transactions on Biomedical Engineering, vol. BME-15, no. 2, pp. 128-129*, April 1968.

[49] W. C. Mueller. "Arrhythmia detection program for an ambulatory ECG monitor", *in Biomedical Science Instrument, vol. 14, pp. 81-85*, April 1978.

[50] S. M. S. Jalaleddine, C. G. Hutchens, R. D. Strattan, W. Coberly. "ECG Data Compression Techniques – A Unified Approach", *in IEEE Transactions on Biomedical Engineering, vol. 37, no. 4, pp. 329-343*, April 1990.

[51] J. P. Abenstein, W. J. Tompkins. "A New Data-Reduction Algorithm for Real-Time ECG Analysis", *in IEEE Transactions on Biomedical Engineering, vol. BME-29, no. 1, pp. 43-48*, January 1982.

[52] L. W. Gardenhire. "Redundancy reduction the key to adaptive telemetry", *in Proceedings 1964 National Telemetry Conference, pp. 1-16,* 1964.

[53] M. Ishijima, S. B. Shin, G. H. Hostetter, J. Sklansky. "Scan-Along Polygonal Approximation for Data Compression", *in IEEE Transactions on Biomedical Engineering, vol. BME-30, no. 11, pp. 723-729*, November 1983.

[54] D. Stewart, G. E. Dower, O. Suranyi. "An ECG compression code", *in Journal of Electrocardiology, vol. 6, no. 2, pp. 173-176,* February. 1973.

[55] U. E. Ruttimann, A. S. Berson, H. V. Pipberger. "ECG Data Compression by Linear Prediction", *in Computers Cardiology, pp. 313-315*, 1976.

[56] U. E. Ruttimann, H. V. Pipberger. "Compression of the ECG by Prediction or Interpolation and Entropy Encoding", *in IEEE Transactions on Biomedical Engineering, vol. BME-26, no. 11, pp. 613-623*, November 1979.

[57] J. R. Cox and K. L. Ripley. "Compact digital coding of electrocardiographic data*", in Proceedings, VI International Conference on System Science, pp. 333-336*, January 1973.

[58] O. Pahlm, P. O. Börjesson, O. Werner. "Compact Digital Storage of ECG's*" in Computer Programs in Biomedicine, vol. 9, no. 3, pp. 293-300*, May 1979.

[59] D. Stewart, D. Berghofer, R. G. Dower. "Data Compression of ECG signals", *in Proceedings of the 1979 Engineering Foundation Conference. Computerized interpretation of the ECG IV, pp. 162-177 and A1-A8,* January 1979.

[60] R. McCaughern, A. M. Rosie, F. C. Monds. "Two methods of asynchronous data compression", *in Electronics Letters, vol. 4, no. 17, pp. 363-364*, August 1968.

[61] T. S. Ibiyemi. "A novel data compression technique for electrocardiogram classification", *in Engineering in Medicine, vol. 15, number. 1, pp. 35-38*, January 1986.

[62] H. Imai, N. Kiraura, Y. Yoshida. "An efficient encoding method for electrocardiography using spline functions", *in Systems and Computers in Japan, vol. 16, no. 3, pp. 85-94,* 1985.

[63] S. M. Jalaleddine, C. Hutchens, W. Coberly, R. D. Strattan. "Compression of Holter ECG data", *in Biomedical Sciences Instrumentation, vol. 24, pp. 35-45*, April 1988.

[64] H. A. M. Al-Nashash. "A dynamic Fourier series for the compression of ECG using FFT and adaptive coefficient estimation", *in Medical Engineering and Physics, vol. 17, no. 3, pp. 197-203*, April 1995.

[65] H. Saberkari, M. Shamsi. "Comparison of different algorithms for ECG signal compression based on transfer coding*", in 2012 IEEE Symposium on Industrial Electronics and Applications (ISIEA), pp. 341-345*. September 2012.

[66] L. V. Batista, E. U. K. Melcher, L. C. Carvalho. "Compression of ECG signals by optimized quantization of discrete cosine transform coefficients*", in Medical Engineering and Physics, vol. 23, no. 2, pp. 127-134*, March 2001.

[67] V. A. Allen, J. Belina. "ECG data compression using the discrete cosine transform (DCT)", *in IEEE Proceedings of Computers in Cardiology 1992, pp. 687-690*, October 1992.

[68] V. Aggarwal, M. S. Patterh. "Quality controlled ECG compression using Discrete Cosine transform (DCT) and Laplacian Pyramid (LP)", *in Multimedia, Signal Processing and Communication Technologies, 2009. IMPACT '09. International, pp. 12-15*, March 2009.

[69] S. Olmos, M. Millan, J. Garcia, P. Laguna. "ECG data compression with Karhunen-Loeve transform", *in Computers in Cardiology, pp. 253-256,* September 1996.

[70] N. Ahmed, P. J. Milne, S. G. Harris. "Electrocardiographic data compression via orthogonal transforms", *in IEEE Transactions on Biomedical Engineering, vol. BME-22, no. 6, pp. 484-487,* November 1975.

[71] M. E. Womble, J. S. Halliday, S. K. Mitter, M. C. Lancaster. "Data compression for storing and transmitting ECG's/VCG's", *in Proceedings of the IEEE, vol. 65, no. 5, pp. 702-706*, May 1977.

[72] T. Y. Young, W. H. Huggins. "The intrinsic component theory of electrocardiography", *in IRE Transactions on Bio-Medical Electronics, vol. 9, no. 4, pp. 214-221*, October 1962.

[73] A. M. Zied, M. E. Womble. "Application of a partitioned Karhunen-Loeve expansion scheme to ECG/VCG data compression", *in Proceedings of the Seventh New England (Northeast) Bioengineering Conference, pp. 102-105*, 1979.

[74] M. E. Womble, A. M. Zied. "A statistical approach to ECG/VCG data compression", *in Optimization of Computer ECG processing, H. K. Wolf and P. W. MacFarlane (Eds.) New York: North-Holland Publishing Company, pp. 91-101*, 1980.

[75] B. R. S. Reddy, I. S. N. Murthy. "ECG data compression using Fourier descriptors", *in IEEE Transactions on Biomedical Engineering, vol BME-33, no. 4, pp. 428-434*, April 1986.

[76] S. Lee, J-H. Lee. "A real-time ECG data compression algorithm for a digital holter system", *in 30th IEEE Annual Conference on Engineering in Medicine and Biology Society EMBS2008, pp. 4736-4739*, August 2008.

[77] W. S. Kuklinski. "Fast Walsh transform data-compression algorithm: ECG applications", *in Medical and Biological Engineering and Computing, vol. 21, no. 4, pp. 465-472*, July 1983.

[78] G. P. Frangakis, G. Papakonstantinou, S. G. Tzafestas. "A fast Walsh transform-based data compression multi-microprocessor system: application to ECG signals", *in Mathematics and Computers in Simulation, vol. 27, no. 5, pp. 491-502*, 1985.

[79] T. A. De Perez, M. C. Stefanelli, F. D'alvano. "ECG data compression via exponential quantization of the Walsh spectrum", *in Journal of Clinical Engineering, vol. 12, no. 5, pp. 373-378*, September-October 1987.

[80] M. Shridhar, M. F. Stevens. "Analysis of ECG data, for data compression", *in International Journal of Bio-Medical Computing, vol. 10, no. 2, pp. 113-128*, March 1979.

[81] B. A. Rajoub. "An efficient coding algorithm for the compression of ECG signals using the wavelet transform", *in IEEE Transactions on Biomedical Engineering, vol. 49, no. 4, pp. 355-362*, April 2002.

[82] Y. Xiang-Guo, Z. Chong-xun. "ECG data compression for Holter system using integer to integer wavelet transform", *in Proceeding of the 20th Annual International Conference of IEEE. Engineering in Medicine and Biology Society, vol. 1, pp. 202-205*, October-November 1998.

[83] B. S. Kim, S. K. Yoo, M. H. Lee. "Wavelet-based low-delay ECG compression algorithm for continuous ECG transmission", *in IEEE Transactions on Information Technology in Biomedicine, vol. 10, no. 1, pp. 77-83*, January 2006.

[84] A. G. Ramakrishnan, S. Saha. "ECG coding by wavelet-based linear prediction", *in IEEE Transactions on Biomedical Engineering, vol. 44, no. 12, pp. 1253-1261*, December 1997.

[85] N. V. Thakor, Y. Sun, H. Rix, P. Caminal. "Multiwave: a multi resolution wavelet-based ECG data compression algorithm", *in IEEE Proceedings on Computers in Cardiology, pp. 393-396*, September. 2005.

[86] Z. Lu, D. Y. Kim, W. A. Pearlman. "Wavelet compression of ECG signals by the set partitioning in hierarchical trees algorithm", *in IEEE Transactions on Biomedical Engineering, vol. 47, no. 7, pp. 849-856*, July 2000.

[87] M. L. Hilton. "Wavelet and wavelet packet compression of electrocardiograms", *in IEEE Transactions on Biomedical Engineering, vol. 44, no. 5, pp. 394-402*, May 1997.

[88] A. M. Al-Busaidi, L. Khriji, F. Touati, M. F. A. Rasid. "Real-time DWT based compression for wearable electrocardiogram monitoring system", *in 8th IEEE GCC Conference and Exhibition (GCCCE), 2015, pp. 1-6*, February 2015.

[89] B. Bradie. "Wavelet packet based compression of single lead ECG", *in IEEE Transactions on Biomedical Engineering, vol. 43, no. 5, pp. 493-501,* May 1996.

[90] J. A. Crowe, N. M. Gibson, M. S. Woolfson, M. G. Somekh. "Wavelet transform as a potential tool for ECG analysis and compression", *in Journal of Biomedical Engineering, vol. 14, no. 3, pp. 268-272*, May 1992.

[91] S. M. Ahmeda, M. Abo-Zahhad. "A new hybrid algorithm for ECG signal compression based on the wavelet transformation of the linearly predicted error", *in Medical Engineering and Physics, vol. 23, no. 2, pp. 117-126*, March 2001.

[92] R. S. S. Kumari, V. Sadasivam. "A novel algorithm for wavelet based ECG signal coding", *in Computers and Electrical Engineering, vol. 33, no. 3, pp. 186-194*, May 2007.

[93] J. Chen, F. Wang, Y. Zhang, X. Shi. "ECG compression using uniform scalar dead-zone quantization and conditional entropy coding", *in Medical Engineering and Physics, vol. 30, no. 4, pp. 523-530*, May 2008.

[94] M. Blanco-Velasco, F. Cruz-Roldan, J. I. Godino-Llorente, J. Blanco-Velasco, C. Armiens-Aparicio, F. Lopez-Ferreras. "On the use of PRD and CR parameters for ECG compression", *in Medical Engineering and Physics, vol. 27, no. 9, pp. 798-802*, November 2005.

[95] M. S. Manikandan, S. Dandapat. "Wavelet threshold based ECG compression using USZZQ and Huffman coding of DSM", *in Biomedical Signal Processing and Control, vol. 1, no. 4, pp. 261-270*, October 2006.

[96] L. Brechet, M. F. Lucas, C. Doncarli, D. Farina. "Compression of biomedical signals with mother wavelet optimization and best-basis wavelet packet selection", *in IEEE Transactions on Biomedical Engineering, vol. 54, no. 12, pp. 2186-2192*, December 2007.

[97] D. L. Donoho. "De-noising by soft-thresholding", *in IEEE Transactions on Information Theory, vol. 41, no. 3, pp. 613-627*, May 1995.

[98] D. Vel, Y. Olivier. "R-wave detection in the presence of muscle artifacts", *in IEEE Transactions on Biomedical Engineering, vol. BME-31, no. 11, pp. 715-717*, March 2007.

[99] http://www.physionet.org/physiobank/database/mitdb/

[100] http://www.mathworks.com/products/matlab/

[101] S. M. R. Rabiul, X. Huang, D. Sharma. "Wavelet based denoising algorithm of the ECG signal corrupted by WGN and Poisson noise", *in 2012 International Symposium on Communications and Information Technologies, pp. 165-168*, October 2012.

[102] CDC.gov – Heart Disease Facts. Report compiled by AHA, CDC, NIH and other sources. http://www.cdc.gov/heartdisease/docs/consumered_heartdisease.pdf

[103] U.S. Preventive Services Task Force (2012). Screening for coronary heart disease with electrocardiography: Recommendation statement. Available online: http://www.uspreventiveservicestaskforce.org/uspstf/uspsacad.htm

[104] P. Kulkarni, Y. Öztürk. "Requirements and design spaces of mobile medical care", *in ACM SIGMOBILE Mobile Computing and Communications Review, vol. 11, no. 3, pp. 12-30*, July 2007.

[105] D. Mozaffarian, E. J. Benjamin, *et al.* on behalf of the American Heart Association Statistics Committee and Stroke Statistics Subcommittee, Heart disease and stroke statistics − 2015 update: A report from American Heart Association. *Circulation*. 2015; 131: e29-e322.

BIOGRAPHICAL SKETCH

Syed Muhammad Abdullah was born in Karachi, Pakistan to Syed Abdul Basit and Talat Anwar. After finishing high school from B.V.S Parsi High School, Karachi, he enrolled at N.E.D. University of Engineering and Technology and completed his Bachelor of Engineering in Computer Systems in 2001. He then joined Hamdard University, Karachi as a telecommunication laboratory engineer from March 2001 to July 2003. He was admitted to the Master of Science program in Electrical Engineering (Communication and Signal Processing) at The University of Texas at Dallas in August 2003. While pursuing Masters, he was an intern at Sychip Incorporation as RF Design Engineer from December 2004 to December 2005. After finishing his M.S.E.E in December 2005, he worked as Sr. RF Module Design Engineer at Murata Wireless Solutions from January 2006 to September 2010. Later, at BlackBerry Corporation he worked as Sr. RF Design Engineer from September 2010 through November 2013. He then moved to NVIDIA Corporation in November 2013 and worked there till June 2015 as Sr. RFIC Design Verification Engineer. He is currently working as Sr. Staff Design Engineer at FLEX in consumer technology group. His research interests include context aware health monitoring systems (design and HW/SW implementation), signal processing techniques in biomedical systems, low power-short range secure wireless system design for industrial, medical, agriculture and consumer products to support M2M communication and wireless co-existence architecture to support multi-band and multi-mode radio architecture.

CURRICULUM VITAE

Syed Muhammad Abdullah

RF/Electrical engineer with 10 years' experience in hardware, system design, simulation, characterization and verification. Self-motivated professional with passion for consumer, industrial and healthcare product design from concept to production. Excellent analytical and problem-solving skills that function well to meet stringent deadlines. An adaptable team player that thrives on challenge with ability to work with cross-functional and cross geographical teams

Technical Skills

Hardware	• Wi-Fi [802.11a/b/g/n/ac]	• Bluetooth4.2	• A/V codecs
	• 9-axis IMU	• RFID/NFC	• Z-wave
	• Image sensor [DVP/MIPI]	• GPS	• ARM Cortex A-9
	• RFIC [4G/3G/LoRA]	• PMIC/DC-DC	• I2C/SPI/USB3.0
Instrumentation	• Vector Network Analyzer	• Logic Analyzer	• Digital Oscilloscope
	• TDR	• LitePoint IQxel80	• CMW500/CMU200
	• Phase noise/NF/Gain	• PXA N9030A	• MT8860
	• Power meter/VSG/VSA	• E5052B SSA	• Power supplies
Software Tools	• OrCAD capture	• Allegro	• MATLAB
	• IxChariot	• ADS	• Wireshark
	• Zuken CR5000	• LabVIEW	• Altium Designer
Languages & OS	• C	• Python	• Linux

Education: MS in Electrical Engineering
The University of Texas at Dallas

BE in Computer Systems
N.E.D. University of Engineering and Technology. Karachi, Pakistan.

Experience:

July '15 – Present   Flex, Plano TX
Sr. Staff Design Engineer

Design, develop and test high volume industrial, health, M2M and consumer IoT products while managing constraints in time, cost, performance and manufacturing. Collaborated with customers, supply chain and PMs on schedule and budget and developed EE project estimates.

Industrial smart hard hat
• Electrical and RF system design of industrial hard hat to comply with IEC60079-0, IEC60079-11 ib [ATEX], FCC part 15, SAR and EMI
• Design to monitor bio-signals [SpO$_2$ and heart rate], temperature, humidity, pressure and external force.
• Gas detector design to detect and process data from CO, H$_2$S, O$_2$ and hydrocarbon gas sensors with actuation and interface with main board using 16/24 bit ADCs.
• Circuit design of wireless connectivity included WLAN 2.4/5GHz, GPS, Bluetooth 4.2, UWB, NFC, RFID and LTE.
• Audio architecture design included dual digital mics for noise cancellation, ANC audio codec and Class D amplifier speakers.
• Video monitoring with still images using OV9732 with OV788 hardware encoder.
• Electrical board design of main board with TI AM4376 [ARM Cortex-A9] processor, PMIC, DDR3, Ethernet, USB2.0, SPI, I^{2}C, SDIO and Buck-Boost.
• Wrote test plans for board bring up and electrical/RF characterization and developed system power tree.
• Worked with PCB designers on board layout of high speed signal routing [memory and digital signals] in accordance with EMI/EMC best practices, RF signal integrity and DFA/DFM reviews.
• Worked with ME designers for placement, thermal analysis and manufacturability.
• Board bring up in lab, debug for hardware/FW issues and performed electrical characterization
• *Chipset: TI AM4376, OV788, TLV320AIC3262, Alphasense gas monitoring sensors, WL1837, TRF970ARHBR, TOBY-L2, OV9732, MT41K12M8RH, DCM03, FSR400.*

Smart clothing accessory
• Electrical and RF hardware design of IP57 smart clothing accessory for monitoring back posture while running, sitting and standing using 9-axis IMU and communicated data to smartphone over BLE.
• Performed system reliability tests including vibration, shock, chemical immersion, temperature cycle test and FCC part 15 emission compliance.
• Worked with suppliers and off-shore Flex manufacturing facilities for design transfer and manufacturing.
• *Chipset: Nordic nRF52832, STM32L, LSM6DS3, LPS25H, LIS3MDL, Ambarella S2Lx*

Smart home gateway
• Home gateway system design to control smart window blinds, door locks and garage doors via smart home application using LoRA and Z-wave
• Performed complete Apple HomeKit certification, wrote compliance test report with SW logs for Bonjour test and self-certification audit test cases

• Worked with SW engineer to perform Z-Wave self-audit test and optimized in-band output power of 433MHz and 850MHz radios to meet FCC Part 15C:15.231.
• *Chipset*: *Semtech SX1276, Freescale iMX28, ZM5202, MFI337S3959*

Nov '13 – June '15   NVIDIA Corporation, Richardson TX
                              Sr. RFIC Design Verification – IC Design Team

Design, debug, lab bring up and characterization of NVIDIA RFIC [WCDMA and LTE] HW platform, non-signaling verification and optimization of TX-RX blocks.

• RFIC bench validation for gain, IIP2, NF, phase noise, S parameter, output power, EVM, ACLR, IQ offset, PLL spurs and settling time, RXBN, spurious analysis, out-band emission measurements, IQ and CS calibration.
• PVT characterization of RFIC [nominal and corner lots] and worked with IC design team for performance optimization of analog, digital and RF blocks.
• Designed hardware platform using Allegro for schematic, board layout and developed test plans for lab and production test environment
• Presented design analysis and recommendations to IC design team and performed detail oriented technical design reviews
• Extensively worked with PXA N9030A, E5052B signal source analyzer, wireless communication analyzer, N5182B MXG, logic analyzer and oscilloscopes.
• Wrote test scripts in MATLAB and Python for bench debug and characterization
• *Chipset*: *ICE9xxx and Vesta RFIC*

Sep '10 – Nov '13   BlackBerry USA, Irving TX
                            Sr. RF Design Engineer

Electrical and RF hardware design of BB7 and BB10 based computing platform that included smartphones and tablets from concept design to production readiness.

• Designed advance wireless connectivity solution with WLAN a/b/g/n/ac/2x2MIMO with BT4.0, BLE and FM using Broadcom, TI and Qualcomm-Atheros SoCs.
• Designed RF front-end that supported downlink LTE CA using APT/ET power amplifier
• Used Zuken for schematic and layout with RF, analog and digital components, DC-DC converters, power management unit [PMU], CPU/AP, RFIC and communication interfaces [HDMI, USB, I^{2}S, MIPI, SPI, Ethernet, I^{2}C] etc.
• Performed RF matching of radio transceiver for optimal RF performance to meet 3GPP and carrier requirements. This included load and source pull for PA and LNA using Maury tuners and subsequent simulation using ADS for best impedance match circuit, component evaluation [FEM, duplexer, diplexer, PA, filter, RF switch etc.] for IMD, stability and measured performance using CMU200, CMW500, VNA, VSA, VSG and power meter.

• Worked closely with engineering/modem development teams on cross-functional issues related to architecture [performance, power consumption, thermal behavior], production [quality, FA and manufacturing] and development [system/board bring up, debugging and integration].
• System level co-existence performance evaluation and front end design of co-located radios – WLAN/BT with CDMA/GSM/UMTS/LTE including co-existence with LTE-B7 and B41.
• Debugged and analyzed digital circuits that involved USB, I^2S, comparators, amplifiers, LDO and DC switchers for skew, group delay, cross-talk, impedance and loss
• Worked with antenna designers for various OTA and SAR measurements to conform to regulatory emission and carrier TRP and TIS requirements.
• Troubleshoot signal de-sense related to display, USB, camera FF/RF, IMU, DC-DC switching frequency and high frequency and high speed memory or system clocks and worked closely with RF/HW/antenna teams to optimize board layout.
• *Chipset: Qualcomm MSM89xx, WTR16xx, PMIC89xx, BCM43xx, TI WL12xx*

Jan '06 – Sep '10   Murata Wireless Solution-Murata Electronics, Plano TX
                    Sr. RF Module Design Engineer

Hardware design of WLAN, Bluetooth, FM, Zigbee and WiMAX modules in single and dual antenna configurations with customized RF front-ends for smartphone, PDA, tablet, data dongle, HVAC and health monitoring devices using leading OEM solutions; Marvell, TI, Broadcom, Ember/Silicon Labs, Atheros, Beceem and Sequans.

• Worked with IC designers at OEM to address issues related to poor EVM due to IQ mismatch, DC power latch-up, on-chip TX calibration optimization, insufficient RF switch timings leading to ACPR failure etc.
• Wrote test plans to characterize IEEE 802.11a/b/g/n, BT, FM, Zigbee modules for EVM, ACPR, sensitivity and transmitter tests using Agilent signal generators, spectrum analyzer, power meters, LitePoint IQ, CBT tester, network analyzer and vector signal analyzer.
• Performed temperature, voltage range, humidity, drop and other reliability tests for production readiness along with statistical analysis [Cpk, Cpl and Cph] for various test parameters.
• On-site customer support to facilitate module seamless integration on customer platform **[HP, Apple, Microsoft]**. Worked extensively with customers in RF/electrical troubleshoot, board bring up and offered high level of customer satisfaction.
• Performed failure analysis including performance and functional failure of modules on customer platform
• *Chipset: Marvel 86xx, TI WL12xx, CSR BC6/BC4/UniFi*